UNIVERSITY OF SOUTHAMPTON

QCD Physics from the AdS/CFT Correspondence

by

Jonathan Phillip Shock

A thesis submitted for the degree of

Doctor of Philosophy

School of Physics and Astronomy

September 2005

(Or: How I Learned to Stop Worrying and Titivate Supergravity)

Dedicated to my family

UNIVERSITY OF SOUTHAMPTON

ABSTRACT

FACULTY OF SCIENCE

SCHOOL OF PHYSICS AND ASTRONOMY

Doctor of Philosophy

QCD PHYSICS FROM THE ADS/CFT CORRESPONDENCE

Jonathan Phillip Shock

The AdS/CFT correspondence is studied in the presence of D7-brane probes which add fundamental matter to the field theory. Using the Dirac-Born-Infeld action of D7-branes in supergravity geometries dual to supersymmetric and non-supersymmetric field theories, the phenomenon of chiral symmetry breaking is studied. We investigate five deformations of the $AdS_5 \times S^5$ geometry where relevant operators have been added to the field theory. Some of the properties of a supergravity background necessary to trigger a quark bilinear condensate in the dual field theory are discovered. A new technique to study the potential felt by a D7-brane in the region of a singularity is developed and used to study QCD phenomena analytically. The low energy effective pion Lagrangian is investigated and predictions made for phenomenological parameters. A preliminary investigation into perfect QCD actions from the AdS/CFT correspondence is also made. The results indicate that the gauge-gravity duality with a low UV cutoff can provide more accurate results than a UV complete theory.

Contents

1 Introduction **1**

1.1 Introduction Overview 1

1.2 The 't Hooft Expansion 4

1.3 String Theory 8

1.3.1 Calculating the Superstring Spectrum 8

1.3.2 World-Sheet Boundary Conditions 10

1.3.3 The World-Sheet Mode Expansion 11

1.3.4 The Type IIB Spectrum 13

1.4 The Type IIB Supergravity Action 14

1.4.1 The Type IIB Supergravity Equations of Motion 17

1.5 D-Branes 18

1.5.1 T-Duality 19

1.5.2 The D3-Brane Solution 21

1.5.3 D3-Brane Distributions 25

2 The AdS/CFT Correspondence **27**

2.1 Open Strings on D-Branes 28

2.2 The Correspondence 29
2.2.1 Global Symmetry Matching 31
2.2.2 Energy-Radius Duality 32
2.2.3 Field-Operator Matching 33
2.2.4 Generalising the Correspondence 35
2.3 Brane Probing 37
2.3.1 BPS Conditions 37
2.3.2 The D-brane Action 39

3 Chiral Perturbation Theory **42**
3.1 Introduction 42
3.1.1 Effective Field Theories 44
3.1.2 The Pion Lagrangian 47
3.2 Naive Dimensional Analysis 49

4 Flavouring the $AdS_5 \times S^5$ Geometry **51**
4.1 Quarks in the AdS/CFT Correspondence 51
4.1.1 The D7-Brane Probe 52
4.2 The D7-Brane Embedding 56
4.2.1 Stable Brane Flow Calculation 58
4.2.2 Meson Mass Spectrum 60
4.2.3 Vector Meson Spectrum 64
4.2.4 The Signatures of Chiral Symmetry Breaking 64

5 The Constable-Myers geometry **66**

5.1 The Background 66
5.1.1 Supersymmetry in the Constable-Myers Geometry 67
5.1.2 The Singularity 68
5.1.3 Dilaton Asymptotics in the Constable-Myers Geometry . . 70
5.1.4 Confinement and Glueballs in the Constable-Myers Geometry 70
5.2 Chiral Symmetry Breaking 73
5.2.1 Stable Brane Flow Calculation 75
5.2.2 The UV Scalar Field Boundary Conditions 77
5.2.3 Numerical Solutions 78
5.2.4 Signatures of Chiral Symmetry Breaking 79
5.2.5 Unstable Flow Solutions 81
5.3 Calculating the Vacuum Energy 83
5.4 Pions and Their Interactions 86
5.5 Higher Order Interactions 91
5.6 Non-Abelian Flavour Symmetry 93
5.7 Vector Mesons and Weakly Gauged Chiral Symmetries 95
5.8 Analytic Investigation of Chiral Symmetry Breaking 98
5.8.1 Brane Wrapping in the $AdS_5 \times S^5$ Geometry 99
5.8.2 Brane Wrapping the Constable-Myers Singularity 100
5.8.3 Analysis of the Brane Wrapping Solutions 102

6 An $\mathcal{N} = 4$ Scalar Deformation **106**

6.1 The Background 106
6.1.1 $\mathcal{N} = 8$ Five-Dimensional Supergravity 107

6.1.2 The Five-Dimensional Supergravity Action 108
6.1.3 The Ten-Dimensional Lift 110
6.1.4 The Ten-Dimensional Solution 111
6.2 Adding Quarks to the $\mathcal{N} = 4$ Scalar Deformation 113
6.2.1 D7-Brane Flow in the Physical Coordinates 115
6.2.2 The Supergravity Background in Physical Coordinates . . 117
6.2.3 The Unphysical Coordinates Revisited 119
6.3 Brane Wrapping the $\mathcal{N} = 4$ Geometry 122

7 A Non-Supersymmetric Scalar Deformation **125**
7.1 The Background 125
7.2 Adding Quarks to the Non-Supersymmetric Scalar Deformation . 129
7.3 Analytic Search for Chiral Symmetry Breaking 131
7.4 Brane Wrapping the Non-Supersymmetric Scalar Deformation . . 133

8 An $\mathcal{N} = 2^\star$ Geometry **136**
8.1 The Background 136
8.2 Adding Quarks to the $\mathcal{N} = 2^\star$ Scalar Deformation 140

9 The Yang-Mills* Geometry **144**
9.1 The Background 144
9.1.1 UV and IR Asymptotics of the Yang-Mills* Geometry . . . 146
9.1.2 The Ten-Dimensional Lift 147
9.2 D3-Brane Probing the Yang-Mills* Geometry 151
9.2.1 UV Asymptotics 151

9.2.2 IR Asymptotics 152
9.3 Glueballs in the Yang-Mills* Geometry 154
9.4 Adding Quarks to the Yang-Mills* Geometry 156
9.4.1 D7-Brane Solutions in the Yang-Mills* Coordinates 158
9.4.2 Boundary Value Problems for PDEs 161
9.4.3 D7-Brane Solutions using the Relaxation Method 162
9.5 Brane Wrapping the Yang-Mills* Geometry 164
9.5.1 Dilaton Behaviour in the IR 167
9.5.2 D7-Brane Wrapping in a Repulsive Potential 168

10 Glueballs and Perfect Actions **171**

10.1 Glueballs from Eleven-Dimensional Supergravity 171
10.2 A UV Cutoff in the AdS/CFT Correspondence 172
10.2.1 Non-Renormalisable Operators in the AdS/CFT Correspondence 174
10.3 The AdS-Schwarzschild Black-Hole Solution 175
10.4 The Eleven-Dimensional Black-Hole Solution 177
10.5 Calculating the 0^{++} Glueball Spectrum 179
10.6 Calculating the 0^{-+} Glueball Spectrum 186

11 Conclusions **189**

A $AdS_5 \times S^5$ Parametrisations **197**

List of Figures

1.1 Two examples of Feynman diagrams in the double line notation contributing to the vacuum amplitude. The left and right diagrams contribute factors N^2 and N^0 respectively. 7

1.2 Plot of the world-sheet for a closed string. The compact and non-compact directions are labelled by σ_2 and σ_1 respectively. 13

2.1 The AdS/CFT correspondence is a duality between a theory of open strings living on a stack of D3-branes, and the supergravity theory living in the singular region of the geometry sourced by the D3-branes. 31

2.2 A small number of D3-brane probes in a background sourced by a large stack of D3-branes. The theory living on the probes is a $U(N_p)$ gauge theory and the strings stretching between the probes and the centre of the space correspond to massive gauge bosons of the broken $U(N)$ gauge symmetry. 41

3.1 Effective mass induced by the interaction of hadrons with the quark condensate. 47

4.1 D7-brane probes in the presence of a background sourced by D3-branes. The open strings between the two live in a quark hypermultiplet. The open strings on the D7-brane correspond to mesons and their superpartners and the fields living on the D3-brane make up N_c $\mathcal{N} = 4$ hypermultiplets. 53

4.2 D7-Brane flows for $m = 1$ with several initial conditions for the condensate value in an $AdS_5 \times S^5$ background. Only the $c = 0$ solution defines a consistent theory. 59

4.3 Calculation of the meson spectrum for $L = 1$ (and $R = 1$) in the AdS background. The dots indicate the spectrum from the analytic calculation. 63

5.1 Plot illustrating the symmetries of the Constable-Myers geometry. Toy examples of symmetry breaking and symmetry preserving flows are also illustrated. 76

5.2 D7-brane flows about the spherical singular region. The upper diagram shows those flows with positive condensate and mass while the lower diagram illustrates those with negative condensate and positive mass. For each graph, the values of m and c are annotated in the form (m, c) for the two highest mass solutions. 79

5.3 Mass plotted against condensate for the consistent solutions to equation 5.24. For $-1.8 \lesssim m \lesssim 1.8$ there are two consistent solutions with opposite sign condensate. The reason for this is discussed in section 5.2.4. The value of the condensate in the massless limit is given by $c = \pm 1.86$. 80

5.4 Plot approximating the logarithmic behaviour of the condensate as a function of the mass. 80

5.5 Graph showing how the two solutions for a given mass can be continuously deformed into one another. 81

5.6 Plots illustrating the apparent minimum seen in the solutions to the D7-brane flows. Using a toy Higgs model, a cross-section in two of the field directions appears to give a second minimum in the potential V. 83

5.7 Plots illustrating the reason for a minimum negative condensate value for the positive mass. 84

5.8 Normalised vacuum potential, $V|_m - V|_{m=0}$. The positive condensate solutions are favoured for a positive mass. 85

5.9 Quark mass plotted against pion mass as calculated numerically from D7-brane flows. This shows excellent agreement with the Gell-Mann-Oakes-Renner prediction from the chiral Lagrangian. . 88

5.10 Plot illustrating that a D7-brane in a circular configuration in $AdS_5 \times S^5$ will collapse into the centre of the space. 100

5.11 Plot of the potential against radius, r, for the $b = 1$ circular wrapping solution. The potential is minimised at $r_0 = 1.29$. 101

5.12 Plot illustrating that a brane stretched artificially to some large radius will collapse to a configuration which is repelled by the central singularity. 102

5.13 Plot of the minimum action spherical D7-brane embedding and the massless quark embeddings in the Constable-Myers Geometry. The black circle represents the singularity in the geometry. 103

5.14 Plot of the minimum action spherical D7-brane embedding and a local minimum embedding action for a massive quark in the Constable-Myers Geometry. 104

5.15 Phases of the Constable-Myers dual field theory as a function of the conformal symmetry breaking parameter b. The ends of each arrow indicate the point at which the property of the background or the field theory stops. 105

6.1 Analytic solutions to the first order equations of motion for the scalar field flow given by equation 6.18. 113

6.2 Singularity structure of the warp factor, H, in the physical coordinate system. The right hand plot demonstrates that the circular singularity is deformed to a disk singularity as expected from the D3-brane distribution. 119

6.3 D7-brane flows in the scalar deformed geometry for different quark masses. The solid lines are the numerical solutions and the dashed lines, the coordinate transform of the full analytic solutions. This plot indicates that the numerical and analytical solutions to the DBI equations of motion for the D7-brane match well. The singularity of the geometry is shown as a black circle. 120

6.4 Apparent values of the quark mass and condensate extracted asymptotically from the flows in figure 6.3. 121

6.5 Wrapping D7-brane (central circle) falling onto singularity (outer circle) at $\chi = \infty$. 124

7.1 Plot of the scalar field $\lambda(u)$ for various values of $\mathcal{M}$ and $\mathcal{C}$. 127

7.2 IR asymptotic behaviour of λ as a function of the mass and condensate defined by the boundary conditions in the UV. The supersymmetric line ($\mathcal{M} = 0$) is on the line of stability between those flows which diverge to $+\infty$ and $-\infty$. As seen from figure 6.1, these supersymmetric flows do diverge. 128

7.3 Sample solutions for a D7-brane embedding in the non-supersymmetric scalar deformation geometry showing the absence of a gap between the solutions and the singularity. 130

9.1 Plot of the IR asymptotic flow of the five-dimensional supergravity field corresponding to a fermion bilinear as a function of the UV boundary conditions. The lower half corresponds to flows which asymptote to negative infinity while those in the top half asymptote to positive infinity. 147

9.2 Plot indicating the link between the IR asymptotic behaviour of the supergravity scalar, $\lambda(r)$, and the UV boundary conditions defined by $\mathcal{M}$ and $\mathcal{K}$. 156

9.3 Plots illustrating the relaxation method for a D7-brane flow in the canonical $AdS_5 \times S^5$ coordinates. Starting from a random discretised brane flow with a fixed UV boundary point ($\rho = 20$), it is possible to find the action minimising solution using the relaxation method. 163

9.4 Asymptotic behaviour of the dilaton as a function of α. The dilaton is independent of r in the IR of the gauge theory. 167

9.5 Attempts to solve the differential equation for a wrapped brane using the usual boundary condition methods (plot calculated using the IR asymptotic form of λ). 169

9.6 Three-dimensional brane wrapping solution about a spherical singularity. This plot is generated using the ansatz $r = r(\alpha)$ and independent of θ_+. The function r is then found using the relaxation method and the three dimensional plot generated from this function. The distance between the brane and the singularity has been exaggerated in order to see the deviation of the brane from a perfect sphere. 170

10.1 Comparison of the QCD gauge coupling (lower curve) and the gauge coupling of the field theory dual to the supergravity backgrounds in the applicable regimes (upper curve). The plots match well in the IR, but not in the UV. 172

10.2 Graph of the potential felt by the scalar field in the non-extremal, AdS-Schwarzschild black-hole background for different values of α. α is the coupling constant for the higher-dimensional operator $\mathrm{Tr}\, F^4$. 182

10.3 Peak position of the potential plotted in figure 10.2 as a function of α. This sets the value of the field theory cutoff, Λ. 183

10.4 Ratio of the first two glueball masses as a function of the parameter α. The lattice value [131, 132] 1.9 is indicated in the diagram. . . 185

List of Tables

1.1 Massless modes from type IIB string theory. The + denotes that the field strength of this 4-form potential is self-dual. This field is of particular importance in the formulation of the AdS/CFT correspondence. 14

4.1 D3- and D7-brane embedding in the $AdS_5 \times S^5$ geometry. Filled dimensions are marked with crosses, those perpendicular to the world-volumes are denoted by a dot. 52

5.1 D3-brane and D7-brane embedding in the Constable-Myers geometry. Filled dimensions are marked with crosses, those perpendicular to the world-volumes are denoted by a dot. 74

5.2 Vector meson spectrum comparing Constable-Myers and pure $AdS_5 \times S^5$ backgrounds. The Constable Myers results are normalised to agree with the $AdS_5 \times S^5$ results for highly excited states. 97

5.3 D3-brane and wrapped D7-brane embedding in the Constable-Myers geometry. Filled dimensions are marked with crosses, those perpendicular to the world-volumes are denoted by a dot. 99

6.1 Geometries representing n-dimensional disk distributions with their supergravity field boundary conditions. 111

6.2 D3- and D7-brane embedding in the $\mathcal{N} = 4$ geometry. Filled dimensions are marked with crosses, those perpendicular to the world-volumes are denoted by a dot. 114

6.3 D3- and D7-brane embedding in the pseudo-Cartesian $\mathcal{N} = 4$ geometry. Filled dimensions are marked with crosses, those perpendicular to the world-volumes are denoted by a dot. 115

8.1 D3-brane and D7-brane embedding in the $\mathcal{N} = 2^\star$ geometry. Filled dimensions are marked with crosses, those perpendicular to the world-volumes are denoted by a dot. 142

9.1 D3- and D7-brane embedding in the Yang-Mills* geometry. Filled dimensions are marked with crosses, those perpendicular to the world-volumes are denoted by a dot. 157

10.1 QCD_4 0^{++} glueball masses from AdS ($\alpha = 0$) and Improved ($\alpha = 0.0855$) geometries along with lattice data [131, 132] . All states are normalised to the 0^{++} ground state. 186

10.2 QCD_4 0^{-+} glueball masses from AdS ($\alpha = 0$) and improved ($\alpha = 0.0855$) geometries along with lattice data [131] . All states are normalised to the 0^{++} ground state. 188

Preface

The work described in this thesis was carried out in collaboration with Dr Nick Evans and Tom Waterson. The following list details our original work and gives the references for the material.

- Chapter 5: N. Evans and J. P. Shock, Phys. Rev. D **70:046002**2004 [arXiv:hep-th/0403279]
- Chapters 5 to 9: N. Evans, J. P. Shock and T. R. Waterson, JHEP **0503:005**2005 [arXiv:hep-th/0502091]
- Chapter: 10 N. Evans, J. P. Shock and T. R. Waterson, Phys. Lett. B **622:165**2005 arXiv:hep-th/0505250

No claims to originality are made for the content of Chapters 1 to 4 which were compiled using a variety of other sources.

Acknowledgements

Firstly, I would like to thank my supervisor Dr Nick Evans who has made the last two and a half years, both intellectually stimulating by coming up with such interesting research projects, and extremely enjoyable. He has always had time to answer my questions and listen to my ramblings, however trivial and frequent. I hope that we can continue collaborating together in the future. I would also like to thank my other collaborator Tom Waterson who I have thoroughly enjoyed working with and, though only beginning the second year of his AdS/CFT career, has helped me to understand many things I had brushed under the carpet, and has corrected me with my ropy maths on many occasions. I would like to thank the rest of the SHEP postgraduates who have made the last three years a truly enjoyable experience, whether it has been in the form of pub quizzes, poker nights, squash matches, being silly in the office or actually talking about physics! The rest of the SHEP team have also been great fun and of immeasurable value in getting me to the point I am in my understanding and love of high energy physics. Next, and of vital importance, my sister Joanna, who has spent many hours going through this tome with me and helping to turn it into a document that is infinitely more readable than I could ever have produced on my own. I am

truly grateful. Last and by no means least, my parents who have not only played a valuable part in proofreading this thesis but supported me without question, through the start of my career in physics. I am hugely grateful for their backing and advice. Special thanks would go to my good friends Adam, Dan and Tim, but unfortunately they've been nothing but trouble.

Chapter 1

Introduction

1.1 Introduction Overview

The progress of gauge theories, from the original conjectures on general relativity [1] through the development of quantum electrodynamics (QED) [2], and finally the discovery of non-Abelian gauge theories in 1954 [3], has heralded a giant leap in our understanding of the structure of the universe. QED has been verified to ever greater accuracy over the past 50 years and in 1965 its creators were awarded the Nobel Prize.

A gauge theory [4] is a model with an invariance under a local symmetry of some of the variables in the theory. In the case of QED, this relabelling means that the phase on all fields can be changed locally and the physics remains identical. For the theory to remain invariant under this change, a gauge field (the photon for QED) is introduced connecting points of local relabelling. In the case of non-Abelian gauge theories this relabelling is performed on a more complicated,

internal space, which takes values in a non-Abelian (non-commuting) Lie group. General relativity can be constructed as a gauge theory with an invariance under local space-time diffeomorphisms. Weyl conjectured incorrectly that the group may be extended to include local scaling invariance (dilations).

The method of Feynman diagrams has made it possible to perform perturbative calculations in gauge theories that previously would have been unthinkable. Perturbation theory relies on the fact that non-interacting systems can often be understood through sets of exactly solvable linear differential equations and, in many cases, the use of harmonic oscillators. A perturbative calculation uses a small, dimensionless parameter to parametrise the deviation from a non-interacting system. A series expansion can often be performed in the small parameter in the hope that each term in the series will be of decreasing significance. The series can be truncated at some order to give a reasonable, though not exact, answer to the problem. This method works only when a small, dimensionless parameter, defining the deviation from the linear case, exists.

Though there have been significant breakthroughs in our understanding of physics at very high energy scales, there remain some important, unanswered questions. Currently, perhaps the most relevant are those concerning the Higgs boson [5] (predicted to give mass to all matter) and the nature of symmetries at higher scales [6, 7, 8]. The limits of the standard model are currently being tested, in the expectation that its predictions, at energy scales above those for which it is an effective theory, will soon deviate from experiment, leading to a deeper insight into the bigger picture. Another significant question concerns the

nature of the strong force. The theory of quantum chromodynamics (QCD) was an important breakthrough in the attempt to understand the large spectrum of particles observed in bubble and spark chambers in the 1950s. Following this discovery, there were great leaps forward in the understanding of non-Abelian gauge theories, in particular the phenomenon of asymptotic freedom [9], discovered in the 1970s, and in 2004 awarded the Nobel prize. Asymptotic freedom describes the force felt by quarks within a nucleon. At small separations, the force between the quarks is small, and so within a nucleon they appear to move freely.

At high energy scales, QCD is in its perturbative regime [10], meaning that its coupling constant (the dimensionless parameter defining the deviation from the free theory) is small. Calculations can be performed in this regime and have been verified to accuracies of a few percent at LEP and many other high-energy particle experiments. However, the big question remains: "how is it possible to calculate QCD quantities efficiently in the strong coupling regime?" Though the perturbative Feynman diagram formulation breaks down in this regime, there are techniques with which this problem can be tackled.

The first is lattice QCD [11] which has proved an immensely valuable tool. Though both time- and computer-intensive, this technique is crucial to the understanding of hadron collider physics.

The use of effective field theories [12] is another essential technique used to study QCD at low-energy scales. In QCD, chiral perturbation theory [13] provides an algebraic link between the quark and meson masses, in addition to an understanding of the condensate picture of chiral symmetry breaking. In chapter

3 a review of this topic is provided.

The third and most salient technique for this thesis is the use of the $\frac{1}{N_c}$ expansion (N_c is the number of colours in an $SU(N_c)$ Yang-Mills theory) [14, 15, 16]. This technique has influenced the AdS/CFT correspondence to such an extent that it is important to understand it in some detail.

1.2 The 't Hooft Expansion

In the strong coupling regime of Yang-Mills theory, the usual perturbative methods of amplitude calculation break down. If another small parameter exists in the theory, it may be possible to use this to parametrise small perturbations from the free theory. 't Hooft [14, 15] showed that in the limit where the number of colours is taken to ∞ while the combination $\lambda = g_{YM}^2 N_c$ (where g_{YM} is the Yang-Mills coupling constant) is kept fixed and large, Yang-Mills theory appears to be described by a perturbative string theory.

The β-function of a gauge theory expresses the rate at which the coupling constant changes with energy. For $SU(N_c)$ pure Yang-Mills theory (Yang-Mills theory with only gauge fields) this is given by

$$\mu \frac{dg_{YM}}{d\mu} = -\frac{11}{3} N_c \frac{g_{YM}^3}{16\pi^2} + \mathcal{O}(g_{YM}^5) \ , \tag{1.1}$$

where μ is the energy scale. Truncating the expression at order g_{YM}^3, this equation can be integrated to give

$$-\frac{1}{2g_{YM}^2 N_c} = -\frac{11}{3 \cdot 16\pi^2} \ln \mu + const \ . \tag{1.2}$$

As N_c is increased, the strong coupling scale, Λ_{YM}, is kept constant by keeping

the combination $\lambda = g_{YM}^2 N_c$ fixed. The strong coupling scale is the energy scale at which the parameter λ becomes large, making perturbative calculations impossible. In QCD, this is not an exact value as the value of the coupling constant constituting strong coupling is a matter of definition.

For QCD, the Lagrangian is given by [17]

$$\mathcal{L} = \bar{\psi}(i \not{\partial} + g A_\mu^a \gamma^\mu t^a - m)\psi - \frac{1}{4} F_{\mu\nu}^a F^{\mu\nu a} \ , \tag{1.3}$$

where ψ is the quark field which is a Dirac fermion in the fundamental of the gauge group (given in QCD by $SU(3)$), m is the quark mass, g is the QCD coupling constant, A is the gluon field (QCD gauge field) which transforms in the adjoint of $SU(3)$ and the parameters f are given by the structure constants of the $SU(3)$ algebra. Greek letters label space-time indices and Roman letters label gauge group indices.

The 't Hooft expansion was originally formulated in terms of a $U(N_c)$ gauge theory, with all matter in the adjoint (though this can be generalised to include fundamental matter). The Lagrangian for this theory can be written with the fields normalised such that the coupling constant appears explicitly only as an overall constant of proportionality. For example, the interaction and kinetic terms of a theory of scalar fields, in the adjoint of the gauge group, with cubic and quartic couplings is given by [18]

$$\mathcal{L} \sim \frac{1}{g_{YM}^2} \left[\mathrm{Tr}\,(d\Phi_i d\Phi_i) + c^{ijk} \mathrm{Tr}\,(\Phi_i \Phi_j \Phi_k) + d^{ijkl} \mathrm{Tr}\,(\Phi_i \Phi_j \Phi_k \Phi_l) \right] \ , \tag{1.4}$$

where $\frac{1}{g_{YM}^2} = \frac{N_c}{\lambda}$. In the large N_c limit, the propagators of adjoint fields in a $U(N_c)$ and an $SU(N_c)$ gauge theory differ by a vanishing term, proportional to

$\frac{1}{N_c}$, and so are treated as identical in this thesis. A $U(N_c)$ theory with matter in the adjoint can be written in a double line notation where each adjoint field is drawn as the direct product of a fundamental and an anti-fundamental field. This double line notation can be used to write a Feynman diagram expansion for a scattering amplitude, propagator or vacuum contribution. It is possible to calculate the powers of N_c and λ associated with a given vacuum diagram. There is a contribution to the amplitude from vertices, propagators and loops, with the following powers of N_c and λ

$$\begin{aligned} \text{Vertex} &: \frac{N_c}{\lambda} , \\ \text{Propagator} &: \frac{\lambda}{N_c} , \\ \textit{Loop} &: N_c . \end{aligned} \tag{1.5}$$

A diagram with V vertices, E propagators and F Loops, includes a factor

$$N^{V-E+F}\lambda^{E-V} = N^{\chi}\lambda^{E-V} , \tag{1.6}$$

where χ is the Euler characteristic (a topological invariant) of the simplicial decomposition. A simplicial decomposition is a triangulation of a polygon in which the propagators become edges and the loops become faces. In terms of the genus of the surface,

$$\chi = 2 - 2h , \tag{1.7}$$

where h is the number of handles (genus). Therefore a diagram with h handles is suppressed by h powers of $\frac{1}{N^2}$. The number of factors λ is independent of number of faces. For large λ, it is believed that a non-perturbative calculation would indicate that the diagrams are filled by propagating fields, that is, the internal

gaps in an individual diagram closes, leaving a surface. This surface is the non-perturbative Yang-Mills string world-sheet. The perturbative calculation in terms of $\frac{1}{N_c}$ is then a topological expansion in the genus of the string in the same form as a perturbative string calculation [19]. Figure 1.2 provides an example of two diagrams contributing to a vacuum amplitude. The left and right diagrams are of Euler character two and zero respectively.

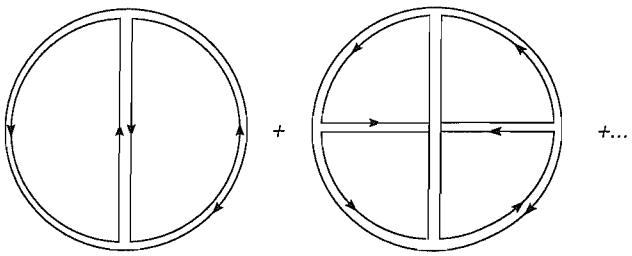

Figure 1.1: Two examples of Feynman diagrams in the double line notation contributing to the vacuum amplitude. The left and right diagrams contribute factors N^2 and N^0 respectively.

The link between strong coupling phenomena and string theory dates from before the 't Hooft expansion. Before the development of QCD, it was discovered that, in certain energy regimes, hadronic scattering amplitudes could be successfully described using the mathematics of string oscillations [20, 21]. In the Regge region [22] (large Mandelstam variable s with fixed t [23]), these calculations matched experimental results to a higher accuracy than the naive point-particle calculations. However, this model did not work well for high-energy scattering at fixed angles. Subsequently QCD was discovered and realised to be the correct

description of high-energy hadronic processes. However, 't Hooft's realisation that, at strong coupling, QCD could really be a string theory, and more recently Maldacena's conjecture [24] of an exact duality between string theory and gauge theory, have meant that these problems are once again being tackled with the techniques of string theory.

1.3 String Theory

The AdS/CFT correspondence [24, 25, 26] is discussed in detail in chapter 2, but it is instructive to note at this point that the correspondence links a string theory and a gauge theory. In the regime of interest for this thesis, the string side of the duality is described by a classical effective field theory. Though many of the complex techniques of string theory are not important for this discussion, it is enlightening to have a clear path between the formulation of string theory and the effective action, discussed in detail in section 1.4. The aim of this section is to obtain the massless spectrum of a specific string theory and to discuss the emergence of D-branes from the underlying dualities of the theory. These results are the essential ingredients necessary to understand the AdS/CFT correspondence.

1.3.1 Calculating the Superstring Spectrum

Though it is common to start with the action for the purely bosonic string, the full supersymmetric action is provided here for completeness [19].

$$S[X,\psi] = \frac{1}{4\pi\alpha'}\int d^2\sigma(\eta^{ab}g_{\mu\nu}\partial_a X^\mu \partial_b X^\nu) + \alpha'(\eta^{ab}g_{\mu\nu}\bar{\psi}^\mu\gamma_a\partial_b\psi^\nu)\ . \tag{1.8}$$

The theory is described by a two-dimensional world-sheet with bosonic fields, X^μ, and fermionic fields, ψ^ν, living on its surface. The world-sheet metric is given by η_{ab} and the coupling constants of the fields are given by $g_{\mu\nu}$. The parameter α' is related to the fundamental string length by $\alpha' = l_s^2$. The bosonic part of the action is motivated by the relativistic point-particle action, where the point-particle's position in space-time is a function of a parameter on its world-line. In the case of the superstring, the positions of the points on the string world-sheet in space-time (with directions X^μ) are given by $X^\mu(\sigma_1, \sigma_2)$, where σ_i are the two directions on the string world-sheet. To label each point on the world-sheet takes D-coordinates, where D is the number of space-time dimensions. Therefore, there are D scalar fields and D fermionic fields living on the world-sheet (μ runs from 1 to D). The fermionic part of the action describes the superpartners of the bosonic excitations. Just as the X^μ describe the position of the string in space-time, so the fermionic degrees of freedom, ψ^μ, describe the position of the world-sheet in superspace. As for a relativistic point-particle, there are several important symmetries of the action (equation 1.8).

The symmetries for the bosonic part of the action are given by:
a diffeomorphism invariance for the metric on the world-sheet:

$$\begin{aligned} X'^\mu(\sigma'_1, \sigma'_2) &= X^\mu(\sigma_1, \sigma_2), \\ \frac{\partial \sigma'^c}{\partial \sigma^a} \frac{\partial \sigma'^d}{\partial \sigma^b} \gamma'_{cd}(\sigma'_1, \sigma'_2) &= \gamma_{ab}(\sigma_1, \sigma_2) \ , \end{aligned} \tag{1.9}$$

and a two-dimensional Weyl invariance:

$$\gamma'_{ab}(\sigma_1, \sigma_2) = e^{2\omega(\sigma_1, \sigma_2)} \gamma_{ab}(\sigma_1, \sigma_2) \ , \tag{1.10}$$

which allows a local rescaling of the world-sheet metric. These symmetries allow

enough freedom to define the world-sheet metric in the flat Minkowski form in the action of equation 1.8. In the case of the superstring, there is also explicit super-Poincaré invariance. The next step in understanding the theory is the calculation of the stress-energy tensor by the variation of the action with respect to the world-sheet metric. This variation vanishes classically. The vanishing of the trace of the stress-energy tensor ensures that Weyl invariance is a good symmetry of the theory, however, this symmetry is anomalous in the full quantum theory. This anomaly is equal to the central charge of the theory, which is related to the variation of the stress-energy tensor under conformal transformations [19]. When the theory is gauge-fixed, ghosts are introduced which, along with the scalar and fermionic fields, contribute to the central charge. The central charge is a function of the number of fields, which is proportional to the number of space-time dimensions. For the central charge to vanish, giving a non-anomalous Weyl symmetry, the theory must be formulated in ten space-time dimensions.

1.3.2 World-Sheet Boundary Conditions

There are several types of string, the properties of which depend on the nature of the boundary conditions of the fields on the world-sheet. Open and closed strings arise from this difference in boundary conditions. It is possible to formulate equations for left- and right-moving modes living on the world-sheet. For the open string, these modes are related, whereas for the closed string, these modes are independent and there are twice as many degrees of freedom as occur in the open string case. A simple trick allows the coordinates on the world-sheet to be

written in terms of two complex numbers, z and $\bar{z}$, where left- and right-moving modes depend on only one of these coordinates (holomorphic and antiholomorphic functions).

1.3.3 The World-Sheet Mode Expansion

The first step in calculating the spectrum of states on the string, is to expand the stress-energy tensor as a Laurent series. This is given (in the purely bosonic case) by

$$T_{zz}(z) = \sum_{i=-\infty}^{\infty} \frac{L_m}{z^{m+2}}, \qquad T_{\bar{z}\bar{z}}(\bar{z}) = \sum_{i=-\infty}^{\infty} \frac{\tilde{L}_m}{\bar{z}^{m+2}} \ , \tag{1.11}$$

where L_m are the Virasoro generators. The Virasoro generators make up an infinite-dimensional algebra which has an infinite number of conserved charges. This algebra is given by

$$[L_m, L_n] = (m-n)L_{m+n} + \frac{c}{12}(m^3 - m)\delta_{m,-n} \ , \tag{1.12}$$

where c is the central charge of the algebra. There is an equivalent algebra for the anti-holomorphic generators $\tilde{L}_m$. There is also a second set of fermionic Virasoro generators which obey an anticommutative algebra and are part of the full super Virasoro algebra.

The bosonic modes, fermionic modes and Virasoro generators can be written in terms of creation and annihilation operators (α_n for the bosonic modes and θ_r for the fermionic modes). The spectrum of operators can be found by defining the ground state as the state which is annihilated by all lowering operators. All physical states are those for which

$$L_m|\phi>=\tilde{L}_m|\phi>=0, \text{ for } m>0 \ , \tag{1.13}$$

and there is a similar condition for the fermionic generators. This condition is a result of the vanishing of the stress-energy tensor. The mass operator for the open string modes can be written in terms of the raising and lowering operators:

$$M^2 = \frac{1}{\alpha'}\left(\sum_{n=1,r=\frac{1}{2}}^{\infty}(\alpha_{-n}\cdot\alpha_n + r\theta_{-r}\cdot\theta_r - a)\right) , \tag{1.14}$$

where a is a normal ordering constant which must be determined by the cancellation of the Weyl anomaly. The spectrum of states is determined using this operator.

For the fermionic fields in the closed string theory, there are two possible boundary conditions given by

$$\text{Ramond (R)} \quad : \quad \psi^\mu(\sigma_2 + 2\pi) = +\psi^\mu(\sigma_2) ,$$

$$\text{Neveu-Schwarz (NS)} \quad : \quad \psi^\mu(\sigma_2 + 2\pi) = -\psi^\mu(\sigma_2) ,$$

where σ_2 is chosen to be the space-like (compactified) direction on the world-sheet. The closed string worldsheet is illustrated in figure 1.2.

Though the world-sheet theory is explicitly supersymmetric, to obtain space-time supersymmetry, a projection of states, the GSO-projection [27] (Gliozzi-Scherk-Olive), is required. The GSO projection also removes the open string tachyon which remains in the purely bosonic string theories.

There is another decision to be made for the left- and right-moving modes. If the R groundstate modes have the same chirality, the theory is labelled type IIB string theory, while if they have opposite chirality, the theory is type IIA. II refers to the number of supersymmetries, as two is the highest number of supersymmetries in ten dimensions that is consistent with a truncation to four dimensions. This is discussed in more detail in section 1.4.

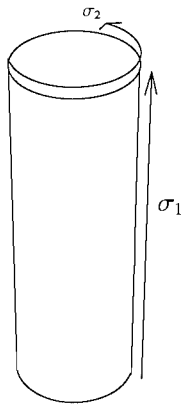

Figure 1.2: Plot of the world-sheet for a closed string. The compact and non-compact directions are labelled by σ_2 and σ_1 respectively.

Type II string theory contains only closed strings (until D-branes are introduced in section 1.5). A string theory which contains open strings necessarily contains closed strings but the reverse is not the case. This is because an open string one-loop amplitude is equivalent to a closed string propagator.

1.3.4 The Type IIB Spectrum

The groundstate (massless) modes fill representations of the little group of the ten-dimensional Lorentz symmetry, given by $SO(8)$. Along with the chirality, these representations are given by $\mathbf{8}_v$ (vector representation of $SO(8)$), $\mathbf{8}_c$ (spinor representation with positive chirality), and $\mathbf{8}_s$ (spinor representation with negative chirality). The existence of three representations can be understood from the triality of the $SO(8)$ Dynkin diagram.

The massless spectrum of type IIB is the direct product $(\mathbf{8}_v \oplus \mathbf{8}_s) \otimes (\mathbf{8}_v \oplus \mathbf{8}_s)$, which decomposes into irreducible representations of the $so(8)$ algebra given in

Table 1.1.

	States	Fields
NS-NS Bosons	$\mathbf{1} \oplus \mathbf{28} \oplus \mathbf{35}$	Φ, B_{MN}, G_{MN}
R-R Bosons	$\mathbf{1} \oplus \mathbf{28} \oplus \mathbf{35}_+$	A_0, A_2, A_4
NS-R Fermions	$\mathbf{8}_s \oplus \mathbf{56}_s$	$\lambda^{(1)}$, $\psi_M^{(1)}$
R-NS Fermions	$\mathbf{8}_s \oplus \mathbf{56}_s$	$\lambda^{(2)}$, $\psi_M^{(2)}$

Table 1.1: Massless modes from type IIB string theory. The + denotes that the field strength of this 4-form potential is self-dual. This field is of particular importance in the formulation of the AdS/CFT correspondence.

1.4 The Type IIB Supergravity Action

This section begins with the low-energy spectrum of string theory, and attempts to take the shortest path to the low-energy effective action which describes these degrees of freedom in terms of a point-particle field theory [28]. The equations of motion of the fields in the effective action are calculated, and finally a specific classical solution to these equations, describing D-branes [29], is obtained.

The string theory of interest is type IIB, which is related to type IIA and eleven-dimensional supergravity [30] by simple duality relations (discussed in section 1.5.1). The highest spin field that a four-dimensional, point-particle field theory can consistently describe (unless it has an infinite tower of spin states or is non-interacting) is spin two [31], the graviton. This restriction implies a

limit on the maximum number of supersymmetries of any theory [19]. Specifically, this limit means that the maximal supersymmetry in four dimensions is $\mathcal{N} = 8$. There is only one possible representation (in the massless case) given by the supergravity multiplet with the following state multiplicities:

$$(-2, -\frac{3}{2}^{8}, -1^{28}, -\frac{1}{2}^{56}, 0^{70}, \frac{1}{2}^{56}, 1^{28}, \frac{3}{2}^{8}, 2) \ . \tag{1.15}$$

The total number of supercharges in this theory is calculated from the $\mathcal{N} = 1$ theory, where there are four supercharges. This is the minimum representation for a Weyl spinor in four dimensions (following from $2^{\frac{d}{2}}$). This implies that, in the maximally extended supersymmetry, there are $4 \cdot 8 = 32$ supercharges. In fact this bound on the total number of supercharges holds for higher dimensions because the four-dimensional theory can be reached from a higher-dimensional compactification. This implies a bound on the maximum number of dimensions for a consistent field theory due to the minimum spinor representations. The highest possible number of dimensions for a consistent supersymmetric field theory is eleven (with some exceptions for multiple time-like dimensions) because min.rep $= 2^{\frac{d-1}{2}}$ in an odd number of dimensions. In ten dimensions, where the minimum representation is 16, the maximal supersymmetry is $\mathcal{N} = 2$.

The massless spectrum of eleven-dimensional supergravity has 256 states which, by the usual supersymmetry rules, are made up of 128 fermions and 128 bosons. The graviton multiplet contains a graviton and an antisymmetric three-index tensor, making up $44 + 84$ bosonic degrees of freedom. These fill two representations of $so(9)$ (the little group of $SO(10, 1)$). The fermionic degrees of freedom are all in a spinor-vector state satisfying $(\Gamma^{\mu})^{\beta\alpha}\psi_{\mu\alpha} = 0$, and a Dirac equation which

reduces its degrees of freedom to 128.

With a limit on the number of derivatives, there is a unique supersymmetric action for this eleven-dimensional spectrum, with the bosonic part given by [18]

$$S_{11} = \frac{1}{2\kappa^2}\int d^{11}x\sqrt{-G}\left(R - \frac{1}{2}|F_4|^2\right) - \frac{1}{12\kappa^2}\int A_3 \wedge F_4 \wedge F_4 \ , \qquad (1.16)$$

where A_3 is the three-form potential and F_4 is its field strength. As explained, the maximum number of supersymmetries in ten dimensions is two. However, there are two possible theories – one includes two supercharges of the same chirality and the other in which they are opposite. By compactifying eleven-dimensional supergravity on a circle and keeping only the massless states, a theory with opposite chirality supercharges (in the **16** and **16′**) is obtained. This is type IIA supergravity. To obtain the IIB theory, a duality transformation must be applied to the IIA theory (T-duality is discussed in more detail in section 1.5.1). The massless spectra of IIA and IIB can be calculated and the IIB spectrum is given in Table 1.1. The antisymmetric rank-four tensor has a self-dual field strength meaning that a satisfactory action which encodes this self-duality does not exist. The self-duality condition must be added as a supplementary condition:

$$\begin{aligned} S_{IIB} &= \frac{1}{4\kappa^2}\int d^{10}x\sqrt{-G}e^{-2\Phi}(2R + 8\partial_\mu\Phi\partial^\mu\Phi - |H_3|^2) \\ &\quad -\frac{1}{4\kappa^2}\int d^{10}x\sqrt{-G}\left(|\tilde{F}_1|^2 + |\tilde{F}_3|^2 + \frac{1}{2}|\tilde{F}_5|^2\right) + S_{fermionic} \ , \\ \tilde{F}_5 &= \star\tilde{F}_5 \ , \end{aligned} \qquad (1.17)$$

where the tildes have been added because the fields in this action are not the same as those in equation 1.16.

1.4.1 The Type IIB Supergravity Equations of Motion

The equations of motion for this supergravity action are now calculated. The formulation of the AdS/CFT correspondence (chapter 2) has only three fields switched on – the graviton, the dilaton and the five-form field strength. The action with these fields turned on can be written as

$$S_{IIB} = \frac{1}{2\kappa^2}\int d^{10}x\sqrt{-G}\left[R - \frac{1}{2}(\partial\Phi)^2 - \frac{1}{2.5!}F_5^2\right] . \tag{1.18}$$

Note that the metric and the dilaton have been redefined to transform the action from the string frame to the Einstein frame, giving an action in the usual Einstein-Hilbert form [29]. It is in this frame that the stress-energy tensor has its usual physical meaning.

The dilaton equation of motion is the least complex, given by [32]

$$\partial_M(\sqrt{G}\partial^M\Phi) = 0 . \tag{1.19}$$

Note that the metric has been written in a Wick rotated form here. The derivative of the determinant of the metric is given by

$$\begin{aligned}\frac{\partial\sqrt{G}}{\partial x^M} &= \frac{\partial G_{NP}}{\partial x^M}\frac{\partial\sqrt{G}}{\partial G_{NP}} \\ &= \partial_M G_{NP}\frac{1}{2\sqrt{G}}GG^{NP} \\ &= \frac{\sqrt{G}}{2}G^{NP}\partial_M G_{NP} .\end{aligned} \tag{1.20}$$

So the equation of motion is

$$\begin{aligned}\sqrt{G}\partial_M(\partial^M\Phi) + \frac{\sqrt{G}}{2}G^{NP}\partial_M G_{NP}\partial^M\Phi &= 0 , \\ \partial_M\partial^M\Phi + \frac{1}{2}G^{NP}\partial_M G_{NP}\partial^M\Phi &= 0 .\end{aligned} \tag{1.21}$$

However, the dot product of a covariant and a partial derivative is

$$\begin{aligned} \nabla_M \partial^M \Phi &= \partial_M \partial^M \Phi + \frac{1}{2} G^{MB} \left[G_{MB,N} + G_{NB,M} - G_{MN,B} \right] \partial^N \Phi \\ &= \partial_M \partial^M \Phi + \frac{1}{2} G^{MB} G_{MB,N} \partial^N \Phi \ , \end{aligned} \tag{1.22}$$

which is equal to the left hand side of equation 1.21. Therefore

$$\nabla_M \partial^M \Phi = 0 \ . \tag{1.23}$$

The equation of motion for the graviton is more complicated. The first term in the action is the Einstein-Hilbert term. The variation of the dilaton term is simple, but the variation of the five-form term is more complex. The equation of motion for the graviton is given by

$$R_{AB} - \frac{1}{2} R G_{AB} = \frac{1}{2} \partial_A \Phi \partial_N \Phi + \frac{1}{2.5!} (5 F_A{}^{C_1 C_2 C_3 C_4} F_{B C_1 C_2 C_3 C_4} - \frac{1}{2} G_{AB} F_5^2) \ . \tag{1.24}$$

The solutions studied in this thesis are all Ricci flat and so the second term in the above equation vanishes. The equation of motion and the Bianchi identity for the five-form are

$$\partial_M (\sqrt{G} F^{M C_1 C_2 C_3 C_4}) = 0, \qquad dF_5 = 0 \ . \tag{1.25}$$

1.5 D-Branes

It is hoped that string theory is the unique, fundamental theory that unifies all the forces of nature. It would be a great achievement if a unique solution could be found to describe the universe we live in. The anthropic principle may be correct – the universe may be this way because, of all the many possibilities, this

is one of few that hold the right conditions to support life. Perhaps, through studying the statistics of string vacua, it can be shown that the type of universe we live in is highly favoured by the landscape [33]. The string landscape defines the space of all possible string vacua, for instance, the value of the dilaton lives on a moduli-space, so, one value of the dilaton is not favoured over any other. Finally, it would be most satisfying if the only fully consistent string solution was that which describes this universe. This would surely be the strongest signal that string theory is the correct description of nature.

In the early 1990s, the community of string theorists was becoming disillusioned. Not only was it known that string theory had many different solutions, it also appeared that there were five independent string theories. The hope of a single unifying theory seemed to be fading. However, the second superstring revolution, started by Ed Witten [34] in 1995 sparked a resurgence in activity when it was shown that the five theories were linked by a series of simple dualities. This meant that all the apparently independent theories were actually different descriptions of the same theory in different regions of parameter space.

1.5.1 T-Duality

T-duality [35] is the most important duality for this thesis. It is a large-small radius duality between type IIB theory with a large compactified dimension and type IIA theory with a small compactified dimension. A closed string in a compactified dimension has two contributions to its energy – a winding energy, which is proportional to both the radius of the compactified direction and the number

of times the string winds around this direction, and a Kaluza-Klein energy which is inversely proportional to the radius. For a dimension of radius R, there is a spectrum of closed strings given by all the possible winding numbers and all the possible Kaluza-Klein states. If the radius, R, is changed to $\frac{1}{R}$, the spectrum will remain exactly the same, as the Kaluza-Klein and winding modes are exchanged. Therefore, a theory with only closed string modes appears to be dual to itself under the interchange of $R \rightarrow \frac{1}{R}$. However, though open strings have Kaluza-Klein modes in the compactified direction, they do not have winding modes. This means that the spectrum will change under the large-small radius interchange and the theories appear different. In contrast to the closed string spectrum, the open string spectrum does change under this duality. By studying the open string modes, it is found that, as a large dimension R is replaced with a small dimension $\frac{1}{R}$, the ends of the open strings become trapped in the small dimension. In the limit $R \rightarrow \infty$, the ends of the open strings become trapped on a hyper-surface of one dimension less then the original space. The physical spectrum of closed strings, however, does not notice this change and so closed strings are free to move around as if the radius of the space had not been altered. The boundary conditions of the open string ends change under this duality from Neumann to Dirichlet in the T-dualised direction,

$$\partial_{\sigma_2} X^{\mu}(\sigma_1, (0,l)) = 0 \leftrightarrow X^{\mu}(\sigma_1, (0,l)) = c^{\mu} \ , \tag{1.26}$$

where $(0,l)$ denote the ends of the string, and μ is the direction that is T-dualised. T-duality exchanges Neumann and Dirichlet boundary conditions and also changes the chirality of the right-moving modes thereby exchanging type IIB

for IIA. By T-dualising, a hyper-surface has appeared which has excitations in the form of open strings. This hyper-surface is the D-brane. Though it seems to be simply a surface in the higher-dimensional space, because open strings can be excited on it, it is truly a dynamical object. Not only are D-branes a consequence of the duality inherent in string theory, but these objects exist as solitonic solutions in the low-energy limit of string theory – supergravity – which are discussed in more detail in section 1.5.2. The two ends of the string, given by 0 and l, can have different boundary values, meaning that an open string can stretch between D-branes. By setting up the boundary conditions appropriately, many D-branes spanning different directions can be introduced.

These D-branes appear to be rather crude constructions, but using another duality (the strong-weak coupling duality under which type IIB is self-dual), the fundamental string is exchanged for the two-dimensional D1-brane. This suggests that D-branes are as fundamental as the strings from which string theory was originally constructed.

1.5.2 The D3-Brane Solution

The ingredients are now in place to find specific solutions to the supergravity action, in particular, the D3-brane solution [36, 32]. This is a solitonic solution to the supergravity equations, and describes a four-dimensional classical solution in ten-dimensional space. This soliton fills four of the dimensions, including the time dimension. The existence of this soliton breaks some of the space-time symmetries of the $SO(9,1)$ Lorentz group, and an ansatz can be postulated which

preserves the symmetries on the brane world-volume and those perpendicular to its surface. The presence of the brane is expected to break the Lorentz group in the following way:

$$SO(9,1) \rightarrow SO(3,1) \times SO(6) \ . \tag{1.27}$$

A four-dimensional soliton has the correct number of dimensions to be a source for a five-form field strength, and indeed the D3-brane solution is just that. In general, a Dp-brane is a source for a $(p+1)$-form R-R gauge potential, the charge density for which is given by

$$Q_p = \int_{S^{8-p}} \star F_{p+2} \ . \tag{1.28}$$

The simplest D3-brane ansatz with the appropriate space-time symmetries is then

$$\begin{aligned} ds_{10}^2 &= H^{-2\alpha}\eta_{\mu\nu}dx^\mu dx^\nu + H^{2\beta}\delta_{ab}dy^a dy^b, \\ A_{(4)} &= H^{-\gamma}dx^0 \wedge dx^1 \wedge dx^2 \wedge dx^3 \ , \\ \Phi &= 0 \ , \\ A_{(0)} &= 0 \ , \end{aligned} \tag{1.29}$$

where, by the symmetries, μ and ν run over four-dimensional Minkowski space-time, and a and b run over six spatial directions with an $SO(6)$ isometry. The warp factor, H, depends only on the distance from the brane. The metric can be written in a simpler form, where the flat six-plane is written in spherical polars:

$$ds_{10}^2 = H^{-2\alpha}\eta_{\mu\nu}dx^\mu dx^\nu + H^{2\beta}\left(dr^2 + r^2 d\Omega_5^2\right) \ , \tag{1.30}$$

where Ω_5 is the metric on a five-sphere. This means that H can only depend on the r direction. By studying the equations of motion, the parameters (α, β, γ),

and the form of $H(r)$ can be constrained. The simplest equation of motion leading to a constraint is given by the Bianchi identity. The five-form can be written as

$$\begin{aligned} F_5 &= dA_4 + \star dA_4 \ , \\ dA_4 &= -\gamma H^{-(\gamma+1)} \partial_r H dr \wedge dx^0 \wedge dx^1 \wedge dx^2 \wedge dx^3 \ , \\ \star dA_4 &= -\frac{\gamma}{5!} H^{-(\gamma+1)} \partial_r H \sqrt{g} g^{rr} (g^{xx})^4 d\omega^1 \wedge ... \wedge d\omega^5 \\ &= -\frac{\gamma}{5!} H^{-(\gamma+1)+4\alpha+4\beta} \partial_r H r^5 d\omega^1 \wedge ... \wedge d\omega^5 \ . \end{aligned} \tag{1.31}$$

Due to the self-duality of the five-form, the Bianchi identity is given by

$$\begin{aligned} d \star dA_4 &= 0 \ , \\ (4\alpha + 4\beta - (\gamma+1))(\partial_r H)^2 \frac{r}{H} + ((\partial_r^2 H) r + 5\partial_r H) &= 0 \ . \end{aligned} \tag{1.32}$$

The next field equation is given by

$$R^M{}_N = \frac{1}{2 \cdot 4!} F^{MABCD} F_{NABCD} \ . \tag{1.33}$$

There are two independent components of this equation to study. The first is given by the rr component. The right hand side of equation 1.33 is given by

$$F^{rx_1x_2x_3x_4} F_{rx_1x_2x_3x_4} = \gamma^2 (\partial_r H)^2 H^{-2(\gamma+\beta+1-4\alpha)} \ , \tag{1.34}$$

and from the left hand side is

$$\begin{aligned} R^r{}_r &= g^{rr} R_{rr} = H^{-2\beta} R_{rr} \\ &= H^{-2(\beta+1)} \left(-r \left(4\alpha^2 - 5\beta + 4\alpha(1+\beta) \right) (\partial_r H)^2 \right. \\ &\quad \left. + H(-5\beta \partial_r H + r(4\alpha - 5\beta)\partial_r^2 H) \right) \ . \end{aligned} \tag{1.35}$$

The xx component of equation 1.33 is calculated in a similar fashion and provides the third constraint.

In order to be a vacuum solution to the Einstein equations, the metric must be Ricci flat. This puts the final constraint on the free parameters:

$$r(10\alpha^2+\alpha(4-16\beta)+5\beta(2\beta-1))(\partial_r H)^2-(4\alpha-5\beta)H(5\partial_r H+r\partial_r^2 H)=0\,. \quad (1.36)$$

From these constraint equations, it can be shown that the consistent solution to the supergravity ansatz is parametrised by

$$\begin{aligned} \alpha &= \frac{1}{4}\,, \\ \beta &= \frac{1}{4}\,, \\ \gamma &= 1\,, \\ \partial_r^2 H &= \frac{-5\partial_r H}{r}\,. \end{aligned} \quad (1.37)$$

If the metric on the ab directions in the ten-dimensional space are left unspecified, it is found that the final constraint means that the warp factor, H, must be a solution to the six-dimensional Laplace equation. In this case, the D3-brane supergravity solution is then

$$\begin{aligned} ds^2 &= H(y)^{-\frac{1}{2}}dx_{//}^2 + H(y)^{\frac{1}{2}}h^{mn}dy_m dy_n\,, \\ A_4 &= H(y)^{-1}dx^0\wedge\ldots\wedge dx^4\,, \\ \Phi &= 0\,, \\ \partial_m(\sqrt{h}h^{mn}\partial_n H(y)) &= 0\,. \end{aligned} \quad (1.38)$$

This calculation can be performed in several other ways. Another method of finding the constraints is by the vierbein and sechsbein formalism with Cartan's structure equations to derive equation 1.37. The original method of Horowitz and Strominger [36] works by writing the metric in an ansatz of the form

$$ds^2 = e^A dx_{//}^2 + e^B dy^2\,. \quad (1.39)$$

This form of the metric is substituted into the supergravity action, and the parameters, A and B, which depend on the transverse direction are treated as fields. The field equations for this action are then calculated and the four equations for the four fields fix the constraints as above.

1.5.3 D3-Brane Distributions

When the space transverse to the D3-brane is written in Euclidean, flat-space coordinates as $\sum_{i=1}^{6} dy_i^2$, the solution to Laplace's equation can be written as a function of the position of the D3-brane, $\vec{y}_1$, as

$$H(y) = 1 + \frac{L^4}{|\vec{y} - \vec{y}_1|^4} , \tag{1.40}$$

where $L^4 = 4\pi g_s \alpha'^2$. This function can be generalised to a solution with N_I branes at different positions, $\vec{y}_I$:

$$H(y) = 1 + \sum_{I=1}^{N} \frac{L^4 N_I}{|\vec{y} - \vec{y}_I|^4} . \tag{1.41}$$

Generally, the solutions of interest will describe a single stack at one position (defining the origin of the six-dimensional space) with a large number of branes. As the limit $N \to \infty$ is taken, the warp factor tends to its near-horizon solution $H(y) = \frac{NL^4}{y^4}$. In this limit, the simplest parametrisation of the metric is given by [18]

$$\left(\frac{4\pi g_s \alpha'^2 N}{r^4}\right)^{-\frac{1}{2}} dx_{//}^2 + \left(\frac{4\pi g_s \alpha'^2 N}{r^4}\right)^{\frac{1}{2}} (dr^2 + r^2 d\Omega_5^2) . \tag{1.42}$$

This is the product space of AdS_5 (five-dimensional Anti-de-Sitter space) and an S^5, both of radius $R^4 = 4\pi g_s \alpha'^2 N$. AdS_5 is a maximally symmetric space (maximum number of Killing vectors) with a negative cosmological constant [37].

It is constructed by taking a hyperboloid in a six-dimensional flat-space with metric $(+++++--)$. The isometry group of AdS_5 is $SO(4,2)$ which is inherited from the six-dimensional embedding. The $AdS_5 \times S^5$ metric can be written in many different ways, and, depending on the most convenient parametrisation for a specific problem, will be rewritten accordingly. Appendix A summarises some of these parametrisations. The $AdS_5 \times S^5$ metric describes the supergravity background used in the formulation of the AdS/CFT correspondence.

A more general solution is formulated by defining a continuous distribution of D3-branes. In this case the sum in the harmonic form becomes an integral over the distribution

$$\begin{aligned} H(y) &= 1 + \int_{\mathcal{M}} d^6y' \frac{L^4}{|\vec{y} - \vec{y'}|^4} \sigma(y') \ , \\ N &= \int_{\mathcal{M}} d^6y' \sigma(y') \ , \end{aligned} \tag{1.43}$$

where $\sigma(y')$ describes the density distribution and the integral is taken over the six-dimensional space perpendicular to the branes. Due to the infinite number of possible brane distributions, there are an infinite number of possible warp factors.

Chapter 2

The AdS/CFT Correspondence

Having introduced the building blocks of the AdS/CFT correspondence, it can now be explored in some detail. Half of the correspondence was investigated in the previous section. A stack of D3-branes [29] can be described by a supergravity solution which is, in the near-horizon limit, $AdS_5 \times S^5$ with a non-zero, five-form field strength and a constant dilaton [18].

The near-horizon geometry is obtained when the number of branes is taken to infinity. Having formulated this solution, the propagation of closed strings in this background can be studied. As the number of branes is taken to infinity and the product $g_s N$ is kept large and constant, the radius of curvature of the AdS space and five-sphere, $R = (4\pi g_s N \alpha'^2)^{\frac{1}{4}}$, becomes much larger than the string scale, $\sqrt{\alpha'} = l_s$. Taking the large N limit means that the supergravity limit of string theory gives an accurate description of the physics.

2.1 Open Strings on D-Branes

One side of the duality is described by closed string modes in the D3-brane supergravity background. The other side is described by open strings on a stack of D3-branes in flat-space [38]. To understand this, the theory of the strings living on the brane must be explored. The ends of open strings are labelled by the branes they are attached to. The strings are oriented, meaning that there are two kinds of string stretching between two branes – one with the left end on the first brane and the right on the second, and the other with the ends reversed. These labels, known as Chan-Paton factors [19], generate a symmetry for the open strings. For a stack of coincident branes, the physics remains invariant under a permutation of the labels. There are N^2 possible string labellings, which fill a single adjoint representation of a Lie group, $U(N)$. As the strings are free to move around on the surface of the branes, and a relabelling can be performed at any point, the symmetry is a local symmetry. Indeed, when the spectrum of strings living on the D-brane is calculated, it is found that there is a massless vector mode – the $U(N)$ gauge boson. As explained in chapter 1, in the large N limit, the $U(N)$ and $SU(N)$ gauge groups can be treated identically. All strings living on the coincident branes are in the adjoint representation of the $U(N)$ gauge group. The spectrum of strings is given by the dimensional reduction of an $\mathcal{N} = 1$ gauge multiplet in ten dimensions to four dimensions:

$$\begin{array}{c} \begin{pmatrix} A^\mu \\ \psi \end{pmatrix} \\ D = 10, \mathcal{N} = 1 \end{array} \quad \rightarrow \quad \begin{array}{c} \begin{pmatrix} A^\mu \\ \psi \end{pmatrix} \begin{pmatrix} \psi \\ \lambda \end{pmatrix} \begin{pmatrix} \psi \\ \lambda \end{pmatrix} \begin{pmatrix} \psi \\ \lambda \end{pmatrix} \\ D = 4, \mathcal{N} = 4 \end{array} \tag{2.1}$$

where A^μ are gauge fields, ψ are gauginos and λ are complex scalars. Six of the ten-dimensional gauge field degrees of freedom become the three complex scalars in the four-dimensional reduction. The ten-dimensional Majorana-Weyl spinor becomes four complex Weyl spinors in four-dimensions. This theory has $\mathcal{N} = 4$ extended supersymmetry. The spinors are in the fundamental of $SU(4)_R$, the scalars are in the **6** and the gauge field is a singlet. The Lagrangian for this $\mathcal{N} = 4$ supersymmetric gauge theory is [18]

$$\begin{aligned} \mathcal{L} &= -\frac{1}{2g_{YM}^2}\mathrm{Tr}\left(F_{\mu\nu}F^{\mu\nu} + 2D_\mu\lambda_i D^\mu\lambda_i - [\lambda_i,\lambda_j]^2\right) \\ &\quad -\frac{i}{g_{YM}^2}\mathrm{Tr}\left(\bar{\psi}\Gamma^\mu D_\mu\psi + i\bar{\psi}\Gamma_i[\lambda_i,\psi]\right) \ . \end{aligned} \tag{2.2}$$

The one-loop β-function for this theory is

$$\beta = \left(\frac{11}{3}N_c - \frac{4}{3}4\frac{N_c}{2} - \frac{3}{3}N_c\right) = 0 \ , \tag{2.3}$$

where the first term comes from the gauge fields, the second from the four gauginos and the third from the three scalar fields. Supersymmetric non-renormalisation theorems [39] can be used to show that there are no additional contributions, and therefore the theory has zero β-function in the full quantum theory [40]. A theory where all fields are massless, and no scale is introduced through dimensional transmutation of a running coupling, is a conformal field theory [41].

2.2 The Correspondence

The AdS/CFT correspondence states that the open string theory living on a stack of D3-branes is dual to the closed string theory living in the space warped by these branes [24, 25, 26]. The theory in the ten-dimensional background can

be divided into three parts: a near-horizon geometry, a flat-space geometry and an interaction between the two. In the small $g_s\alpha'$, low-energy limit the interaction term disappears. In the large N limit, the space deformed by the branes becomes $AdS_5 \times S^5$. As $\alpha' \to 0$ and $N \to \infty$ the closed string theory becomes classical supergravity. As this limit is taken, the open string theory on the branes is described by the large, constant $\lambda = g_{YM}^2 N = g_s N$, infinite N, $SU(N)$ $\mathcal{N} = 4$ gauge theory. The conjecture states that the classical supergravity theory, in which calculations are simple, is dual to a strongly-coupled gauge theory, where calculations are often intractable. Conversely, at weak coupling on the field theory side, the closed string theory is strongly-coupled. This strong-weak coupling duality allows full control of one side at a time.

The equivalence is given by an equality in the actions:

$$S_{\text{Open strings on D3-branes}} = S_{\text{Closed strings in } AdS_5 \times S^5}$$

$$\text{Strongly coupled } \mathcal{N} \simeq 4 \text{ Super Yang-Mills} = \text{Classical supergravity on } AdS_5 \times S^5$$

A diagrammatic sketch of the duality is illustrated in figure 2.1.

This duality is remarkable because, while the left hand side is a four-dimensional field theory, the right hand side is a ten-dimensional supergravity theory. This type of duality is known as a holographic correspondence and was first conjectured for black-holes with the statement that the entropy of a black-hole is given by its area [42, 43, 44]. This means that all the information enclosed inside the black-hole is encoded in a lower-dimensional surface. The conjecture of the AdS/CFT correspondence states that the information in a ten-dimensional theory of gravity

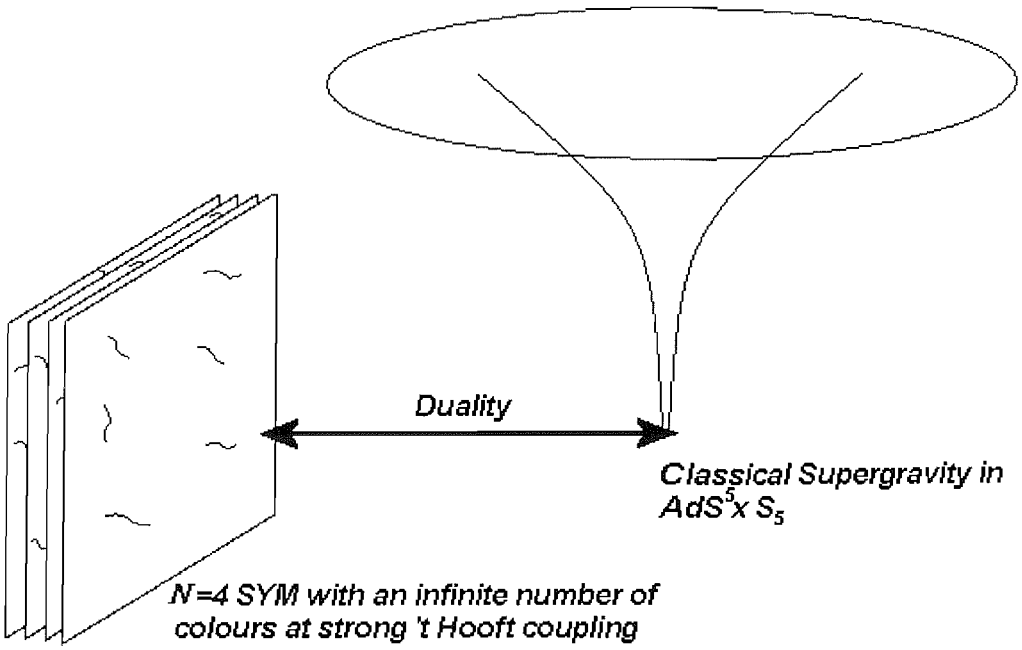

Figure 2.1: The AdS/CFT correspondence is a duality between a theory of open strings living on a stack of D3-branes, and the supergravity theory living in the singular region of the geometry sourced by the D3-branes.

can be encoded in a four-dimensional field theory.

2.2.1 Global Symmetry Matching

The AdS/CFT duality was first established [24] by studying the symmetries of the two sides of the correspondence. The supergravity side is formulated in a space which has the isometry group $SO(4,2) \times SO(6)$ corresponding to $\mathrm{AdS}_5 \times \mathrm{S}^5$. On the field theory side, the global symmetry group is $SO(4,2) \times SU(4)_R$ which is locally the same as the isometry group on the supergravity side. These symmetries correspond to the conformal group and the R-symmetry group. The number of

supercharges (16) match on both sides of the correspondence.

This correspondence is useful only if there is a concrete means to calculate physical quantities on both sides [26]. The equivalence is established through the equality of the actions and is the fundamental equation describing the AdS/CFT correspondence:

$$\boxed{< e^{\int d^4x \phi_0(x)\mathcal{O}(x)} >_{CFT} = \mathcal{Z}_{string}\left[\phi(x,r)|_{r=\infty} = \phi_0(x)\right]} \tag{2.4}$$

where x runs over the four directions parallel to the branes and r is in the radial direction of the $AdS_5 \times S^5$ space. This means that the generating functional for correlation functions with a source, $\phi_0(x)$, for an operator, $\mathcal{O}$, is equal to the supergravity partition function, with boundary condition that the supergravity field, ϕ, at $r = \infty$, is equal to the source for the field theory operator.

More simply, this means that boundary values for supergravity fields correspond to sources for field theory operators. In order to find which supergravity field corresponds to each field theory operator, it is necessary to find a combination (including the d^4x in the action) that is a singlet under all the symmetries of the theory. For instance, the source for an operator charged in the 4 of $SU(4)_R$ must be in the $\bar{4}$ of the $SO(6)$ isometry group.

2.2.2 Energy-Radius Duality

The field theory side of the duality has a conformal symmetry. It is important to understand what this conformal scaling corresponds to on the supergravity side. [18]. One of the generators of the conformal group is the dilatation operator which rescales dimensionful quantities. This means that, in the field theory, there is the

freedom to rescale distances and fields with the action remaining unchanged:

$$x \to \beta x, \qquad \lambda \to \frac{\lambda}{\beta} \,. \tag{2.5}$$

On the supergravity side, the metric is invariant under this scaling if $r \to \frac{r}{\beta}$ as $x \to \beta x$. This means that under the four-dimensional conformal scaling, the distance r transforms like an energy scale. This relationship between energy and radius can be understood from another point of view. For an observer at the boundary of $AdS_5 \times S^5$, a photon emitted from a distance r from the centre of the space is redshifted. The closer to the centre of the space, the larger the redshift and so, for an observer at the boundary, the photon appears to have lower energy as it is emitted from smaller r. The energy-radius duality indicates that, rather than there being a field theory only on the boundary of $AdS_5 \times S^5$, there is a field theory description at all four-dimensional slices, at different values of r, corresponding to field theories at varying energy scales.

Throughout this thesis, the radius of the AdS space is referred to in terms of an energy scale. The small r limit is labelled the IR and the large r limit is labelled the UV as these are the low and high energy limits respectively in the field theory.

2.2.3 Field-Operator Matching

To find the field theory operator corresponding to a specific supergravity field, it is necessary to calculate the equations of motion for the supergravity fields in the $AdS_5 \times S^5$ background, and to study their possible boundary conditions [25].

As an example, the action for a scalar field, ϕ, of mass m in the $AdS_5 \times S^5$

background is given by

$$S_{scalar} = \int d^{10}\zeta \sqrt{-|g|} \left((\partial_\zeta \phi)^2 + m^2 \phi^2 \right) . \tag{2.6}$$

The simplest solution to ϕ for this action has dependence only on the radial direction in $AdS_5 \times S^5$. This solution is

$$\phi = A r^{-(4-\Delta)} + B r^{-\Delta} , \tag{2.7}$$

where $\Delta = 2 \pm \sqrt{4 + m^2}$. For a scalar field with $m^2 = 0$, $\Delta = 4$ or 0, so the solution is $\phi = A + \frac{B}{r^4}$. Because supergravity fields do not scale under the four-dimensional conformal scaling, the parameter A must have conformal mass dimension zero, and the parameter B must have conformal mass dimension four. If the boundary value of the supergravity field is to act as the source for an operator, its symmetries must be understood. The supergravity field is a scalar under the $SO(6)$ isometry group which corresponds to the $SU(4)_R$ symmetry group of the field theory. This means that the operator corresponding to this field must also be a scalar under this symmetry. The field is a space-time scalar and so has no indices to contract with anything other than a scalar operator. The parameter A is of scaling dimension zero and therefore must be the source for a mass dimension four operator which can only be $\mathrm{Tr}\, F^2$. The parameter B is of scaling dimension four and corresponds to the vacuum expectation value (vev) of this gauge field operator: $< \mathrm{Tr}\, F^2 >$. For this particular supergravity field its dual field theory operator has been identified. Remarkably, there is a one-to-one correspondence between fields and operators which has been proved explicitly for the infinite set of operators and the infinite tower of Kaluza-Klein states on the five-sphere [45].

2.2.4 Generalising the Correspondence

The explicit correspondence between a supergravity theory and a field theory has now been introduced. This allows for the calculation of gauge theory quantities, even in the strong coupling regime. This ability is extremely important; however, in the form introduced so far, the correspondence has some deficiencies which must be discussed. Crucially, the field theory is not very similar to QCD and so does not describe the universe in which we live [46, 47, 48, 49, 50]. The field theory is both conformal and highly supersymmetric, as well as being strongly-coupled in the UV and having an infinite number of colours. The first two problems are addressed in the bulk of this thesis while the problem of the strongly-coupled UV is tackled in chapter 10.

The correspondence provides a recipe by which to turn on any operator in field theory by finding the appropriate supergravity field to act as its source. In the original formulation of the duality, the only couplings that are switched on, are those of the $\mathcal{N} = 4$ Lagrangian (equation 2.1). This corresponds to having a graviton, a constant dilaton and a five-form field strength on the supergravity side. The field theory has two phases: one where the potential is zero, corresponding to the super-conformal phase for which the vevs of all scalars are zero and the other, where at least one of the scalars has a vev (the Coulomb phase). The induction of a vev for M of the scalars generates an $SU(N) \rightarrow SU(N-M) \times U(1)^M$ gauge theory. On the D-brane side, this corresponds to pulling M D-branes from the stack in different directions in the space transverse to their world-volume. The magnitude of the vevs correspond to the distance between the isolated branes

and the remaining stack.

By switching on masses and vevs for operators, the superconformal symmetry can be broken explicitly. The inclusion of any mass scale in the field theory automatically breaks the conformal invariance, while switching on different masses for fields in a supermultiplet breaks the supersymmetry. As indicated in equation 2.4, to turn on these operators, the boundary values for supergravity fields must be set appropriately. The correspondence is explicitly realised only in the region where the supergravity background is $AdS_5 \times S^5$ corresponding to the field theory in its superconformal phase. It is in this regime only that scaling dimensions do not change under renormalisation group flow and so the field-operator matching can be performed.

Though turning on a mass for one of the fields breaks the superconformal invariance, the symmetry is restored in the high energy limit where the mass is negligible compared to the energy scale. By breaking the symmetries on the field theory side, the isometries on the supergravity side that match up through the duality are also broken. Specifically, breaking the conformal symmetry corresponds to warping the AdS_5 section of the geometry, and breaking some of the supersymmetries corresponds to deforming the five-sphere. The act of breaking these symmetries is called a deformation and explicit examples of this procedure are discussed in the following chapters.

Though there are more details which could be discussed on both the structure of superconformal theories [41, 51, 52] and the geometry of $AdS_5 \times S^5$ [26, 53, 32], the topic of this thesis concentrates on theories in which most of the symmetries

are broken in order to obtain theories that closely resemble QCD. For this reason, references to some of the extensive literature on the subject are given without discussion.

2.3 Brane Probing

Brane probing [54, 55, 56, 57] is the most direct technique employed to study the gauge theory dual to a specific supergravity background. In the limit of an infinite number of branes, adding an extra one and studying the theory on its surface does not disturb the background geometry. In the large N limit, adding an extra brane is identical to pulling a single brane from the stack and studying its action in the closed string background. As discussed in section 2.2.4, this corresponds to moving into the Coulomb phase of the field theory. Though the presence of the brane does not alter the metric, the $U(1)$ gauge theory living on its surface has half as many supersymmetries as the background theory without the probe. In the case of undeformed $AdS_5 \times S^5$, the theory on the brane surface is $\mathcal{N} = 2$ supersymmetric. This is because D-branes are Bogomol'nyi-Prassad-Sommerfield (BPS) objects which break half of the supersymmetries.

2.3.1 BPS Conditions

The BPS conditions [58, 32, 19] arise from studying the massive representations of a supersymmetry algebra. The anticommutation relation for the supersymmetry generators in the rest frame, $P^\mu = (M, 0, 0, 0...)$, is

$$\{\mathcal{Q}^a_{\alpha\pm}, (\mathcal{Q}^a_{\beta\pm})^\dagger\} = \delta^a_b \delta^\beta_\alpha (M \pm Z_a) \ , \tag{2.8}$$

where

$$\begin{aligned} \mathcal{Q}^a_{\alpha\pm} &= \frac{1}{2}(Q^{1a}_\alpha \pm \sigma^0_{\alpha\dot{\beta}} \left(Q^{2a}_\beta\right)^\dagger) \ , \\ Z &= diag(\epsilon Z_1, ..., \epsilon Z_r, \#) \ , \\ \epsilon^{12} &= -\epsilon^{21} = 1 \ , \\ \mathcal{N} &= 2r + 1 \ , \\ a &= 1, ..., r \ . \end{aligned} \tag{2.9}$$

Z is the central charge of the supersymmetry algebra and $\#$ is zero for odd $\mathcal{N}$ and absent for even $\mathcal{N}$. For unitary particle representations, the left hand side of equation 2.8 must be greater than or equal to zero. This puts a bound on M in terms of Z of

$$M \geq |Z_a|, \qquad a = 1, ..., r = \left[\frac{\mathcal{N}}{2}\right] \ . \tag{2.10}$$

If this bound is saturated for one of the Z_a, either $\mathcal{Q}^a_{\alpha+}$ or $\mathcal{Q}^a_{\alpha-}$ must vanish and the amount of supersymmetry is reduced. A state which saturates this bound is known as a BPS state, and one for which the bound is saturated for r_0 of the central charges is denoted as a $\frac{1}{2^{r_0}}$ BPS state which has dimension $2^{2(\mathcal{N}-r_0)}$. By studying its tension, and charge under the five-form potential, it can be shown that a D-brane is a half-BPS state and so its presence breaks half of the supersymmetries. This explains why a D-brane probe reduces the supersymmetry from $\mathcal{N} = 4$ to $\mathcal{N} = 2$.

2.3.2 The D-brane Action

There are an infinite number of parametrisations of $AdS_5 \times S^5$. It is possible to calculate the action of a D-brane probe in $AdS_5 \times S^5$, or one of its deformations, and this action defines the $U(1)$ gauge theory living on the brane surface. A general set of $AdS_5 \times S^5$ coordinates will not give the gauge theory in its canonically normalised form. Therefore, the D-brane probe can sometimes be used to find the 'physical' coordinates with which to describe the gauge theory. In order to perform this calculation, the form of a Dp-brane action in a general supergravity background must be understood. The action is given by the following expression, known as the Dirac-Born-Infeld Wess-Zumino (DBI-WZ) action [59, 60]:

$$\begin{aligned} S_{brane} &= -T_p \int d^{p+1}\zeta \mathrm{Tr}\left(e^{-\Phi}\left[det\left(G_{ab}+B_{ab}+2\pi\alpha' F_{ab}\right)\right]^{\frac{1}{2}}\right) \\ &\quad +iT_p \int_{p+1} \mathrm{Tr}\left[exp(2\pi\alpha' F_2 + B_2)\wedge \sum_q C_q\right] , \end{aligned} \tag{2.11}$$

where ζ are the coordinates on the brane, and a and b only run over these coordinates. C_q are the pullbacks of the q-form potentials, F is the gauge field living on the brane, and G and B are the pullbacks of the symmetric and antisymmetric tensors from the bulk to the brane world-volume. The pullback is given by

$$G_{ab} = G_{\mu\nu}\frac{\partial X^\mu}{\partial \zeta^a}\frac{\partial X^\nu}{\partial \zeta^b} . \tag{2.12}$$

The first term in equation 2.11 gives the volume of the brane and is exactly the same as that used to describe the action for a soap bubble in curved space. The perpendicular directions to the brane are described by scalar fields living on the brane world-volume just as the string world-sheet appears to be a scalar field theory on a two-dimensional surface. The second term describes the pullback of

the antisymmetric two-form, which is not switched on for most of the examples in this thesis. The third term describes the $U(1)$ gauge fields living on the brane. The second integral is the topological Wess-Zumino term that gives the interaction of the brane with the other closed string modes. This term is unimportant in the majority of the work that follows.

There is a choice of how to define the directions on the brane with respect to the directions in the bulk space. The static gauge will always be chosen where the space-time directions on the brane coincide with $p+1$ of those in the world volume, in the rest-frame of the brane.

The theory living on a D3-brane probe in $\mathrm{AdS}_5 \times \mathrm{S}^5$ is a $U(1)$, $\mathcal{N}=2$ supersymmetric gauge theory with a single $\mathcal{N}=2$ hypermultiplet. The theory also includes two massive gauge bosons and one scalar vev, corresponding to the open strings stretching between the brane probe and the central stack. This is illustrated in figure 2.2.

When the brane probe is taken to the origin containing the rest of the branes, the theory on the probe returns to the $\mathcal{N}=4$ superconformal phase as the scalar vev returns to zero. Using these probing techniques, it is possible to study the theory living on a stack of branes, provided the number of brane probes is significantly smaller than the number of branes in the stack creating the background geometry. For N_p brane probes, their world-volume theory is an $\mathcal{N}=2$, $U(N_p)$ gauge theory. The fields living on the brane (including those corresponding to the directions perpendicular to its world-volume) become matrix-valued. These matrices are the generators of the $U(N_p)$ gauge group. All fields living on the

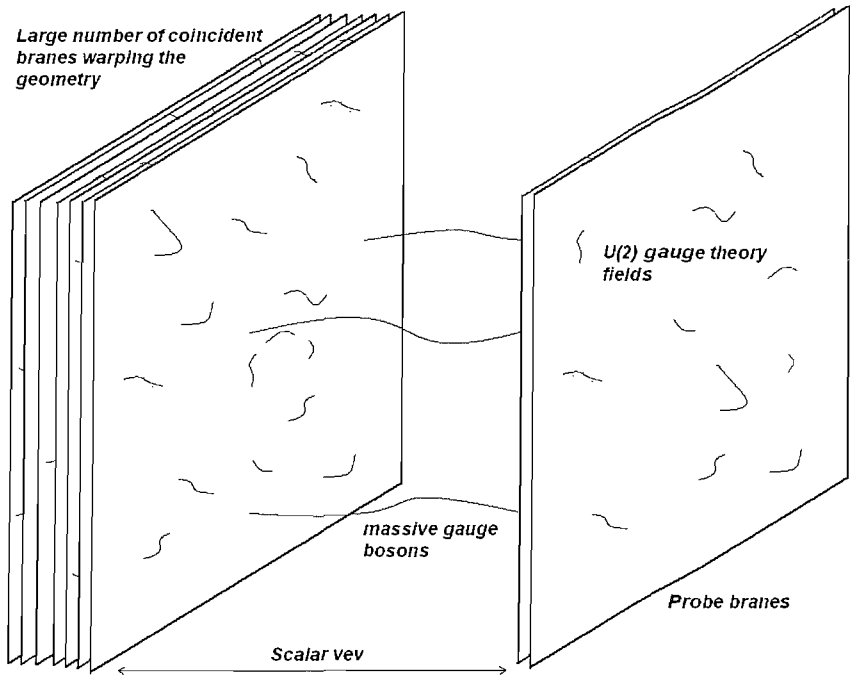

Figure 2.2: A small number of D3-brane probes in a background sourced by a large stack of D3-branes. The theory living on the probes is a $U(N_p)$ gauge theory and the strings stretching between the probes and the centre of the space correspond to massive gauge bosons of the broken $U(N)$ gauge symmetry.

brane stack are charged in the adjoint of the $U(N_p)$ gauge group and are singlets under the colour group associated with the stack of branes distorting the geometry. To make comparisons with the usual gauge theory action, the square root in the DBI action must be expanded. In the non-Abelian case, this expansion is not fully understood to all orders. For this reason, in chapter 5, when a multi-probe action is studied, the highest order terms in the action contain the fourth power of the derivatives, for which a fully consistent DBI action is known.

Chapter 3

Chiral Perturbation Theory

3.1 Introduction

The motivation behind this research is to use the AdS/CFT correspondence to gain some insight into the structure of strongly-coupled gauge theories. String theory originated from the calculation of scattering amplitudes for the strong force. However, it became clear, once QCD was discovered, that this was actually the correct theory to describe the strong force. Experiments have verified this conclusion many times in the past 30 years. The QCD Lagrangian is trivial to write; however, there is still no efficient way to calculate QCD observables when the coupling is strong. Lattice QCD has been very successful and is a vital link between theory and experiment, but it is a resource-intensive process. Any method which can perform the same calculations faster, and also provide further qualitative insight into the properties of QCD in the strong coupling regime, is a valuable tool.

In order to use the AdS/CFT correspondence to explain QCD-like phenomena, it is important to understand the tools used in the current research of low-energy QCD, and how these tie in with experimental measurements. Chiral perturbation theory [61, 62, 63] is an essential tool which deserves some discussion before it is possible to compare lattice calculations with AdS/CFT calculations.

Both experiments and β-function calculations indicate that quarks are confined in QCD. At low energies, and therefore in the strong coupling limit, quarks are clearly not the right variables to describe QCD in a perturbative language. This idea is a familiar one in many areas of science, including biology and chemistry. Moving from small to large distance scales, the degrees of freedom used by a theorist to describe the physical system they are interested in will change. At the Ångstrom scale, physicists are not interested in the dynamics of quarks but use the theory of atoms to describe their experiments. This theory is formulated through experiments at the atomic energy scale and so, though this physics is determined by higher energy processes, the higher energy degrees of freedom have been 'integrated out'. This process of integrating out high-energy behaviour determines the couplings and masses of the theory at lower energy. This is how the pion Lagrangian is constructed. Below the scale at which QCD becomes strongly-coupled, the degrees of freedom are the low-energy observables at that scale. These degrees of freedom are the pions and vector mesons associated with the approximate symmetries to be discussed in section 3.1.1.

3.1.1 Effective Field Theories

It was shown by Steven Weinberg [12] that to construct the most general low-energy Lagrangian as an effective theory [61], it is sufficient for the effective Lagrangian to be local and to incorporate the symmetries of the high-energy completion of the theory. This effective theory is non-renormalisable just as the Fermi interaction is not a renormalisable interaction but is perfectly well-defined up to the mass of the weak interaction gauge bosons.

The first step is to find the symmetries of the underlying theory, by studying the QCD Lagrangian. The quark sector of the QCD Lagrangian is given by

$$\mathcal{L}_{QCD} = \bar{Q}_L \not{D} Q_L + \bar{Q}_R \not{D} Q_R + \bar{Q}_L M Q_R + \bar{Q}_R M^\dagger Q_L \ , \tag{3.1}$$

where Q_L and Q_R are vectors of Weyl fermions. These can be defined in terms of Dirac fermions using the chiral projections:

$$Q_{L,R} = \frac{1 \pm \gamma_5}{2} Q \ , \qquad \bar{Q}_{L,R} = \bar{Q} \frac{1 \pm \gamma_5}{2} \ . \tag{3.2}$$

Considering the generic case of N_f flavours of quark, Q is an N_f-vector of Dirac fermions. If $M = 0$, there is a symmetry that acts on the left and right-handed quarks with different charge as $U(3)_L \times U(3)_R$:

$$Q_{L,R} \to U_{L,R} Q_{L,R} \ , \qquad \bar{Q}_{L,R} \to \bar{Q}_{L,R} U^\dagger_{L,R} \ , \tag{3.3}$$

where $U_{L,R} \in U(N_f)_{L,R}$. In fact, the $U(1)_L - U(1)_R$ (axial) part of this product symmetry group is anomalous. This is broken by instanton contributions associated with the QCD θ-angle. Most of the research in this thesis is concerned with exactly this anomalous part of the symmetry. In the 't Hooft limit (as

$\frac{N_f}{N_c} \to 0$), the anomaly vanishes and the chiral symmetry is restored as a quantum symmetry. This means that the $U(1)_A$ symmetry is a good symmetry in the strongly-coupled theories investigated here. The vector $U(1)$ symmetry is also preserved but simply corresponds to quark number and will not be discussed further.

If an equal mass is introduced for each quark, the product symmetry is broken to the diagonal vector subgroup where the left- and right-handed quarks can still be rotated, but must have the same charge under the rotation group. In this case, the axial subgroup is explicitly broken. When a general set of quark masses is added, the vector symmetry is also broken. The entire $SU(3)_L \times SU(3)_R$ symmetry group can be preserved in the presence of quark masses if the quark mass matrix is interpreted as being a spurion which transforms under

$$M \to U_L M U_R^\dagger \,. \tag{3.4}$$

It is important to understand whether chiral symmetry is a good classical symmetry in QCD. The masses of the u and d quarks can be neglected as they are much smaller than Λ_{QCD}, which is the only other scale in the theory. It is debatable if the s quark mass is significant and this is an important issue in lattice QCD. However, it is of no concern here as, in general, only a single flavour of quark is considered. In this research, a QCD-like theory is studied with N_f quarks, all with $m << \Lambda_{QCD}$. Therefore, classically, the chiral symmetry can be treated as a good approximate symmetry. At low energies, however, strong coupling physics is believed to alter the symmetries of the theory. There are several pieces of evidence to suggest that only some of the classical symmetries remain in the full quantum

theory, the most obvious being the great hierarchy in the QCD spectrum. The pions (Π^-, Π^0, Π^+) and the kaons ($K^\pm, K^0, \bar{K}^0$) are the lightest mesons, with the pions being around four times lighter than the kaons. Most other hadronic states are at least twice the mass of the kaons. As all hadrons are made of the same basic building blocks, it is intriguing that a few of them are substantially lighter than the others.

The second piece of evidence is the absence of a parity-doubled spectrum. If the chiral symmetry were good, there would be a positive parity hadron for every negative parity hadron, which is clearly not the case. The proton is isospin $\frac{1}{2}$, spin $\frac{1}{2}$, positive parity and has a mass of 938Mev, whereas its parity partner has a mass of around 1500Mev.

From this evidence, it appears that chiral symmetry is broken. The simplest way to break this symmetry spontaneously is to induce a condensate for the quark bilinear $\bar{q}q$. Simulations on the lattice support this conjecture and the quark bilinear condensate model is used throughout this thesis.

It is useful to summarise the conjecture of chiral symmetry breaking. In the small quark mass limit, the vacuum breaks the chiral symmetry. This broken symmetry will have associated with it a set of pseudoscalar, pseudo, Goldstone bosons – the pions. The interaction of the mesons with the quark bilinear condensate provides the dynamical mass needed to explain the discrepancy between the constituent quark mass and the hadron spectrum (see figure 3.1).

The following expression defines the coupling between the pions and the axial

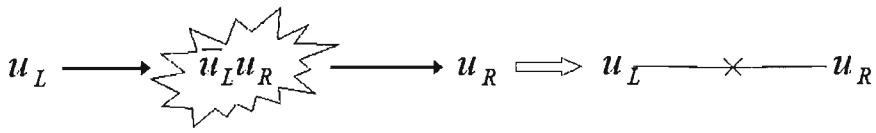

Figure 3.1: Effective mass induced by the interaction of hadrons with the quark condensate.

vector current:

$$< \pi^b(p)|\bar{q}\gamma_\mu\gamma_5 T^a q(0)|0 >= -if_\pi p_\mu \delta^{ba} \ , \tag{3.5}$$

where T^a is a generator of the broken symmetry group and f_π is the pion decay constant. For an $SU(2)$ chiral symmetry, three pions are expected, which consist of only two types of quark.

3.1.2 The Pion Lagrangian

Having found the degrees of freedom and the symmetries of the high energy completion of the pion theory, it should be possible, according to Weinberg, to build a phenomenological effective Lagrangian which respects the remaining unbroken symmetries. It was shown by Vafa and Witten that these symmetries are not broken spontaneously [64]. The most general chiral Lagrangian [62] is given by

$$\begin{aligned}
\mathcal{L}_{lin+quad} &= \frac{f_\pi^2}{4}\mathrm{Tr}\,(D^\mu U D_\mu U^\dagger) + \nu^3 \mathrm{Tr}\,(MU^\dagger + UM^\dagger) \ , \\
\mathcal{L}_{int} &= L_1 \mathrm{Tr}\,(D^\mu U D_\mu U^\dagger)^2 + L_2 \mathrm{Tr}\,((D^\mu U D^\nu U^\dagger)(D_\mu U D_\nu U^\dagger)) + L_3 (D^\mu U D_\mu U^\dagger D^\nu U D_\nu U^\dagger) \\
&\quad + L_4 \mathrm{Tr}\,(D^\mu U D_\mu U^\dagger)\mathrm{Tr}\,(M^\dagger U + MU^\dagger) + L_5 \mathrm{Tr}\,(D^\mu U D_\mu U^\dagger)(M^\dagger U + MU^\dagger) \\
&\quad + L_6 (M^\dagger U + MU^\dagger)^2 + L_7 Tr(M^\dagger U - MU^\dagger) + L_8 \mathrm{Tr}\,(M^\dagger U M^\dagger U + MU^\dagger MU^\dagger) \\
&\quad + iL_9 \mathrm{Tr}\,(F^R_{\mu\nu} D^\mu U D^\nu U^\dagger + F^L_{\mu\nu} D^\mu U D^\nu U^\dagger) + L_{10} \mathrm{Tr}\,(U^\dagger F^R_{\mu\nu} U F^{L\mu\nu}) \\
&\quad + L_{11} \mathrm{Tr}\,(D^2 U D^2 U^\dagger) + L_{12} \mathrm{Tr}\,(M^\dagger D^2 U + M D^2 U^\dagger) \ ,
\end{aligned}$$

(3.6)

where

$$U = e^{\frac{2i\pi^a T^a}{F_\pi}}, \qquad U \to L^\dagger U R \,. \tag{3.7}$$

The final expression indicates that the symmetry is non-linearly realised on the pions. The terms $L_1, ..., L_{12}$ are known as the Gasser-Leutwyler coefficients and are the coupling constants of the pion effective Lagrangian. It is possible to expand the exponential and write a series expansion in the pion fields. For a mass matrix $M = m_q \mathcal{I}_{N_f}$ and a normalisation of the $SU(N_f)$ generators, $\mathrm{Tr}\, T^a T^b = \frac{\delta^{ab}}{2}$, the first terms in the expansion are

$$\mathcal{L} = 2N_f \nu^3 m_q + \frac{1}{2}(\partial^\mu \pi^a)^2 - \frac{4\nu^3 m_q}{2f_\pi^2}(\pi^a)^2 \,. \tag{3.8}$$

From the path-integral formalism of quantum field theory, m_q is a source for the quark bilinear condensate. For every quark flavour there will be a contribution to the total vacuum energy, so as

$$< \bar{q}q >= \frac{1}{\mathcal{Z}} \frac{d\mathcal{Z}}{dm}\bigg|_{m=0} \,, \tag{3.9}$$

the following equality can be made

$$\nu^3 = \frac{1}{2} < \bar{q}q > \,. \tag{3.10}$$

The pion mass and quark mass can be related by studying the term which is quadratic in the pion fields. This is the Gell-Mann-Oakes-Renner relation:

$$m_\pi^2 = \frac{2m_q < \bar{q}q >}{f_\pi^2} \,. \tag{3.11}$$

It is interesting to study this relationship from the dual gravity perspective using AdS/CFT techniques.

3.2 Naive Dimensional Analysis

It is possible to calculate the strength of the non-renormalisable couplings in an effective field theory using a method, formulated in [65, 66], known as naive-dimensional-analysis. This method works for QCD-like theories which may differ in numbers of colours and flavours where, below some scale, chiral symmetry is broken and the theory is given in terms of an effective chiral Lagrangian. The method of calculation is simple and depends on only two parameters: the value of the pion decay constant, f_π, and the value of the strong coupling constant, Λ. The method is given by a straightforward algorithm:

1. Each coupling will have an overall factor of $f_\pi^2\Lambda^2$.

2. Each strongly interacting field (pions for example) comes with a factor of $\frac{1}{f_\pi^2}$.

3. p factors of Λ are included to get the correct dimensions of the coupling.

The pion decay constant can be written in terms of the strong coupling constant and the number of colours:

$$f_\pi^2 \sim \frac{N}{(4\pi)^2}\Lambda \ . \tag{3.12}$$

From this, the order of the other coefficients in the chiral Lagrangian can be calculated. For instance, the Gasser-Leutwyler coefficient L_{11} is given by

$$\begin{aligned} &f_\pi^2\Lambda^2 \mathrm{Tr}\left(\frac{D^2}{\Lambda^2}U\frac{D^2}{\Lambda^2}U^\dagger\right), \\ &L_{11} = \frac{f_\pi^2}{\Lambda^2} \sim \frac{N_c}{4\pi^2} \ . \end{aligned} \tag{3.13}$$

In chapter 5, this value is compared with that calculated using the AdS/CFT correspondence.

Chapter 4

Flavouring the $AdS_5 \times S^5$ Geometry

4.1 Quarks in the AdS/CFT Correspondence

As it stands in chapter 2, the AdS/CFT correspondence has many useful ingredients which allow the study of both supersymmetric and non-supersymmetric, strongly-coupled gauge theories. However, there is one key ingredient missing which will make the gauge theories significantly more like QCD: this is the introduction of quarks [67, 68, 69, 70, 71, 72, 73, 74, 75, 76, 77, 78, 79, 80, 81, 82, 83]. All of the matter discussed in chapter 2 was in the adjoint of the $SU(N_c)$ colour group. This is because both ends of the open strings start on the same type of brane – a D3-brane – and so are indistinguishable. To study quarks it is necessary to introduce a new object which will allow open strings that start on a D3-brane and end on this new object. These strings are labelled in the fundamental of the

colour group, and the fundamental of the group determined by the new objects. These new objects are D7-branes. By probing a background sourced by D3-branes with a D7-brane, the strings stretching between the two are colour-fundamental hypermultiplets. Chapters 4–9 detail the introduction of quarks via D7-brane probes in various supergravity backgrounds. D7-branes, rather than any other higher dimensional object, are introduced due to the number of supersymmetries that they preserve, as well as the local symmetries of the fields living on their world-volume. This is discussed in section 4.1.1.

4.1.1 The D7-Brane Probe

The $AdS_5 \times S^5$ metric can be written in the form

$$ds^2 = \frac{u^2}{R^2} dx_{//}^2 + \frac{R^2}{u^2} \sum_{i=1}^{6} du_i^2 \ , \tag{4.1}$$

which is dual to the large N_c, $\mathcal{N} = 4$ gauge theory at the origin of its moduli-space. A D7-brane probe can be chosen to fill the $x_{//}$ directions and four of the u_i directions. This is illustrated in table 4.1, where the dimensions filled by both the D3- and D7-branes are shown.

	x_0	x_1	x_2	x_3	u_1	u_2	u_3	u_4	u_5	u_6
D3	×	×	×	×	.	.	.	.	.	.
D7	×	×	×	×	×	×	×	×	.	.

Table 4.1: D3- and D7-brane embedding in the $AdS_5 \times S^5$ geometry. Filled dimensions are marked with crosses, those perpendicular to the world-volumes are denoted by a dot.

The configuration is illustrated in figure 4.1 where a stack of N_f D7-brane probes is in a background sourced by a large number of D3-branes.

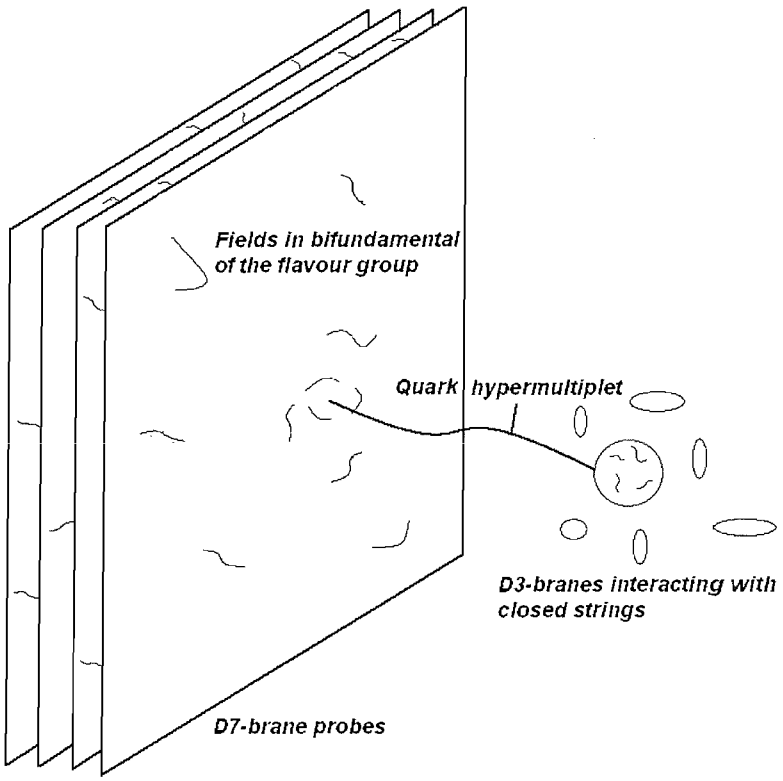

Figure 4.1: D7-brane probes in the presence of a background sourced by D3-branes. The open strings between the two live in a quark hypermultiplet. The open strings on the D7-brane correspond to mesons and their superpartners and the fields living on the D3-brane make up N_c $\mathcal{N} = 4$ hypermultiplets.

Due to the limited number of dimensions of a piece of paper, figure 4.1 is illustrated with only one of the two directions perpendicular to the D7-brane world-volume drawn explicitly. These two directions correspond to scalar fields as discussed in more detail in section 4.2.

The D3-brane has three complex scalars living on its world-volume. The position of the brane, in the six perpendicular directions to its world volume, give the magnitude of the scalar condensates. There is an interaction term between the $\mathcal{N} = 2$ chiral supermultiplet (connecting the D3 and D7-brane stack) and the $\mathcal{N} = 4$ supermultiplet, Λ, living on the brane. When the scalars of the supermultiplet, λ_i, acquire a vev by moving in the perpendicular direction away from the D7-branes, the vev of the scalar associated with the directions u_5 and u_6 ($\lambda_{5,6}$), which is also perpendicular to the D7-brane stack, corresponds to giving a mass to the quarks:

$$\bar{Q}\lambda_{56}Q \rightarrow m\bar{Q}Q \text{ as } \lambda_{56} \text{ acquires a vev.} \tag{4.2}$$

The existence of this interaction is particularly important when the flavour group is extended in section 5.6.

To calculate the number of supersymmetries preserved by a D7-brane in a D3-brane background, the result of a system of Dp and Dp'-branes, where $|p-p'| = 4$, is used [84]. The simplest case is $p = 5$, which preserves $SO(5,1) \times SO(4)$ space-time symmetry. This background preserves eight unbroken supersymmetries which corresponds to a world-volume theory on the D5-brane of a six-dimensional $\mathcal{N} = 1$ field theory. This D-brane setup can be T-dualised twice in two of the spatial directions parallel to the D5-brane, which results in a D3-D7 system. The four-dimensional field theory on the D3-brane has the same number of super-charges as the theory before T-dualising, and therefore this corresponds to an $\mathcal{N} = 2$ field theory. The introduction of a D7-brane has broken half of the supersymmetries of the original D3-brane configuration. This is the same number

of broken supersymmetries as the D3-brane probe off moduli-space. The probe limit of the D7-branes means that, though sources are added for the quarks (see figure 4.1), the probe does not back-react with the metric. This corresponds to the quenched approximation where quark loops are neglected. That is, the D3-branes (and therefore the gauge fields) only feel the presence of the D7-branes through the quark sources and not through higher dimension quark operators (ie. quark loops). This is exactly the same as the quenched approximation in lattice QCD.

Though the $\mathcal{N} = 2$ theory has a β-function proportional to $\frac{N_f}{N_c}$, in the probe limit, the theory is conformal. Therefore, as long as the space being probed is asymptotically $AdS_5 \times S^5$, the fields living on the D7-brane can be understood in exactly the same way as those living on a D3-brane probe.

The fact that a D7-brane is probing a D3-brane background means that there is no charge to stabilise the D7-brane from decay, so it must be stabilised in another way. This is achieved by wrapping the brane on a non-trivial three-cycle in the five-sphere.

The full action for a D7-brane in this background is given by

$$S_{D7} = -T_7 \int d^8\zeta \sqrt{-det(P[G]_{ab} + 2\pi\alpha' F_{ab})} + \frac{(2\pi\alpha')^2}{2} T_7 \int P[C^{(4)}] \wedge F \wedge F \,. \quad (4.3)$$

For now, the field strength of the $U(1)$ gauge field will not be studied (but will be in chapter 5). This means that the action is calculated from the term associated with the pullback of the ten-dimensional metric onto the D7 world-volume. In section 4.2.3, when the gauge-fields are reintroduced, only those gauge fields with no R-charge corresponding to vectors with no indices on the three-sphere will be

of interest. The WZ term vanishes for this case.

4.2 The D7-Brane Embedding

The D7-brane embedding is chosen such that the directions u_5 and u_6 are orthogonal to its world-volume [69]. Throughout this thesis, static gauge is always used in which the space-time directions on the D7-brane coincide with the ten-dimensional space-time directions in its rest-frame. The distance between the D7-brane and the stack of D3-branes, sets a scale and breaks the conformal symmetry of the gauge theory. This distance gives the mass of the lightest string states in the $\mathcal{N} = 2$ hypermultiplets which include the quarks and therefore $m_q \propto L$. As there is a $U(1) \sim SO(2)$ symmetry between u_5 and u_6, there is a freedom to choose a direction in this plane to separate the D7-brane from the D3-brane stack. This $U(1)$ symmetry corresponds to the axial symmetry of a single-flavour QCD model. In QCD, as explained in chapter 3, this symmetry is anomalous. However, in the 't Hooft limit the symmetry is restored. The Goldstone boson associated with this symmetry in QCD is the η'. In the 't Hooft limit, the pions and the η' are degenerate in mass so throughout this thesis, the Goldstone mode for this spontaneously broken symmetry is called a pion.

The excitations of the D7-brane in the directions perpendicular to its world-volume correspond to scalar fields, which are singlets under the colour group and in the adjoint of the flavour group. These states include mesons. There is also a $U(1)$ gauge field living on the brane which will be discussed in chapter 5. As the theory is supersymmetric, there will be other states, including fermions, living on

the brane but these are not explored in this research.

Due to the supersymmetry, a fermion bilinear condensate cannot be induced meaning that, though quarks have been introduced, the chiral symmetry is not expected to be broken as it is in QCD. Non-supersymmetric deformations must be studied to find this phenomenon, which form the bulk of this thesis. However, to understand the D7-brane probe and the dictionary between the fields on the brane and the degrees of freedom of the chiral Lagrangian, the simplest example to start with is the D7-brane probe in an $AdS_5 \times S^5$ background.

Neglecting the gauge field living on the brane, the DBI action for the D7-brane is given by

$$S_{DBI} = -T_7 \int d^8\zeta \frac{\rho^3}{R^3} \sqrt{1 + \left(\frac{\partial u_5}{\partial \rho}^2 + \frac{\partial u_6}{\partial \rho}^2\right) + \frac{R^2}{u^2}\left(\frac{\partial u_5}{\partial x}^2 + \frac{\partial u_6}{\partial x}^2\right)} , \qquad (4.4)$$

where the ten-dimensional metric has been written in the form

$$ds^2 + \frac{u^2}{R^2} dx_{//}^2 + \frac{R^2}{u^2}(d\rho^2 + \rho^2 d\Omega_3^2 + du_5^2 + du_6^2) , \qquad (4.5)$$

where $u^2 = \rho^2 + u_5^2 + u_6^2$. Before examining the x-dependent fluctuations of the scalar fields (corresponding to mesons), it is important to understand how the D7-brane lies in the ρ direction. In the large ρ limit, ρ corresponds to the energy scale of the field theory on the brane. As explained in section 2.2.2, the ρ-dependence of the fields will provide information about the vev and source for the scalar fields. Due to the existence of the $U(1)$ symmetry in the (u_5, u_6) plane, there is a freedom to choose in what direction the D7-brane flows. The D7-brane is chosen to flow away from the D3-branes in the u_5 direction. In this limit, where the x-dependence of the fields is neglected, the square root is expanded

to quadratic order in the scalar fields and the equation of motion for $u_5(\rho)$ is calculated:

$$\partial_\rho \left(\frac{\rho^3 \partial_\rho u_5}{\sqrt{1+\partial_\rho u_5^2}} \right) = 0 \ . \tag{4.6}$$

At the boundary of the AdS space where $u = \infty$, this equation has solution

$$u_5 = m + \frac{c}{\rho^2} \ . \tag{4.7}$$

As u_5 has conformal dimensions of a mass in the four-dimensional field theory, the parameter m corresponds to a mass for the $\bar{q}q$ operator and the parameter c (which has mass dimension three) corresponds to the vev for the $\bar{q}q$ corresponding to the quark bilinear operator.

4.2.1 Stable Brane Flow Calculation

For a given mass, it can now be investigated whether there is a particular value of the condensate which gives a consistent field theory. For a consistent field theory, the D7-brane must be well-behaved throughout its flow. The field theory of interest must have a unique description at a given energy, meaning that as the D7-brane flows in the ρ direction from ∞, the sum $u_5^2 + \rho^2$ must decrease monotonically. There is also a symmetry of the metric given by $\rho \to -\rho$. A brane configuration with a kink will have an infinite contribution to the action. This means that the well-behaved solutions must be configurations that have $\partial_\rho u_5|_{\rho=0} = 0$ and $u_5|_{\rho=0} \neq \pm\infty$. Figure 4.2.1 shows three flows for $m = 1$ with $c = -1, 0$ and 1.

For any mass, a non-zero condensate makes the flow unstable. As expected for a supersymmetric theory, a condensate is not allowed to form. In this case,

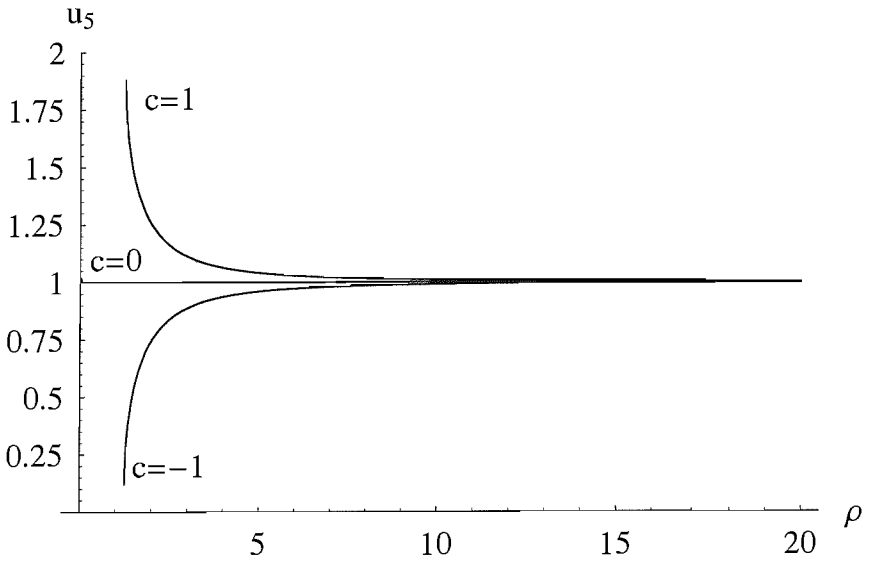

Figure 4.2: D7-Brane flows for $m = 1$ with several initial conditions for the condensate value in an $AdS_5 \times S^5$ background. Only the $c = 0$ solution defines a consistent theory.

the fact that a condensate cannot form can be shown analytically from equation 4.2. The full solution to this equation is known for all values of ρ and is given by

$$u_5(\rho) = A \cdot i \cdot hypergeom\left[\frac{1}{6}, \frac{1}{2}, \frac{7}{6}, \rho^6\right] + B \ . \tag{4.8}$$

This function is complex unless $A = 0$, meaning that only a constant value of u_5 is well-behaved. This agrees with the numerical analysis shown in figure 4.2.1.

The symmetries of the system can now be studied. Before the D7-brane was placed in the background, there was a $U(1)$ symmetry in the (u_5, u_6) plane. There was a choice of where to start the flow in the UV. If the flow starts at $u_5 = u_6 = 0$, because no condensate is allowed, and from the numerical analysis, this flow will remain at $u_5 = u_6 = 0$ all the way into the IR. This situation preserves the $U(1)$ symmetry from the UV to the IR of the theory and corresponds to a theory with

massless quarks. Starting the flow in the UV at a non-zero value in the (u_5, u_6) plane, corresponds to a non-zero quark mass which explicitly breaks the $U(1)$ symmetry. The aim of this thesis is to find backgrounds where this symmetry is broken dynamically by a condensate, even in the limit that there is no quark mass

4.2.2 Meson Mass Spectrum

The next step is to calculate the spectrum of mesons in this background [69]. Mesons correspond to x-dependent fluctuations of the fields u_5 and u_6 on the D7-brane world-volume. To find the meson spectrum, the mesons are treated as small fluctuations on the brane surface, meaning that the DBI action can be expanded to quadratic order giving no interactions between meson fields. Because of this, the mesons can be treated as freely moving plane-waves which will allow their spectrum to be calculated. In this case, the ρ-dependent flow of the brane (u_5) is a constant, so the following field redefinition is possible

$$u_5 = m + \chi(x, r), \qquad u_6 = \phi(x, r) \ , \tag{4.9}$$

where the $U(1)$ freedom has been utilised to choose the ρ-dependent flow to be the u_5 direction. The induced metric on the D7-brane can be written as

$$ds^2 = \frac{\rho^2 + L^2}{R^2} dx_{//}^2 + \frac{R^2}{\rho^2 + L^2} d\rho^2 + \frac{R^2 \rho^2}{\rho^2 + L^2} d\Omega_3^2 \ , \tag{4.10}$$

where $\rho^2 = u^2 - L^2$. L and m are used interchangeably here; there is a constant of proportionality between the two, though for this study of the qualitative behaviour this is unimportant. Then the Lagrangian for the fields χ and ϕ is given

by

$$\mathcal{L} = -T_7\sqrt{-detG_{ab}}\left(1 + 2(R\pi\alpha')^2\frac{g^{cd}}{\rho^2+L^2}(\partial_c\chi\partial_d\chi + \partial_c\phi\partial_d\phi)\right) . \qquad (4.11)$$

The equations of motion for ϕ and χ are identical, so these fields are generically labelled Φ whose equation of motion is

$$\frac{R^4}{(\rho^2+L^2)^2}\partial^\mu\partial_\mu\Phi + \frac{1}{\rho^3}\partial_\rho(\rho^3\partial_\rho\Phi) = 0 . \qquad (4.12)$$

This equation differs from that in [69] where R-charged fields, which are ignored here, were considered. The non-interacting, plane-wave assumption for the x-dependence of the mesons is given by

$$\Phi = f(\rho)e^{ik.x} , \qquad (4.13)$$

where $k^2 = -M^2$. Again, only those solutions which are normalisable correspond to consistent field theories. M^2 (equivalently k^2) is tuned to find the well-behaved field solutions. Equation 4.12 has a UV asymptotic solution, given by

$$f(\rho) = a + \frac{b}{\rho^2} . \qquad (4.14)$$

The field $\bar{q}q$ has conformal scaling dimension three in the UV, therefore, because Φ has scaling dimension one, the parameter b has the correct dimensions to correspond to the $\bar{q}q$ operator. It is possible to solve the above equation exactly in terms of Legendre polynomials to find the meson spectrum. However, this analytic luxury will not be available in the more complicated geometries so numerical calculations are performed at this stage in order to compare to the analytic solutions found in [69]. To find the numerical solutions, a shooting technique is used. A trial mass is used in equation 4.12 which is then solved numerically with the

correct UV boundary conditions for $f(\rho)$ ($a = 0$) and the IR behaviour is studied (note that the value of b drops out of the equation of motion). If the solution is not well-behaved in the IR, the value of M^2 is altered slightly and the process is performed again. M^2 is tuned through a range of values. Those values which produce well-behaved flows give the mass spectrum. Instead of shooting one trial mass after another, there is a simple algorithm for finding this spectrum:

- Define the equation of motion for the field $f(\rho)$ in terms of an undetermined parameter M.

$$eq1 = \frac{R^4 M^2}{(\rho^2 + L^2)^2} f(\rho) = \frac{1}{\rho^3} \partial_\rho (\rho^3 \partial_\rho f(\rho)) \ . \tag{4.15}$$

- Define a function which numerically solves the equation of motion for the field with the correct UV boundary conditions.

$$func(\rho, M) = solve \left\{ eq1|_{f(\infty)=\frac{1}{\rho^2}} \right\} \ . \tag{4.16}$$

- Define a new function

$$g(M) = sign \left\{ \partial_\rho func(\rho, M)|_{\rho=\rho_{IR}} \right\} \ , \tag{4.17}$$

  and plot this as a function of M.

- The values of M in this plot where the value changes from $+1$ to -1 define the most stable flows (those which don't asymptote to $\pm\infty$) and therefore give the meson mass spectrum.

Figure 4.3 illustrates the output for this spectrum calculation. This example is given for $L = R = 1$.

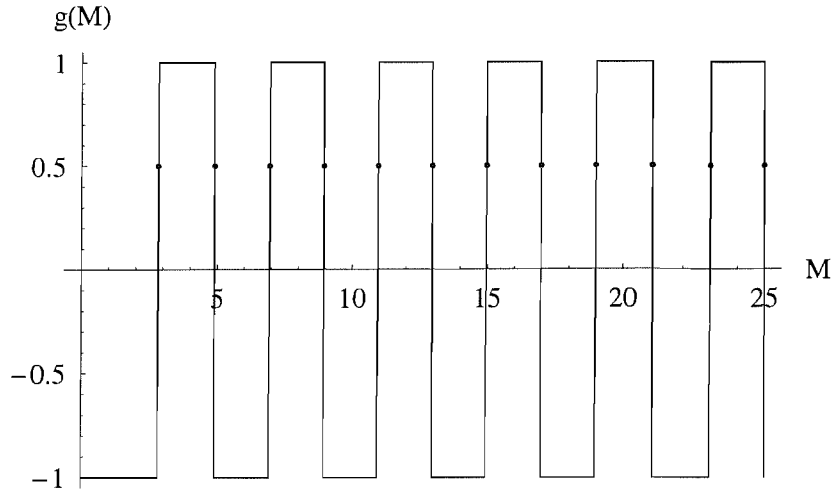

Figure 4.3: Calculation of the meson spectrum for $L = 1$ (and $R = 1$) in the AdS background. The dots indicate the spectrum from the analytic calculation.

The numerical eigenvalues in figure 4.3 agree to a very high accuracy with the analytic solution for the R-chargeless meson spectrum, given by

$$M(n) = \frac{2L}{R^2}\sqrt{(n+1)(n+2)}\,. \tag{4.18}$$

This is an important result which means that the numerical analysis which gives the same answer as the analytical result can be used in more complicated geometries where exact results will not be available.

As the quark mass (given by L) is reduced, the meson spectrum gets closer and closer to zero. In the numerical studies as well as the above analytic result, a massless meson spectrum is found in the massless quark limit.

In this case, their is no potential felt by the D7-brane. For this reason, the meson spectrum associated with the u_5 and u_6 fields coincide. This will not be the case when there is a potential felt by the fields living on the brane.

One important point to note here is that the meson mass is proportional to the quark mass. This relationship is expected to change in theories where chiral symmetry breaking is dynamically induced.

4.2.3 Vector Meson Spectrum

Now, the $U(N_f)$ gauge field living on the D7-brane is reintroduced in the DBI action. By including only the background x-independent values for the u_5 directions, the spectrum for the vector mesons can be calculated in exactly the same way as the pseudo-scalar meson spectrum by giving an ansatz for the gauge field potential of the form

$$A^\mu = g(\rho)e^{ik.x}e^\mu \ , \tag{4.19}$$

where e^μ is a unit vector in the $x_{//}$ directions and $g(\rho)$ is a function to be determined using the equations of motion. For this ansatz, the vector mesons have exactly the same spectrum as the pseudo-scalar mesons. Again, this is not surprising as they live in an $\mathcal{N} = 2$ hypermultiplet so are expected to have the same mass. In the non-supersymmetric theories studied from chapter 5 onwards, this degeneracy is not expected.

4.2.4 The Signatures of Chiral Symmetry Breaking

At this point, it is constructive to postulate what sort of behaviour is likely in a theory which does exhibit chiral symmetry breaking. The aim is to find a theory with a $U(1)$ symmetry in the UV which is broken dynamically in the IR. To have a theory with this $U(1)$ symmetry in the UV, the quarks must be in their massless

limit. It will then be necessary to have a potential which forces the brane out from the origin of the (u_5, u_6) plane to break the $U(1)$ symmetry dynamically. Because of the original symmetry, there should be a freedom in choosing which direction to break the $U(1)$. This dynamical symmetry breaking will be associated with a $\bar{q}q$ condensate. An understanding of the Higgs mechanism indicates that there will be light modes associated with oscillations in the flat directions orthogonal to the condensate. These modes will be the Goldstone bosons of the spontaneously broken symmetry. It will be interesting to calculate the relationship between the meson mass and quark mass in the massless limit. It has been shown in this chapter that in the case where there is no chiral symmetry breaking, there is a linear relationship between the quark and meson mass. This is in contrast to the relationship predicted by the effective action of a theory with chiral symmetry breaking which predicts a quadratic relationship (equation 3.11).

Chapter 5

The Constable-Myers geometry

In Chapter 4, quarks were introduced into the field theory dual to the $AdS_5 \times S^5$ background by embedding D7-brane probes. This simple example has provided some insight into the techniques that are essential for this chapter, where quarks are introduced to a more realistic field theory. Before adding quarks to this non-supersymmetric, non-conformal field theory, the background geometry and the field theory in the absence of quarks are studied.

5.1 The Background

The Constable-Myers dilaton flow geometry, first studied in [85], is a consistent solution to the type IIB supergravity equations of motion. Similar geometries have been studied in [86, 87]. Though it has a naked singularity, its analytic form and asymptotic behaviour, as well as its non-supersymmetric nature, make it an ideal candidate to use for studying chiral symmetry breaking in its field theory dual. The solution is asymptotically $AdS_5 \times S^5$ in the UV limit and has a non-

trivial profile for the dilaton and five-form field strength. The set of solutions are parameterised by a single dimensionful parameter b which characterises the size of the singularity. The background in the Einstein frame is given by the metric

$$ds^2 = \frac{1}{\sqrt{H}}\left(\frac{\omega^4+b^4}{\omega^4-b^4}\right)^{\frac{\delta}{4}} dx_4^2 + \sqrt{H}\left(\frac{\omega^4+b^4}{\omega^4-b^4}\right)^{\frac{2-\delta}{4}} \frac{\omega^4-b^4}{\omega^4} \sum_{i=1}^{6} d\omega_i^2 \ , \qquad (5.1)$$

where

$$\begin{aligned} H &= \left(\frac{\omega^4+b^4}{\omega^4-b^4}\right)^{\delta} - 1, \\ e^{2\phi} &= e^{2\phi_0}\left(\frac{\omega^4+b^4}{\omega^4-b^4}\right)^{\Delta}, \\ C_{(4)} &= -\frac{1}{4H} dt \wedge dx \wedge dy \wedge dz \ , \\ \Delta^2+\delta^2 &= 10 \ , \qquad \delta = \frac{R^4}{2b^4} \ . \end{aligned} \qquad (5.2)$$

For future convenience, the flat Euclidean six-plane can be written as

$$\begin{aligned} \sum_{i=1}^{6} d\omega_i^2 &= d\rho^2 + d\omega_5^2 + d\omega_6^2 + \rho^2 d\Omega_3^2 \ , \\ \omega^2 &= \rho^2 + \omega_5^2 + \omega_6^2 \ , \end{aligned} \qquad (5.3)$$

where b is the dimensionful parameter which sets the scale at which the supersymmetry and conformal symmetry are broken, and R is the radius of the AdS space and five-sphere.

5.1.1 Supersymmetry in the Constable-Myers Geometry

To calculate whether a given background allows any degree of supersymmetry, the Killing spinor equations are studied. From [88], an integrability condition relating the Ricci tensor to the variation of the dilaton indicates when a background is

supersymmetric:

$$R_{mn}(h) = P_m^\star P_n + P_m P_n^\star \ , \tag{5.4}$$

$$P_m = ie^{2i\theta}\frac{\partial_m \tau}{2\tau_2} \ , \tag{5.5}$$

$$\tau = \tau_1 + i\tau_2 = \chi + ie^{-\phi} \ , \tag{5.6}$$

where the metric has been written in the form:

$$ds^2 = e^{2A(x^m)}\eta_{\mu\nu}dx^\mu dx^\nu + e^{2B(x^m)}h_{mn}dx^m dx^n \ , \tag{5.7}$$

and $R_{mn}(h)$ is the Ricci scalar of the metric on the six coordinates perpendicular to the D3-brane stack. In the case of the dilaton flow geometry, there is an undeformed Euclidean six-plane so the relevant metric is

$$h_{mn}dx^m dx^n = d\omega^2 + \omega^2 d\Omega_5^2 \ . \tag{5.8}$$

The Ricci scalar vanishes for this metric. The vector P_m has a single non-zero component given by

$$P_\omega = -e^{2i\theta}\frac{\sqrt{40 - \frac{R^8}{b^8}}\omega^3 b^4}{\omega^8 - b^8} \ . \tag{5.9}$$

So that the right hand side of equation 5.4 is

$$\frac{2\omega^6(40b^8 - R^8)}{(b^8 - \omega^8)^2} \ . \tag{5.10}$$

Clearly, the integrability condition is not satisfied unless $b = \frac{R}{40^{\frac{1}{8}}}$ or $b = 0$, corresponding to the $AdS_5 \times S^5$ limit of this geometry, at which point the dilaton is a constant, and the integrability condition is satisfied trivially.

5.1.2 The Singularity

A black-hole horizon is a region of space-time where the Killing vectors change from time-like to space-like. A vector field defines a flow on a manifold, and

the change of another vector or tensor field as it travels along this flow can be calculated. A Killing vector defines a flow which preserves the metric as it flows on the manifold:

$$\mathcal{L}_X g = 0 \ , \tag{5.11}$$

defining the Lie derivative in the direction of the Killing vector X. The number of Killing vectors provides a measure of the isometries of a space. A d-dimensional, maximally symmetric space, for instance Euclidean flat-space, has $\frac{d(d+1)}{2}$ Killing vectors corresponding to d translations and $\frac{d(d-1)}{2}$ rotations.

It has been shown that, in the dilaton flow geometry, this boundary does not exist for $\omega \geq b$; therefore the singularity is naked. It may be that when stringy corrections are included in the calculation of this geometry, the D3-brane distribution sourcing the background becomes fuzzy and the naked singularity is removed. In the current context, the existence of a naked singularity is unimportant. As discussed in chapter 2, the 't Hooft limit corresponds to a small curvature in the supergravity background. In this case, as ω tends to b the curvature tends to infinity. Assuming all calculations are performed in the region away from the singularity, the supergravity approximation holds. In fact, in the 't Hooft limit, as long as calculations are not performed on the singularity, the radius of the space can be scaled (by increasing R) such that the region of interest is sufficiently far from the singularity to be flat compared to the string scale.

In this background, b is a free parameter, which when varied can give qualitatively different geometries. For instance, for $b < R \cdot 40^{-\frac{1}{8}}$, the dilaton is complex, and appears to correspond to a complex coupling constant on the gauge theory

side. Other values of b are studied in different contexts in the following sections to understand how this affects the physics.

5.1.3 Dilaton Asymptotics in the Constable-Myers Geometry

To understand the gauge theory dual of this geometry, the asymptotics of the dilaton are studied. In the large ρ limit (UV of the field theory), the form of the dilaton is

$$e^{\phi} \sim e^{\phi_0}\left(1+\frac{\sqrt{40b^8-R^8}}{2\rho^4}\right) . \tag{5.12}$$

The coefficient of $\frac{1}{\rho^4}$ has scaling dimension four and is a singlet under the isometries of the five-sphere. The dilaton is a massless, ρ-dependent supergravity field and therefore this term corresponds to the R-singlet operator of dimension four – $< \mathrm{Tr}\, F^2 >$ – and the size of this vev is given by the coefficient of the ρ^4 term. This deformation breaks the supersymmetry from $\mathcal{N}=4$ to $\mathcal{N}=0$ on the gauge theory side. If the relevant operator addition is to be real, the dilaton must be real. The addition of a complex vev would not make sense and so b is always set larger than $R \cdot 40^{-\frac{1}{8}}$.

5.1.4 Confinement and Glueballs in the Constable-Myers Geometry

Before moving on to chiral symmetry breaking in the field theory dual of this supergravity background, it is worthwhile reviewing some of the previous research into this geometry [85] to discover its properties in the absence of quarks.

Confinement in a four-dimensional field theory can be studied by calculating the Nambu-Goto action for a fundamental string in the geometry dual to the field theory. This was first argued in [89] where confinement was studied by calculating the energy of a quark-antiquark pair as a function of their separation. The AdS/CFT correspondence provides a method for calculating expectation values of field theory operators in the large 't Hooft coupling limit. In this case, the operator in question is the Wilson loop, given by

$$W(\mathcal{C}) = \frac{1}{N}\mathrm{Tr}\, P e^{i\int_{\mathcal{C}} A} \ , \tag{5.13}$$

where the integral is taken around a closed loop, $\mathcal{C}$, and A is the gauge field, path ordered by the operator P. The Wilson loop is related to the holonomy of the gauge connection and the operator acts to create a quantum excitation which is localised on the loop. In Euclidean field theory with a square contour, defined with sides of length T and L, it is possible to calculate the energy of a quark-antiquark pair by finding the expectation value of the Wilson loop in the $T \to \infty$ limit. This is given by

$$< W(\mathcal{C}) >= A(L) e^{-TE(L)} \ , \tag{5.14}$$

where $E(L)$ is the energy of a quark-antiquark pair and A is the amplitude for the Wilson loop. It was conjectured by Maldacena that this expectation value is dual to the fundamental string in a supergravity background:

$$< W(\mathcal{C}) > \sim e^{-S} \ , \tag{5.15}$$

where S is the Nambu-Goto action for the string and is equal to the area of the string world-sheet. Therefore, it is possible to calculate the energy of a quark-

antiquark pair by studying the action of a fundamental string. The displacement of the quark and antiquark pair is equal to the length of the string and confinement corresponds to a minimum energy configuration for a finite string length. In pure $AdS_5 \times S^5$, quarks do not confine as the size of their bound-state would set a scale and break the conformal symmetry.

Confinement

In the Constable-Myers geometry, a string at position ω has a minimum action when its length is

$$r_{min}^4 = \frac{2b^4}{\left(\frac{|\Delta|+\delta}{|\Delta|-\delta}\right)^{\frac{1}{\delta}} - 1} \,. \tag{5.16}$$

The action is minimised for finite r_{min} provided, $b > \frac{R}{20^{\frac{1}{8}}}$ [85, 86]. The value of r_{min} tends to infinity as this bound is saturated and, and therefore this bound must be obeyed for confinement to be exhibited in the dual field theory. Note that this bound is stronger than the reality bound for the dilaton discussed in section 5.1.2. It is interesting that, when the above bound is saturated and the string length tends to infinity, the QCD string tension is the same as that for a string in flat, empty space.

Glueballs

The glueball spectrum for this background has also been investigated [85]. The details of this calculation are covered fully in chapter 10. Using the WKB approximation, this background is found to give a discrete glueball spectrum with a mass gap. The WKB approximation is a common method for solving simple

Schrödinger-type potential problems perturbatively. However, in this research, numerical methods are generally relied upon instead.

5.2 Chiral Symmetry Breaking

Having investigated the field theory dual of the Constable-Myers geometry in the absence of fundamental matter, quarks are introduced using the D7-brane techniques developed in chapter 4, in order to study chiral symmetry breaking.

Chiral symmetry breaking was first discovered in the dilaton flow geometry using the AdS/CFT correspondence in [71] and has subsequently been investigated in several other backgrounds [83, 76, 90, 91]. The method is the same as that used in the non-deformed, $AdS_5 \times S^5$ case as studied in chapter 4. A D7-brane is used to probe the geometry to introduce fundamental matter, including quarks, into the field theory. By calculating the world-volume action, a $U(1)$ gauge theory with mesons can be studied. In the case of the Constable-Myers geometry, as the only deformation is a non-constant dilaton and five-form field strength, there is no contribution to the WZ term for the D7-brane world-volume action (unless an R-charged field strength is studied). Just as in the $AdS_5 \times S^5$ case, for the D7-brane to be stable it must wrap a three-cycle. The Constable-Myers background is particularly simple because the five-sphere is undeformed and so there is an undeformed three-cycle to wrap. The D7-brane lies in the Minkowski space-time and the ρ-direction, and wraps the three-sphere. The two directions orthogonal to the brane are parametrised in terms of a complex coordinate, defined as

$$\Phi = \omega_6 + i\omega_5 = \sigma e^{i\theta} \ . \tag{5.17}$$

The dimensions filled by the D7- and D3-brane directions are indicated in table 5.1

	x_0	x_1	x_2	x_3	r	Φ	ω_1	ω_2	ω_3
D3	×	×	×	×	.	.	.	.	.
D7	×	×	×	×	×	.	×	×	×

Table 5.1: D3-brane and D7-brane embedding in the Constable-Myers geometry. Filled dimensions are marked with crosses, those perpendicular to the world-volumes are denoted by a dot.

There are two free dimensionful parameters in the theory: R, the AdS radius, given by $R^2 = \sqrt{4\pi g_s N}\alpha'$, and b which determines the scale of conformal and supersymmetry breaking. At this stage all dimensionful quantities are written in units of R, meaning that $b \to Rb$. The mass scale of the dual gauge theory is then

$$\Lambda_b = \frac{Rb}{2\pi\alpha'} , \tag{5.18}$$

which is the mass of a string with length b. Though it is understood from section 5.1 that changing b alters the properties of the gauge theory, at this point it is set to one, setting the QCD scale. In section 5.8, this constraint will be relaxed and chiral symmetry will be sought for varying values of b.

With this constraint on b and reparametrisation of dimensionful quantities, the metric is

$$ds^2 = \frac{1}{\sqrt{H}}\left(\frac{\omega^4+1}{\omega^4-1}\right)^{\frac{\delta}{4}} dx_4^2 + R^2\sqrt{H}\left(\frac{\omega^4+1}{\omega^4-1}\right)^{\frac{2-\delta}{4}} \frac{\omega^4-1}{\omega^4}\sum_{i=1}^{6} d\omega_i^2 , \tag{5.19}$$

where

$$H = \left(\frac{\omega^4+1}{\omega^4-1}\right)^{\delta} - 1, \qquad e^{2\phi} = e^{2\phi_0}\left(\frac{\omega^4+1}{\omega^4-1}\right)^{\Delta} . \tag{5.20}$$

The Einstein-frame DBI action for the D7-brane is given by

$$S_{D7} = -\frac{1}{(2\pi)^7\alpha'^4 g_s}\int d^8\zeta e^{\phi}\sqrt{-det(P[G_{ab}])} . \tag{5.21}$$

As in chapter 4, $P[G_{ab}]$ is the pullback of the background metric onto the D7-brane world-volume. Though the pullback of the metric is rather complicated, with 28 of the 49 elements being non-zero, the determinant is relatively simple. Most of the cross-terms in the determinant cancel out leaving the following action for the D7-brane

$$\begin{aligned} S_{D7} &= -\frac{1}{(2\pi)^7\alpha'^4 g_s}\int d^8\zeta \left(\frac{\omega^4+b^4}{\omega^4-b^4}\right)^{\frac{\Delta}{2}} \rho^3\left(\frac{\omega^8-b^8}{\omega^8}\right) \\ &\quad \cdot \sqrt{1+(\partial_\rho\omega_5)^2+(\partial_\rho\omega_6)^2+H\left(\frac{\omega^4+b^4}{\omega^4-b^4}\right)^{\frac{4-\delta}{8}}\frac{\omega^4-b^4}{\omega^4}((\partial_x\omega_5)^2+(\partial_x\omega_6)^2)} . \\ &= -\frac{1}{(2\pi)^7\alpha'^4 g_s}\int d^8\zeta \left(\frac{\omega^4+b^4}{\omega^4-b^4}\right)^{\frac{\Delta}{2}} \rho^3\left(\frac{\omega^8-b^8}{\omega^8}\right) \\ &\quad \cdot \sqrt{1+|\partial_\rho\Phi|^2+H\left(\frac{\omega^4+b^4}{\omega^4-b^4}\right)^{\frac{4-\delta}{8}}\frac{\omega^4-b^4}{\omega^4}|\partial_x\Phi|^2} , \end{aligned} \tag{5.22}$$

where

$$\omega^2 = \rho^2 + |\Phi|^2 = \rho^2 + \omega_5^2 + \omega_6^2 . \tag{5.23}$$

5.2.1 Stable Brane Flow Calculation

As in the undeformed geometry in chapter 4, quark fields are introduced by embedding a D7-brane probe. The scalar fields living on the brane correspond to colourless operators in the bifundamental of the flavour gauge symmetry. The first aim of this investigation is to study the mass and condensate of the scalar

fields associated with the directions perpendicular to the brane-probe. The x-dependent excitations of the scalar fields (corresponding to mesons) are small compared to the ρ-dependence, and to first order are not included in the action. Just as in the undeformed geometry, it is important to note the symmetries of the background ten-dimensional space. The translational symmetry of the three directions, ω_5 , ω_6 and ρ, is broken by the singularity. However, there is an $SO(2)$ symmetry between the ω_5 and ω_6 directions. This is broken by the presence of the brane, unless the brane has the solution $\omega_5(\rho) = \omega_6(\rho) = 0$ for all values of ρ. Though this is a solution of the equations of motion, it is not a physical solution as it flows directly into the singularity. An example of the possible symmetry breaking and symmetry preserving solutions are illustrated in figure 5.1

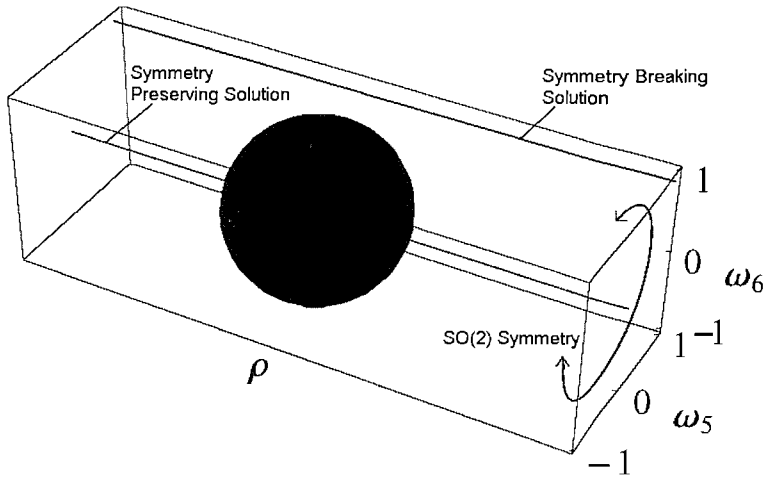

Figure 5.1: Plot illustrating the symmetries of the Constable-Myers geometry. Toy examples of symmetry breaking and symmetry preserving flows are also illustrated.

The equation of motion for the complex field Φ as a function of ρ is given by

$$\begin{aligned}\frac{d}{d\rho}\left(\frac{e^{\phi}G(\rho,|\Phi|)}{\sqrt{1+|\frac{d\Phi}{d\rho}|^2}}\frac{d\Phi}{d\rho}\right) &= \frac{b^4\rho^3\Phi e^{\phi}\left(4b^4-\sqrt{40-\frac{1}{b^8}(\rho^2+|\Phi|^2)}\right)}{(\rho^2+|\Phi|^2)^5}\,, \\ G(\rho,|\Phi|) &= \rho^3\frac{(\rho^2+|\Phi|^2)^4-b^8}{(\rho^2+|\Phi|^2)^4}\,. \end{aligned} \tag{5.24}$$

5.2.2 The UV Scalar Field Boundary Conditions

As the gauge-gravity correspondence is only quantitatively understood when the gravity side is $AdS_5 \times S^5$, the UV limit of this equation of motion, where the space returns to the near-horizon limit, must be studied. It is in this limit that the values of the couplings and vevs for relevant operators can be calculated. In this limit, the equation of motion is given by

$$\frac{d}{d\rho}\left(\rho^3\frac{d\Phi}{d\rho}\right)=0\,. \tag{5.25}$$

As there is an $SO(2)$ symmetry in the background (the (ω_5,ω_6) plane), the phase of the function $\Phi(\rho)$ is a free choice. In this case, the choice is made to flow in the direction of real Φ. Therefore, the solution to the $AdS_5 \times S^5$ equation of motion is

$$\Phi = m + \frac{c}{\rho^2}\,. \tag{5.26}$$

This choice of phase corresponds to a brane solution which flows in the ω_6-direction and remains at $\omega_5 = 0$ throughout the flow. The parameter m, in equation 5.26, is interpreted as a source (dimension one) and parameter c as a condensate (dimension three) for a $\bar{q}q$ operator.

Having calculated the UV boundary behaviour for the scalar fields, the flow of the brane into the IR is investigated. As in the case of $AdS_5 \times S^5$, the solutions

to the equation of motion which describe real physics in the dual field theory are those which are well-behaved in the IR. This is defined by flows which neither fall into the singularity nor asymptote to infinity as the brane flows in. They must also monotonically approach the singularity all along their flow, so that there is a unique field theory for each radial slice corresponding to an energy scale.

For a given value of m, corresponding to the quark mass, a range of values of the condensate are tested to find which one gives a well-behaved brane solution. This involves flowing from the UV to the IR numerically. However, using the symmetry of the background, at $\rho = 0$ the derivative of the scalar field must vanish. The equation of motion with this boundary condition can then be solved to find the flow from the IR to the UV. The value of the mass and condensate for the given IR boundary conditions can be found by calculating the behaviour in the UV asymptotic region.

5.2.3 Numerical Solutions

When these numerical calculations are performed, and the mass and condensate are calculated, there appear to be four quantitatively different types of behaviour. Two of these are shown in the plots in figure 5.2. The other two are mirror images of these plots in the ρ-axis. The upper plot corresponds to solutions with positive mass and positive condensate. Due to the symmetry $\Phi \leftrightarrow -\Phi$ there are also solutions with negative mass and negative condensate. The lower plot shows a set of solutions with positive mass and negative condensate.

From the flows in Figure 5.2 and their mirror images, a graph of the consistent

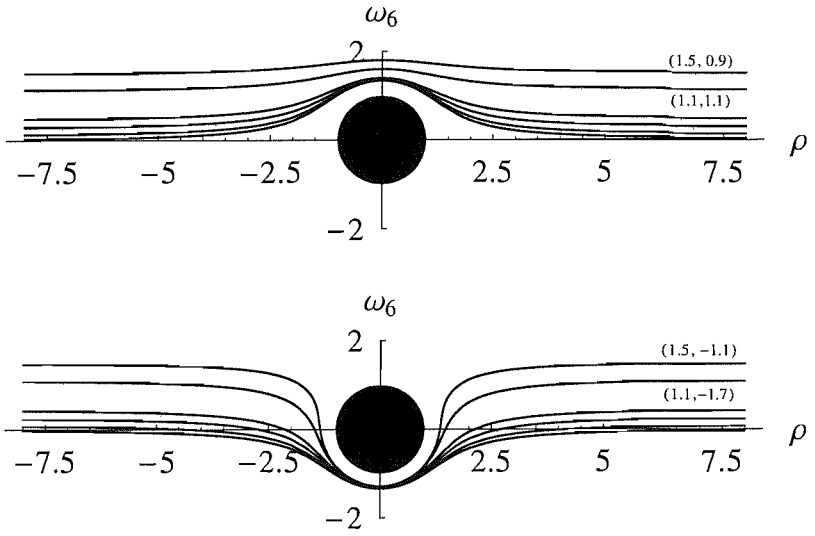

Figure 5.2: D7-brane flows about the spherical singular region. The upper diagram shows those flows with positive condensate and mass while the lower diagram illustrates those with negative condensate and positive mass. For each graph, the values of m and c are annotated in the form (m, c) for the two highest mass solutions.

condensate values against mass is plotted in figure 5.3.

It is worth noting at this point, that the relation between mass and condensate, though not known analytically, is found to be of a logarithmic nature as shown in figure 5.4.

5.2.4 Signatures of Chiral Symmetry Breaking

In the $AdS_5 \times S^5$ case it was found that there was no condensate for any of the stable brane flows. In the case of a D7-brane probe in the Constable-Myers geometry, there is a condensate, and most significantly, there is one for the mass-

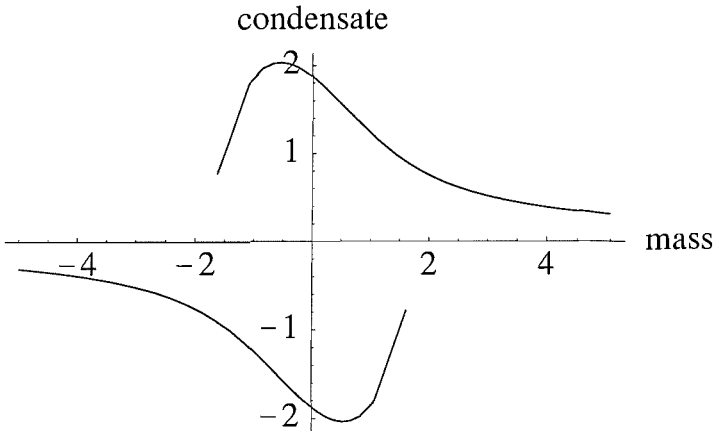

Figure 5.3: Mass plotted against condensate for the consistent solutions to equation 5.24. For $-1.8 \lesssim m \lesssim 1.8$ there are two consistent solutions with opposite sign condensate. The reason for this is discussed in section 5.2.4. The value of the condensate in the massless limit is given by $c = \pm 1.86$.

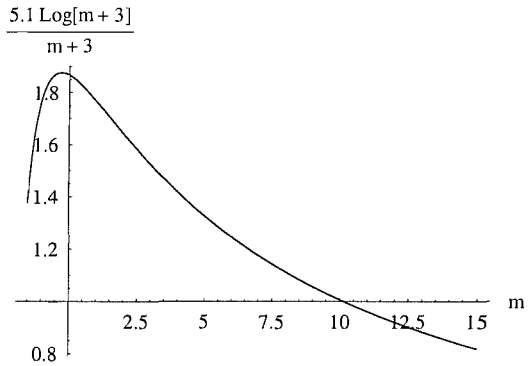

Figure 5.4: Plot approximating the logarithmic behaviour of the condensate as a function of the mass.

less quark limit. This is the first sign of chiral symmetry breaking, discussed in chapter 3. Not only is there a non-zero value for the condensate, the symmetry breaking pattern is exactly as expected. In the UV, there is an $SO(2)$ symmetry (corresponding to a chiral symmetry) in the geometry, which is respected by the

massless quark, D7-brane flow. However, the brane solution breaks this symmetry as it flows into the IR. These are the signatures of chiral symmetry breaking.

In the search for the signatures of chiral symmetry breaking, the next stage is to study the pion mass and compare this with the Gell-Mann-Oakes-Renner relation (equation 3.11) [63]. However, before calculating chiral Lagrangian parameters, it is worthwhile investigating these brane flows a little further.

5.2.5 Unstable Flow Solutions

For a given quark mass (with $-1.8 \lesssim m \lesssim 1.8$) there are apparently two different condensate solutions, but, only one of these is stable. By picturing the brane flow in the $(\rho, \omega_5, \omega_6)$ plane, the two solutions for a given mass can be continuously deformed into one another by pulling the brane around in the (ω_5, ω_6) plane as indicated in figure 5.5.

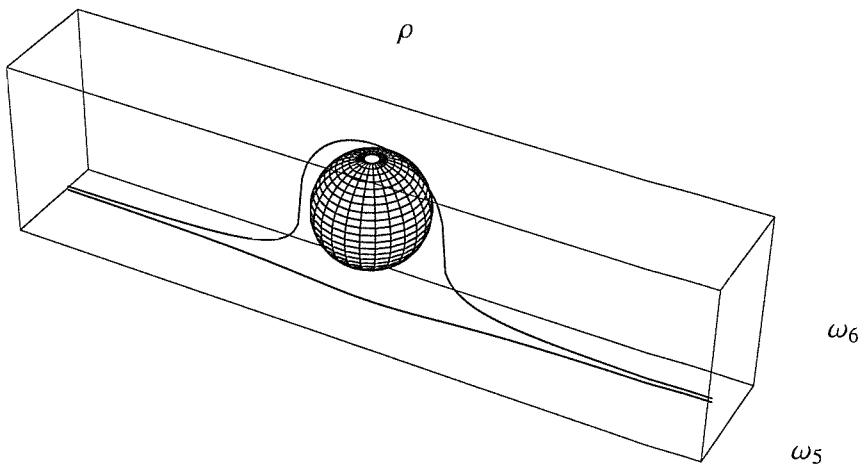

Figure 5.5: Graph showing how the two solutions for a given mass can be continuously deformed into one another.

It is important, however, to understand which of the two solutions is stable. This can be found by calculating the action for each configuration. It is also possible to understand which is stable from the field theory side by looking at a Higgs field breaking an $SO(2)$ symmetry. The two horizontal axes in the Higgs potential (figure 5.6) correspond to the (ω_5, ω_6) plane. The decision is made to break the symmetry in the ω_6 direction. For $m = 0$, this is an arbitrary choice as there is a continuous set of minima, and a maximum corresponding to the solution where the brane flows straight into the singularity. In the case that a mass is added in the ω_6 direction (corresponding to a linear term $m\bar{q}q$ on the Higgs plot) there is a single minimum. However, as the $\omega_5 = 0$ choice is taken, the flows in Figure 5.2 have been projected onto the two-dimensional space where there appears to be a second minimum. This solution is continuously deformable into the true minimum (as seen in figure 5.5) even though, in the two-dimensional plots, this is not explicitly apparent. Therefore, the solutions that have opposite signs for mass and condensate are not stable.

For positive masses, there is a minimum negative condensate solution that exists (~ -1.8 as seen in the lower line in figure 5.3). Figure 5.7 illustrates that the higher the mass, the more the brane stretches as it passes around the other side of the singularity. For a high enough mass, the minimum action for the brane consists of two pieces: one that wraps all the way around the singularity and one that becomes the positive condensate solution for the given mass.

However, this picture is not physical, as explained above. In the full three-dimensional picture, the brane deforms around the singularity when the sign of

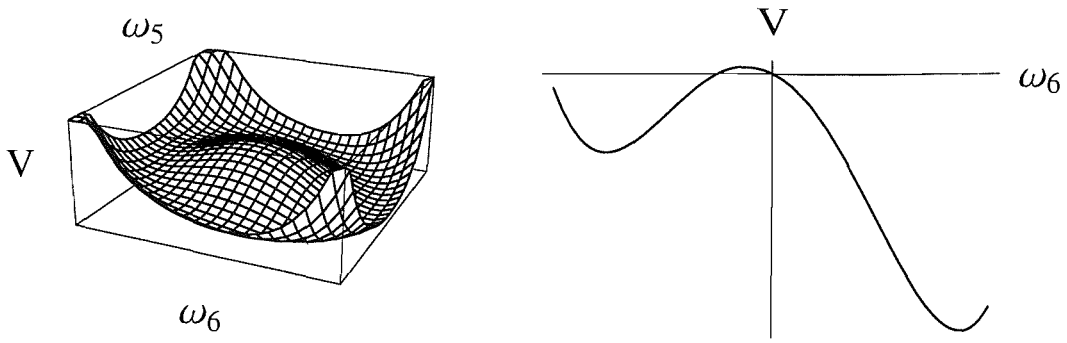

Figure 5.6: Plots illustrating the apparent minimum seen in the solutions to the D7-brane flows. Using a toy Higgs model, a cross-section in two of the field directions appears to give a second minimum in the potential V.

the mass changes.

The value of the condensate in the massless limit in figure 5.3 is given by $c = 1.86$. The massless limit where chiral symmetry is realised is of particular interest in this research.

5.3 Calculating the Vacuum Energy

It is now possible to start calculating the coupling constants of the chiral Lagrangian [61, 62]. Pion fields have yet to been introduced, so at this stage, only the vacuum energy can be calculated. This corresponds to calculating the four-dimensional cosmological constant. Having set $b = 1$, all dimensionful quantities are in units of Λ_b. To compare the DBI action with the chiral Lagrangian, the

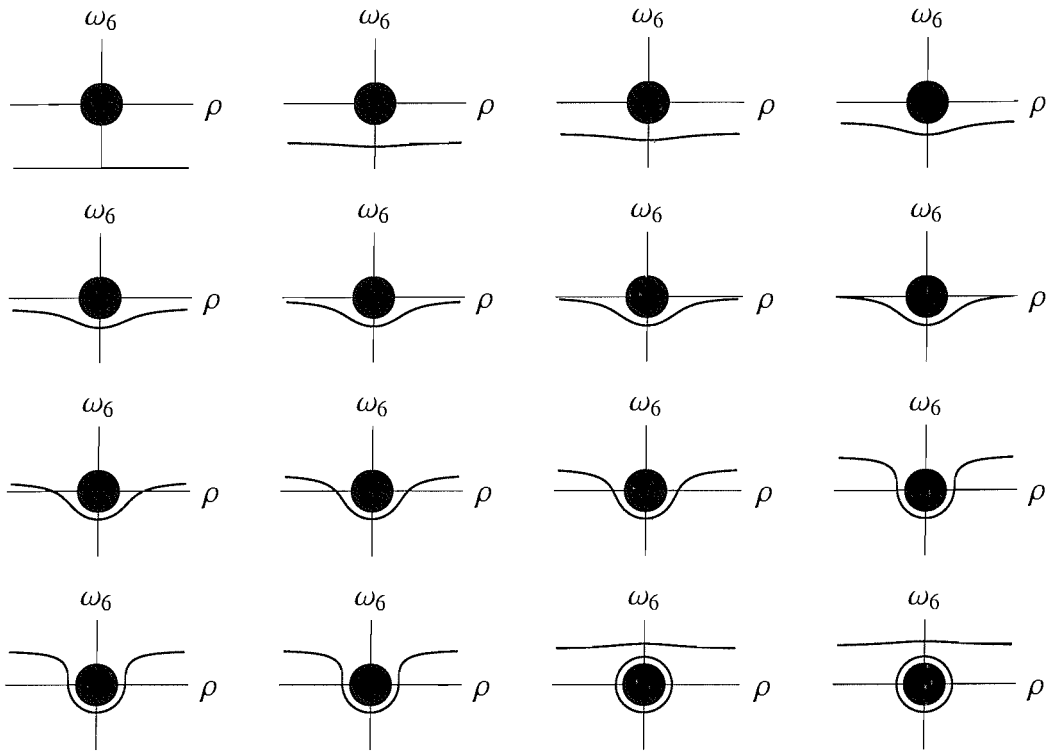

Figure 5.7: Plots illustrating the reason for a minimum negative condensate value for the positive mass.

vacuum energy must be divided by Λ_b. Therefore, the quantity of interest is

$$\frac{\Omega^4}{\Lambda_b^4} = -\frac{R^4}{(2\pi)^7\alpha'^4 g_s}\int d^8\zeta e^{\phi}\mathcal{G}(\rho,\Phi)\sqrt{1+\left(\frac{d\Phi}{d\rho}\right)^2} = \frac{1}{2\pi g_s}\mathcal{I}_0\ , \qquad (5.27)$$

$$\mathcal{I}_0 = -\frac{1}{2}\int d\rho\zeta e^{\phi}\mathcal{G}(\rho,\Phi)\sqrt{1+\left(\frac{d\Phi}{d\rho}\right)^2}\ , \qquad (5.28)$$

where Ω^4 is the four-dimensional cosmological constant and the integral over the three-sphere provides a factor $2\pi^2$. To compare the value of the vacuum term with that in the chiral Lagrangian, the normalisation of the quark fields must be studied. The quark fields in the chiral Lagrangian are canonically normalised, whereas, in the brane analysis they have an extra factor of $\frac{1}{\sqrt{2\pi g_s}}$ that must be

absorbed into the field definitions in order to compare the two. The integral in equation 5.27 is UV divergent, because UV asymptotically, $\Omega^4 \sim \rho_{UV}^4$. This divergence is identical for any D7-brane configuration corresponding to any quark mass and condensate in the theory, due to the quark mass becoming negligible in the UV. The form of the normalised vacuum potential, as a function of the quark mass, is regularised by subtracting the zero quark mass solution for $\frac{\Omega^4}{\Lambda_b^4}$. As equation 5.27 is equal to $-V$, the potential is the negative of this integral. This normalised potential is plotted in figure 5.8, along with the spurious negative condensate solutions corresponding to the unphysical metastable brane flows.

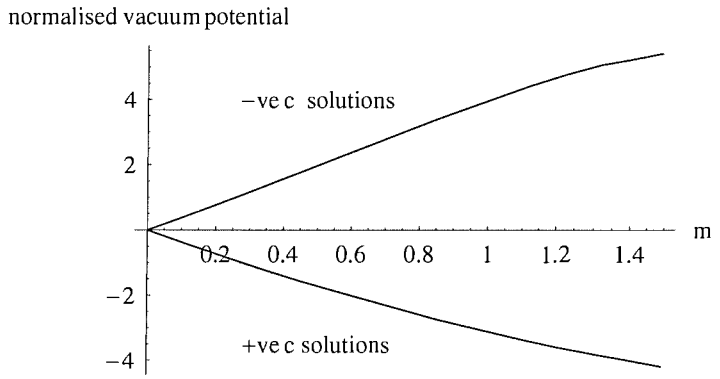

Figure 5.8: Normalised vacuum potential, $V|_m - V|_{m=0}$. The positive condensate solutions are favoured for a positive mass.

This demonstrates that the negative condensate solutions are unstable for a positive mass.

Comparing the D7-brane action with the chiral Lagrangian, the parameter ν^3 from equation 3.1.2 can now be computed. In the single-flavour case, this is

predicted to be

$$\Omega^4 = 2\nu^3 m = < \bar{q}q > m \ . \tag{5.29}$$

Therefore, the gradient of the graph in figure 5.8 provides another way to calculate the value of $< \bar{q}q >$. The numerical value is found to be

$$< \bar{q}q >= 1.86 \ , \tag{5.30}$$

which is the same as the value calculated from the well-behaved brane flows up to the third decimal place. It appears that any deviation in the two answers is likely to be due to numerical inaccuracies. This identification confirms the original prediction that c is indeed the quark bilinear condensate.

5.4 Pions and Their Interactions

Having calculated the vacuum condensate of the quark bilinear operator, the low-energy, dynamical degrees of freedom described by excitations along the moduli-space (in this case lifted by the quark masses), can be studied. At this point, it is most convenient to describe the pions using the circular coordinate system, (σ, θ), of equation 5.17. The decision to have the mass and vev defined in the ω_6 direction (real Φ) corresponds to a vev in the $\theta = 0$ direction. The pions correspond to x-dependent excitations of the θ direction. The pion interactions are treated as negligible so only the quadratic, kinetic and mass terms involving the pion fields are considered. This means that the pions can be treated as plane-waves and the ρ- and x-dependence can be parametrised as

$$\theta(\rho, x) = f(\rho)e^{ik.x} \ . \tag{5.31}$$

To calculate the pion mass, the DBI action is expanded to quadratic order in θ with the background solutions ($\sigma = \sigma_0 = \Phi(\rho)$) calculated for the mass and vev. Again, the three-sphere is integrated over giving a factor of $2\pi^2$:

$$\begin{aligned} S &= \frac{2\pi^2}{(2\pi)^7 \alpha'^4 g_s} \int d\rho d^4x e^{\phi} R^4 \mathcal{G} \sqrt{1 + (\partial_\rho \sigma_0)^2} \\ &\quad \cdot \left[1 + \frac{1}{2(1 + (\partial_\rho \sigma_0)^2)} \left(g^{\rho\rho} g_{\theta\theta} (\partial_\rho \theta)^2 + g^{\mu\nu} g_{\theta\theta} (\partial_\mu \theta)(\partial_\nu \theta) \right) \right] . \end{aligned} \tag{5.32}$$

From this, the equation of motion for θ is calculated. The second derivative with respect to the Minkowski space-time directions gives a factor of $k^2 = -M^2$:

$$\frac{d}{d\rho} \left[\frac{e^{\phi} \mathcal{G}}{\sqrt{1 + (\partial_\rho \sigma_0)^2}} \sigma_0^2 (\partial_\rho f) \right] + \frac{H R^2 M^2 e^{\phi} \mathcal{G}}{\sqrt{1 + (\partial_\rho \sigma_0)^2}} \left(\frac{(\rho^2 + \sigma_0^2)^2 + 1}{(\rho^2 + \sigma_0^2)^2 - 1} \right)^{\frac{1-\delta}{2}} \frac{(\rho^2 + \sigma_0^2)^2 - 1}{\rho^2 + \sigma_0^2} \sigma_0^2 f = 0 . \tag{5.33}$$

Taking the UV limit of this equation of motion, including the UV behaviour of σ_0 gives

$$\frac{d}{d\rho} \left[m^2 \rho^3 \frac{df}{d\rho} \right] = 0 . \tag{5.34}$$

The solution to this equation of motion is $f = A + \frac{B}{\rho^2}$. The x-dependent oscillations correspond to excitations of the $\bar{q}q$ field which has dimension three. As the fields living on the brane correspond to directions perpendicular to the brane surface, f has scaling dimension of an energy. This means that B has scaling dimension three corresponding to the excitations of $\bar{q}q$. If the solution with non-zero A were chosen, this would correspond to x-dependence in the quark mass, which does not describe a QCD-like theory. Therefore the boundary conditions for the field f are given by $f = \frac{B}{\rho^2}$. f should be normalised by scaling B, however, the value of B drops out of the equation of motion, so for this calculation the normalisation is unimportant. The equation of motion is now solved numerically with the above boundary condition for the field θ, and the background flow for

the field σ_0. Those solutions which are well-behaved in the interior are then studied. In this calculation, the tunable parameter is MR. For a given mass and condensate for the quarks there is a discrete spectrum for MR, which produces a well-behaved brane flow. By using a background flow for σ_0 (corresponding to setting the quark mass) the relationship between the meson and quark mass is found (figure 5.9). These results provide a good match to the prediction of the Gell-Mann-Oakes-Renner relation:

$$MR = \kappa\sqrt{m} \ , \tag{5.35}$$

where κ has the numerical value 2.61. Note that the parameter labelled m here is actually $\frac{m_q}{\Lambda_b}$.

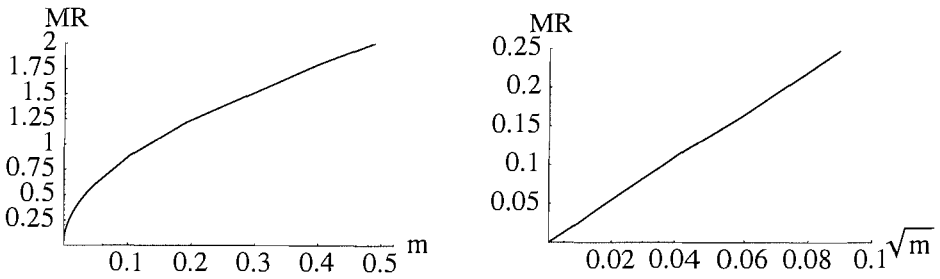

Figure 5.9: Quark mass plotted against pion mass as calculated numerically from D7-brane flows. This shows excellent agreement with the Gell-Mann-Oakes-Renner prediction from the chiral Lagrangian.

Note that the right hand plot in figure 5.9 only extends to $m = 0.1$ but the relationship between quark and meson mass changes for large m. This is exactly as expected. For a brane flow corresponding to a large quark mass, the brane is far away from the deformed region of the geometry and exhibits the same

behaviour as in the $AdS_5 \times S^5$ background. For large m, the quark mass and meson masses are proportional, as expected for a theory with no chiral symmetry breaking. This signals the return of a parity-doubled spectrum and more research is planned on this subject in the near future.

The pion decay constant is calculated using the chiral Lagrangian relationship between the pion mass and quark mass:

$$M_\pi^2 = \frac{4\nu^3 m_q}{f_\pi^2} \ . \tag{5.36}$$

The value of ν^3 has been calculated in equation 5.30 by studying the vacuum energy contribution from the condensate. Equation 5.35, provides a relationship between the meson mass and the quark mass:

$$\begin{aligned} M^2 &= \frac{\kappa^2 m_q}{R^2 \Lambda_b^2} \ , \\ \frac{M^2}{\Lambda_b} &= \frac{\kappa^2 m_q}{\Lambda_b} \frac{4\pi^2 \alpha'^2}{4\pi g_s N \alpha'^2} = \frac{\kappa^2 m_q \pi}{\Lambda_b g_s N} \ , \end{aligned} \tag{5.37}$$

and the vacuum energy given by the chiral Lagrangian and the DBI action are

$$\begin{aligned} \frac{\Omega^4}{\Lambda_b^4} &= \frac{2\nu^3 m_q}{\Lambda_b^4} \text{ (from the chiral Lagrangian)} \\ &= \frac{m_q c}{2\pi g_s \Lambda_b} \text{ (from the DBI action)} \ . \end{aligned} \tag{5.38}$$

Equating these two terms gives a relationship between ν^3 and c

$$\frac{\nu^3}{\Lambda_b^3} = \frac{c}{4\pi g_s} \ . \tag{5.39}$$

Therefore, combining equations 5.36 – 5.39 and using the numerical value of κ

given by the gradient of the MR against $\sqrt{m}$ plot in figure 5.9:

$$\begin{aligned} \frac{4\nu^3 m_q}{f_\pi^2 \Lambda_b^2} &= \frac{\kappa^2 m_q \pi}{\Lambda_b g_s N} , \\ \frac{f_\pi^2}{\Lambda_b^2} &= \frac{Nc}{\pi^2 \kappa^2} \\ &= 0.246 \frac{N}{\pi^2} . \end{aligned} \tag{5.40}$$

This has the expected N-dependence and matches the estimate from naive-dimensional-analysis of section 3.2 [65].

This expression can be compared with the standard model value for the pion decay constant. Using $N = 3$ and $\Lambda \sim 300MeV$, the value of the pion decay constant is found to be

$$f_\pi = 82MeV . \tag{5.41}$$

When compared with the standard model value of $92MeV$, this result is remarkably close and it appears that the difference between this theory and QCD, along with extra $\frac{1}{N}$ corrections, do not make a large difference.

To formulate the action for the pions, the plane wave is replaced with the correctly normalised pion field $2\pi\alpha'\Pi(x)$. The solution $f(\rho)$, used to calculate the mass spectrum, is used so that the function θ is given by

$$\theta = 2\pi\alpha' f(\rho)\Pi(x) . \tag{5.42}$$

Therefore the action for the pion fields up to quadratic order is

$$\mathcal{L} = \frac{R^6}{16\pi^3 \alpha' g_s} \mathcal{I}_1 \left[\frac{1}{2} (\partial^\mu \Pi)^2 - \frac{1}{2} M^2 \Pi^2 \right] , \tag{5.43}$$

where

$$\begin{aligned} \mathcal{I}_1 &= \int d\rho f(\rho)^2 \frac{e^\phi \mathcal{G}}{\sqrt{1 + (\partial_\rho \sigma)^2}} H \left(\frac{(\rho^2 + \sigma_0^2)^2 + 1}{(\rho^2 + \sigma_0^2)^2 - 1} \right)^{\frac{1-\delta}{2}} \frac{(\rho^2 + \sigma_0^2)^2 + 1}{(\rho^2 + \sigma_0^2)^2} \sigma_0^2 \\ &= 0.144 . \end{aligned} \tag{5.44}$$

The pion kinetic term is then canonically normalised to match the chiral Lagrangian.

5.5 Higher Order Interactions

This investigation into models of chiral symmetry breaking aims to compare the DBI action of a D7-brane probe to the phenomenological chiral Lagrangian. So far, the vacuum term and mass term for the pions have been studied, and from this, the value of the condensate and the pion decay constant have been calculated. These appear to be in remarkable agreement with QCD results. The next stage is to study higher order interactions terms, however there are a couple of points to note before continuing.

Firstly, the pions are described by the excitations in the angular direction in the $\bar{q}q$ plane. This statement is exact when the quark mass is zero, but when a finite quark mass is added, excitations in the θ direction will have a component in the direction of the induced condensate (see the left hand plot in figure 5.6). To separate the mixing between the Higgs and the Goldstone modes, the shape of the vacuum manifold, about which the Goldstone modes oscillate, must be understood. This is a complex calculation and may not provide any more insight into chiral dynamics than taking the massless limit where the angular oscillations correspond exactly to the Goldstone modes.

The second point to note is that in the case of a single D7-brane, where the flavour symmetry is Abelian, the Gasser-Leutwyler coefficients cannot be studied separately. While in the non-Abelian case L_1, L_2 and L_3 differ in their

trace structure, the trace over the Abelian group is trivial. In the Abelian case, looking at the quartic pion terms only, the following combination can be studied:

$$L_1 \mathrm{Tr}\,(\partial^\mu U \partial_\mu U^\dagger)^2 + L_2 \mathrm{Tr}\,((\partial^\mu U \partial^\nu U^\dagger)(\partial_\mu U \partial_\nu U^\dagger)) + L_3 \mathrm{Tr}\,(\partial^\mu U \partial_\mu U^\dagger \partial^\nu U \partial_\nu U^\dagger)$$
$$\sim \frac{4(L_1+L_2+L_3)}{f_\pi^4}(\partial_\mu \Pi)^4 = \frac{4L}{f_\pi^4}(\partial_\mu \Pi)^4 \ . \tag{5.45}$$

The same term in the DBI action can now be studied, using the ansatz for θ and looking for the $(\partial_\mu \Pi)^4$ term:

$$\begin{aligned} \mathcal{L} &= \frac{2\pi^2 R^4}{(2\pi)^7 g_s \alpha'^4} \int d\rho e^\phi \mathcal{G} \sqrt{1+(\partial_\rho \sigma_0)^2} \left[-\frac{1}{4} \frac{(g_{\theta\theta} g^{\mu\nu})^2}{1+(\partial_\rho \sigma_0)^2} (\partial_\mu \theta) \right] \\ &= -\frac{R^8}{16\pi g_s} \mathcal{I}_2 (\eta^{\mu\nu} \partial_\mu \Pi \partial_\nu \Pi)^2 \ , \end{aligned} \tag{5.46}$$

where

$$\begin{aligned} \mathcal{I}_2 &= \int d\rho e^\phi \mathcal{G} \frac{f(\rho)^4 \sigma_0^4}{(1+(\partial_\rho \sigma_0)^2)^{\frac{3}{2}}} \left[H^2 \left(\frac{\omega^4+1}{\omega^4-1} \right)^{\frac{1}{2}} \left(\frac{\omega^4-1}{\omega^4} \right)^2 \right] \\ &= 0.0061 \ . \end{aligned} \tag{5.47}$$

Canonically normalising the pion fields and matching the coefficients of the pion interaction terms gives

$$\frac{L}{f_\pi^4} = \frac{16\pi^5 \alpha'^4 g_s}{R^4} \frac{\mathcal{I}_2}{\mathcal{I}_1^2} \ , \tag{5.48}$$

so that

$$L = \frac{(g_{ym}^2 N) N c^2}{\kappa^4 2\pi^4} \frac{\mathcal{I}_2}{\mathcal{I}_1^2} \ , \tag{5.49}$$

where $g_{ym}^2 N$ is a fixed parameter defining the strong coupling of the theory. This can be compared with the naive-dimensional-analysis estimate [65] by using the values of κ and c, along with the numerical values for the integrals which gives

$$\begin{aligned} L_{DBI} &= (g_{ym}^2 N) 0.0001 N \ , \\ L_{NDA} &= 0.006 N \ . \end{aligned} \tag{5.50}$$

These values are equal for a 't Hooft parameter of 60 which seems to be a reasonable strong coupling value.

5.6 Non-Abelian Flavour Symmetry

It would be interesting to promote the axial symmetry from an Abelian to a non-Abelian symmetry by introducing more flavours of quark [92, 93]. Though more quarks can be introduced, the symmetry group cannot be enhanced. In the UV of the field theory, there is a superpotential term $\tilde{Q}AQ$ (see section 4.1) which breaks the extended axial symmetry explicitly, meaning that the addition of more quark flavours does not enhance the axial flavour group. However, the adjoint scalar, A, is expected to have a mass of order Λ and therefore an accidental chiral symmetry is possible. To enhance the D7-brane to a stack of D7-branes, the perpendicular directions to the stack take values in the adjoint of the $U(N_f)$ flavour group:

$$\Phi = \sigma_0 e^{i\Pi^a T^a} \ , \tag{5.51}$$

where T^a are the broken generators of the Lie group. The DBI-Lagrangian of the field for two pions takes the form

$$\begin{aligned} \mathcal{L} \ &= \ \mathcal{A}[(\partial_\mu \Pi_1(x))^2 + (\partial_\mu \Pi_2(x))^2] \\ &\quad + \mathcal{B}[2\Pi_1(x)\Pi_2(x)(\partial_\mu \Pi_1(x)\partial^\mu \Pi_2(x)) - \Pi_1^2(\partial_\mu \Pi_2(x))^2 + \Pi_2^2(\partial_\mu \Pi_1(x))^2] \ , \end{aligned} \tag{5.52}$$

where

$$\begin{aligned}
\mathcal{A} &= \frac{2\pi^2 R^4}{(2\pi^7\alpha'^4 g_s)}(2\pi\alpha' R)^2\mathcal{I}_1 \ , \\
\mathcal{B} &= \frac{2\pi^2 R^4}{(2\pi^7\alpha'^4 g_s)}(2\pi\alpha')^4\mathcal{I}_3 \ , \\
\mathcal{I}_3 &= \int d\rho e^{\phi}\mathcal{G}H\left(\frac{\omega^4+1}{\omega^4-1}\right)^{\frac{1}{4}}\frac{\omega^4-1}{\omega^4}\frac{\sigma_0^2 f^4}{\sqrt{1+(\partial_\rho\sigma_0)^2}} \\
&= 0.0139 \ . \qquad (5.53)
\end{aligned}$$

The equivalent term in the chiral Lagrangian expansion is

$$\begin{aligned}
\mathcal{L}_\chi &= \frac{1}{2}((\partial_\mu\Pi_1(x))^2+(\partial_\mu\Pi_2(x))^2)+\frac{1}{3f_\pi^2}(\Pi_1(x)\Pi_2(x)(\partial_\mu\Pi_1(x)\partial^\mu\Pi_2(x))) \\
&\quad -\frac{1}{6f_\pi^2}(\Pi_1(x)^2(\partial_\mu\Pi_2(x))^2+\Pi_2(x)^2(\partial_\mu\Pi_1(x))^2) \ . \qquad (5.54)
\end{aligned}$$

The pion decay constant can be calculated in exactly the same way as for the Abelian case, and it is found that all the extra numerical factors associated with the non-Abelian nature of this action cancel out, leaving the same answer as the Abelian case. This is unsurprising as the axial flavour symmetry cannot be enhanced by the addition of new quark flavours. However, comparing the interaction terms of the chiral Lagrangian with those in the DBI action with coefficients $\mathcal{B}$ allows for an alternative method by which to calculate the pion decay constant. Again, the kinetic term must be canonically normalised and compared to the chiral Lagrangian parameter which gives the equality

$$\begin{aligned}
\left(\frac{f_\pi}{\Lambda_b}\right)^2 &= \frac{\mathcal{A}^2}{\mathcal{B}}\frac{1}{6\Lambda_b^2} \\
&= \frac{\mathcal{I}_1^2}{\mathcal{I}_3}\frac{N}{6\pi^2} \\
&= 0.246\frac{N}{\pi^2} \ . \qquad (5.55)
\end{aligned}$$

This is exactly the same answer as calculated from the pion quadratic term in both the Abelian and the non-Abelian cases. This calculation is important because the integrals being evaluated are non-trivial, meaning that the numerical results which are obtained may not be trustworthy; however, having obtained the same result twice with two separate sets of integrals is confirmation that the numerics are reliable.

5.7 Vector Mesons and Weakly Gauged Chiral Symmetries

There is a further bosonic field in the low-energy DBI action for the D7-brane – the gauge field partner of the scalar Φ. The field strength, F_{ab}, for this field, enters the DBI action in the form

$$S_{DBI} = -T_7 \int d^8\zeta e^{\phi} \sqrt{-det(P|G_{ab}| + 2\pi\alpha' P|F_{ab}|)} \ . \tag{5.56}$$

The parameter α' is small, so the results of the previous calculations are not altered greatly by this additional field. The leading term in the Lagrangian for the field in a background solution of σ_0 is

$$\mathcal{L} = \frac{2\pi^2 R^4}{(2\pi)^7 \alpha'^4 g_s} \int d\rho e^{\phi} \mathcal{G} \left(\sqrt{1 + (\partial_\rho \sigma_0)^2} H \left(\frac{(\rho^2 + \sigma_0^2)^2 - 1}{(\rho^2 + \sigma_0^2)^2 + 1} \right)^{\frac{1}{4}} (2\pi\alpha')^2 \frac{1}{4} F^{\mu\nu} F_{\mu\nu} \right.$$
$$\left. \cdot \frac{1}{2R^2} \frac{1}{\sqrt{1 + (\partial_\rho \sigma_0)^2}} \left(\frac{(\rho^2 + \sigma_0^2)^2 - 1}{(\rho^2 + \sigma_0^2)^2 + 1} \right)^{\frac{1}{2}} \frac{(\rho^2 + \sigma_0^2)^2}{(\rho^2 + \sigma_0^2)^2 - 1} F^{\mu\nu} F_{\mu\nu} \right) \ , \tag{5.57}$$

where μ, ν run over four-dimensional space-time indices. A coupling between the gauge field living on the brane and the four-form $C_{(4)}$, described by a Wess-

Zumino term, could be included here. However, this term is only relevant for gauge fields with a vector index on the three-sphere which is not the case for the vector mesons of interest in QCD studies. The gauge field is written in the form

$$A^\mu = a(\rho)e^{ik.x}\epsilon^\mu \ , \tag{5.58}$$

where the function $a(\rho)$ is determined by the equations of motion and, again, the non-interacting plane-wave approximation for the form of the space-time-dependence of the gauge field is taken. The meson spectrum can now be studied using a shooting technique, varying $k^2 = -M^2$, to find the well-behaved solutions. The equation of motion for this field is given by

$$e^\phi \mathcal{G}\sqrt{1+(\partial_\rho\sigma_0)^2}M^2R^2a(\rho)H\left(\frac{\omega^4-1}{\omega^4+1}\right)^{\frac{1}{4}} + \partial_\rho\left(\frac{e^\phi\mathcal{G}\partial_\rho a(\rho)}{\sqrt{1+(\partial_\rho\sigma_0)^2}}\frac{\omega^4}{\sqrt{\omega^8-1}}\right) = 0 \ . \tag{5.59}$$

In the UV limit of this equation, there are two independent solutions. The first is given by $a(\rho) = \text{const}$, which corresponds to introducing a background gauge field associated with the $U(1)$ baryon number symmetry in the field theory. In the UV, the Lagrangian for this field is

$$\mathcal{L} \simeq \frac{N}{4\pi^2}\log\frac{\Lambda_{UV}}{\Lambda_b}\frac{1}{4}F^{\mu\nu}F_{\mu\nu} \ , \tag{5.60}$$

which reflects the logarithmic running of the flavour gauge coupling.

The second solution corresponds to the mesons of the vector symmetry associated with the operator $\bar{q}\gamma^\mu q.$ and is $a(\rho) \sim \frac{1}{\rho^2}$. The algorithm used in section 4.2.2 is employed, with these boundary conditions for $a(\rho)$, to find the vector meson spectrum. The results of this analysis can be compared to those for pure

$AdS_5 \times S^5$ where the spectrum is known analytically:

$$M^2_{vector,AdS} R^2 = 4(n+1)(n+2) \ . \tag{5.61}$$

The results of the Constable-Myers analysis and the pure $AdS_5 \times S^5$ calculation are given in table 5.2.

n	*AdS case*	*CM case*
0	2.83	2.06
1	4.90	4.63
2	6.93	6.73
3	8.94	8.78
4	11.0	10.8
5	13.0	12.9
6	15.0	14.9
7	17.0	16.9
8	19.0	19.0

Table 5.2: Vector meson spectrum comparing Constable-Myers and pure $AdS_5 \times S^5$ backgrounds. The Constable Myers results are normalised to agree with the $AdS_5 \times S^5$ results for highly excited states.

5.8 Analytic Investigation of Chiral Symmetry Breaking

The couplings and masses in the field theory dual to the dilaton flow geometry, have now been calculated using D7-brane probes. All the calculations performed have been numerical but it would be useful to employ analytical methods to investigate some of these properties. It transpires that it is possible to calculate whether chiral symmetry will be broken in a given model using analytical techniques.

As explained in section 5.2.4, there appears to be a link between the geometrical symmetry breaking of the D7-brane and the chiral symmetry breaking of the field theory. The symmetry breaking is induced by a deformation in the centre of the space which repels the brane from the singular region. Therefore it is key, as far as chiral symmetry breaking is concerned, that the D7-brane feels a repulsive potential from the singularity. The brane flow from the UV into the IR can only be solved numerically. There is, however, a brane configuration for which the repulsive potential felt by the D7-brane can be calculated analytically. This configuration simplifies the equations because, using the symmetry properties of the background space, the differential equation can be reduced to an algebraic equation. This configurations corresponds to a brane which does not flow from the UV to the IR, but instead wraps around the singularity like an elastic band around a ball. This configuration is clearly unstable as the band can slip off the ball and collapse. However, the configuration can still be used to study the po-

tential. Rather than calculating ω_6 as a function of ρ, the coordinates are altered again and the (ω_6, ρ) plane is written in circular coordinates:

$$\sum_{i=1}^{6} d\omega_i^2 = dr^2 + r^2(d\alpha^2 + \cos^2\alpha d\phi^2 + \sin^2\alpha d\Omega_3^2) \ . \tag{5.62}$$

The action for a brane wrapping the singularity is then written in terms of a scalar field r as a function of the angular coordinate α. This embedding is given in table 5.3.

	x_0	x_1	x_2	x_3	r	α	ϕ	ω_1	ω_2	ω_3
D3	×	×	×	×	.	.	.	.	.	.
D7	×	×	×	×	.	×	.	×	×	×

Table 5.3: D3-brane and wrapped D7-brane embedding in the Constable-Myers geometry. Filled dimensions are marked with crosses, those perpendicular to the world-volumes are denoted by a dot.

5.8.1 Brane Wrapping in the $AdS_5 \times S^5$ Geometry

As explained, this configuration does not have a stable field theory description but this is unimportant here. Before calculating the solution to this deformed case, it is enlightening to see what happens in the pure $AdS_5 \times S^5$ case. The action for the wrapped brane in the $AdS_5 \times S^5$ geometry is given by

$$S_{wrappedD7} = -T_7 \int d^8\zeta \sin^3(\alpha) r(\alpha)^2 \sqrt{1 + \frac{1}{r(\alpha)^2}\left(\frac{dr(\alpha)}{d\alpha}\right)^2} \ , \tag{5.63}$$

There is a solution to this action which is

$$r(\alpha) = 0 \ . \tag{5.64}$$

This means that, when a brane starts in a circular configuration, it will collapse into the centre of the space. This is illustrated in figure 5.10

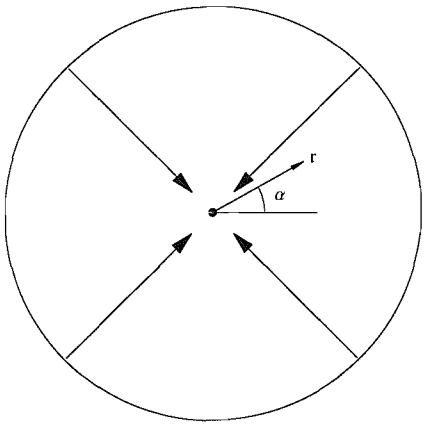

Figure 5.10: Plot illustrating that a D7-brane in a circular configuration in $AdS_5 \times S^5$ will collapse into the centre of the space.

This will be important when calculating the solutions in the deformed geometries. Without the deformations, the brane collapses and the question is now whether a deformation can prevent this collapse.

5.8.2 Brane Wrapping the Constable-Myers Singularity

In the Constable-Myers geometry, it has been shown in figure 5.2, that there is a repulsive potential felt by the brane caused by the singular region. This calculation is performed numerically, but it would be ideal to get the same result analytically using a wrapped brane. The action for a brane wrapping the Constable-Myers singularity is given by

$$S_{wrappedD7} = -T_7 \int d^8\zeta \sin^3(\alpha) r(\alpha)^4 e^{\phi}(r(\alpha)) g_{\mu\nu}^2 g_{rr}^2(r(\alpha)) \sqrt{1 + \frac{1}{r(\alpha)^2}\left(\frac{dr(\alpha)}{d\alpha}\right)^2}\,, \tag{5.65}$$

where the integral runs over $(x_{//}, \Omega_3, \alpha)$. At this stage, b is reinstated as a free parameter to allow the behaviour for different sized singularities to be studied. The equation of motion for this action is rather complicated, however, there is a solution where, just as for $AdS_5 \times S^5$, $r(\alpha)$ is constant. This is the circular wrapping solution of interest. To find the solution, the potential is minimised with respect to the radius, $r(\alpha)$. The existence of this symmetric solution is due to the symmetries of the background space which have been used to reduce the original differential equation to a simple algebraic equation.

For $b = 1$, the potential as a function of r is plotted in figure 5.11.

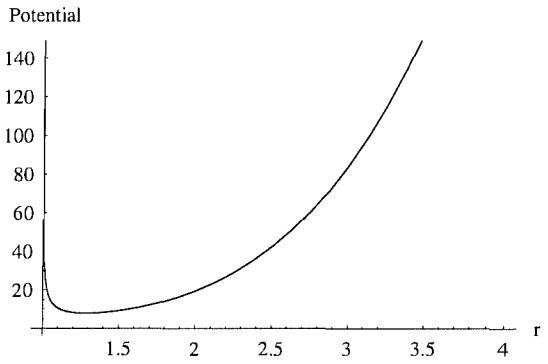

Figure 5.11: Plot of the potential against radius, r, for the $b = 1$ circular wrapping solution. The potential is minimised at $r_0 = 1.29$.

For a general singularity size, b, the radius, r_0, which minimises the potential is given by one of the solutions to

$$r_0^8 - b^4\sqrt{10 - \frac{1}{4b^8}}r_0^4 + b^8 = 0 \ , \tag{5.66}$$

where all variables are in units of R. This equation has eight solutions. Four of

which are real, two are positive and for

$$b \geq \left(\frac{1}{24}\right)^{\frac{1}{8}} , \tag{5.67}$$

there is a solution where $r_0 \geq b$. Provided that the above inequality is satisfied, a brane wrapping solution exists which is repelled from the singularity. If the inequality is saturated, the brane lies on the surface of the singularity. If the inequality is not obeyed, the largest solution of r_0 lies inside the singularity and there will be no chiral symmetry breaking. Configurations which saturate the bound are investigated in more detail in the following chapters.

A solution with $b \geq \left(\frac{1}{24}\right)^{\frac{1}{8}}$ is illustrated in figure 5.12 indicating that the brane solution lies slightly off the singularity.

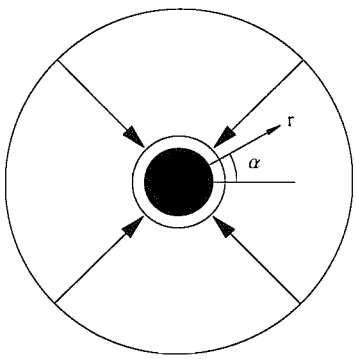

Figure 5.12: Plot illustrating that a brane stretched artificially to some large radius will collapse to a configuration which is repelled by the central singularity.

5.8.3 Analysis of the Brane Wrapping Solutions

For the $b = 1$ solution, a plot of the minimum action radius, r_0, and the UV/IR flow for zero quark mass, is shown in figure 5.13. There is a small gap between

the two configurations at $\rho = 0$.

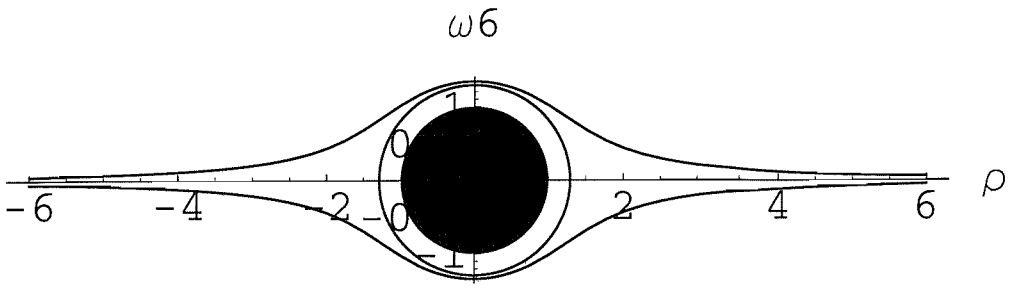

Figure 5.13: Plot of the minimum action spherical D7-brane embedding and the massless quark embeddings in the Constable-Myers Geometry. The black circle represents the singularity in the geometry.

Figure 5.14 is a plot of the circular embedding solution and the UV/IR flow solution which has the largest positive mass for which a negative condensate solution exists (see figure 5.3). Figure 5.7 demonstrates that, as the quark mass of a UV/IR brane flow increases from a negative to a positive value, there is a maximum mass for which a negative condensate solution exists. Above this mass, the solution is not stable and there is a single solution to the equations of motion – that with a positive condensate. It appears that the circular wrapping distance corresponds to the closest point a UV/IR flowing brane can come to the singularity. Note again that these are not stable solutions. The positive mass-negative condensate solution will deform to the stable positive mass-positive condensate solution, while the wrapping brane configuration will slip off the singularity and collapse.

As b decreases, so does the distance between the wrapped brane and the singularity and, when the inequality (equation 5.67) is saturated, the brane falls

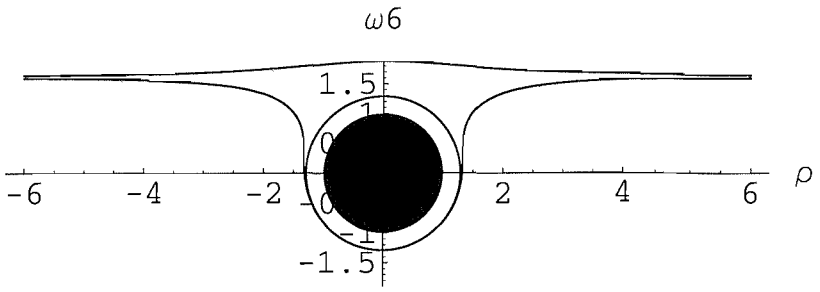

Figure 5.14: Plot of the minimum action spherical D7-brane embedding and a local minimum embedding action for a massive quark in the Constable-Myers Geometry.

onto the singular surface. Similarly, the zero quark mass solution of figure 5.13 approaches the singularity as b decreases. Due to the gap between the solutions, there is a range of values for b where there is no wrapping configuration (with $r_0 > b$) but chiral symmetry breaking is exhibited. The wrapping technique gives a good indication of the potential felt by the brane, but is not a perfect analytic test of chiral symmetry breaking.

A plot of the phase-space of the field theory for varying b is plotted in figure 5.15.

It is particularly interesting to note that there exists a region of parameter space where there is no confinement but chiral symmetry breaking occurs. It is possible that this region may disappear when stringy corrections are included.

Though the circular wrapping technique has not led to any more insight into the physics of chiral symmetry breaking, it is an extremely useful tool for more complex geometries. Geometries with no known analytic form for the metric, dilaton or other R-R fields are investigated in chapters 6 to 9.

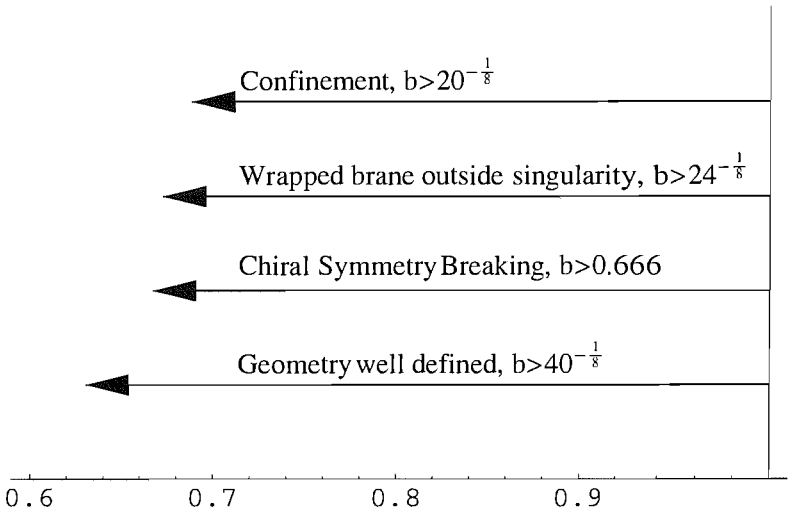

Figure 5.15: Phases of the Constable-Myers dual field theory as a function of the conformal symmetry breaking parameter b. The ends of each arrow indicate the point at which the property of the background or the field theory stops.

Chapter 6

An $\mathcal{N} = 4$ Scalar Deformation

The last two chapters have been concerned with introducing quarks to the field theories dual to qualitatively different supergravity backgrounds. In this chapter, a more complicated geometry is studied and fundamental matter is added in a further attempt to investigate chiral symmetry breaking.

6.1 The Background

In chapter 2, the duality between an $\mathcal{N} = 4$ super-Yang-Mills theory and ten-dimensional supergravity on $AdS_5 \times S^5$ was discussed in detail. In section 2.2.4, it was indicated how this duality could be generalised by deforming the supergravity background, thereby introducing relevant operators to the field theory. In this chapter, a specific deformation is discussed which retains all the supersymmetry of the undeformed background.

It is possible to truncate an eleven-dimensional supergravity background to four dimensions. Conversely, it has been shown in [94] that every formulation of

$\mathcal{N} = 8$ gauged supergravity in four dimensions can be uniquely lifted to eleven-dimensional supergravity compactified on an S^7. It is believed that the same relationship holds between $\mathcal{N} = 8$ gauged supergravity in five dimensions and IIB supergravity compactified on an S^5. This means that all five-dimensional truncations are consistent, due to the isomorphism between the five- and ten-dimensional theories.

In this chapter, a specific five-dimensional supergravity solution is discussed and its lift to ten dimensions provided.

6.1.1 $\mathcal{N} = 8$ Five-Dimensional Supergravity

A set of solutions to five-dimensional supergravity [95, 96, 97] were found in [98, 99] and their lifts to ten dimensions were calculated. It was discovered that this family of supergravity solutions corresponds to D3-branes distributed in disk configurations in the six-dimensional space perpendicular to their world-volume. The algorithm for the consistent lift is complicated and so only a brief outline of this process is discussed here.

It is important to understand the dictionary between fields in the five-dimensional supergravity theory and operators in the field theory. There are a total of 42 scalars in five-dimensional $\mathcal{N} = 8$ gauged supergravity. These fill representations of a coset group given by $E_{6(6)}/USp(8)$. This group has an unbroken $SO(6)$ subgroup and the 42 scalars are in the $(\mathbf{10}, \bar{\mathbf{10}}, \mathbf{20}, \mathbf{1}^2)$ representations of $SO(6)$. In this particular example, the field (labelled M) in the $\mathbf{20}$ is turned on. Using the AdS/CFT dictionary, a field with mass $m^2 = -2$, corresponds to both source and

vev for a dimension two operator. This dimension two operator is given by

$$\mathcal{O} = \mathrm{Tr}\,\lambda^2 \ . \tag{6.1}$$

The solutions to the equation of motion for M correspond to switching on different coefficients for the six real scalar field bilinears. The $SO(6)$ symmetry corresponds to the $SU(4)_R$ symmetry of the field theory.

6.1.2 The Five-Dimensional Supergravity Action

The action for the field M, in the **20** of $SO(6)$, is written in terms of a set of fields, α_i, which are related to M by the parametrisation

$$\begin{pmatrix} \beta_1 \\ \beta_2 \\ \beta_3 \\ \beta_4 \\ \beta_5 \\ \beta_6 \end{pmatrix} = \begin{pmatrix} \frac{1}{\sqrt{2}} & \frac{1}{\sqrt{2}} & \frac{1}{\sqrt{2}} & 0 & \frac{1}{\sqrt{6}} \\ \frac{1}{\sqrt{2}} & -\frac{1}{\sqrt{2}} & -\frac{1}{\sqrt{2}} & 0 & \frac{1}{\sqrt{6}} \\ -\frac{1}{\sqrt{2}} & -\frac{1}{\sqrt{2}} & \frac{1}{\sqrt{2}} & 0 & \frac{1}{\sqrt{6}} \\ -\frac{1}{\sqrt{2}} & \frac{1}{\sqrt{2}} & -\frac{1}{\sqrt{2}} & 0 & \frac{1}{\sqrt{6}} \\ 0 & 0 & 0 & 1 & -\sqrt{\frac{2}{3}} \\ 0 & 0 & 0 & -1 & -\sqrt{\frac{2}{3}} \end{pmatrix} \begin{pmatrix} \alpha_1 \\ \alpha_2 \\ \alpha_3 \\ \alpha_4 \\ \alpha_5 \end{pmatrix}$$

where the field M is given by

$$M = diag(e^{2\beta_1}, e^{2\beta_2}, e^{2\beta_3}, e^{2\beta_4}, e^{2\beta_5}, e^{2\beta_6}) \ . \tag{6.2}$$

The action for the scalars, α, is

$$\mathcal{L} = -\frac{1}{4}R + \sum_{i=1}^{5} \frac{1}{2}(\partial\alpha_i)^2 - P \ , \tag{6.3}$$

where R is the Ricci scalar of the five-dimensional space and P is given by

$$P = -\frac{g^2}{32}\left[(\mathrm{Tr}\,M)^2 - 2\mathrm{Tr}\,M^2\right] \ , \tag{6.4}$$

where g is the coupling constant for the scalar field interactions. P can be written in terms of a superpotential W where

$$W = -\frac{1}{4}\mathrm{Tr}\, M \ . \tag{6.5}$$

There is a simple condition on the superpotential which guarantees the existence of 16 supercharges (giving $\mathcal{N} = 8$ in five dimensions):

$$\frac{d\alpha_i}{du} = \frac{g}{2}\frac{\partial W}{\partial \alpha_i} \ , \qquad \frac{dA}{du} = -\frac{g}{3}W \ , \tag{6.6}$$

where u is the radial coordinate in a warped five-dimensional AdS space with metric

$$ds^2_{\mathcal{M}} = e^{2A(u)}dx^2_{//} - du^2 \ . \tag{6.7}$$

There is a set of solutions to α where the magnitude, but not the direction, of the vector β is a function of u. These solutions to β_a are given by

$$\beta_a = \gamma_a \mu(u) \ , \tag{6.8}$$

where γ is a fixed vector and $\mu(u)$ is a scalar function of the direction u. These supersymmetric solutions are parametrised by the boundary value of μ at infinite u. As discussed in section 6.1.1, turning on this scalar deforms the field theory by the addition of the operator $\mathrm{Tr}\,\lambda^2$. In this supersymmetric case, the size of μ at infinite u gives the size of the vev of this operator. The components of the vector, γ_a, give the coefficients of the fermion bilinears in the form $\sum_{a=1}^{6} \gamma_a \lambda_a^2$. The non-supersymmetric generalisation of this solution corresponds to switching on a source for this operator. The size of the source is related to the derivative of $\mu(u)$ at infinite u.

6.1.3 The Ten-Dimensional Lift

To lift this geometry from five to ten dimensions, it is necessary to find the map between the five-dimensional field solutions and deformed metrics on the five-sphere. The ten-dimensional space is a product space between a non-compact component, $\mathcal{M}$, and a compact component, $\mathcal{K}$, which is the deformed five-sphere, given by

$$ds^2 = \Delta^{-\frac{2}{3}} ds^2_{\mathcal{M}} + ds^2_{\mathcal{K}} \ , \tag{6.9}$$

where the warp factor Δ is a function of components of the five-sphere. The metric on the compact space can have dependence on the non-compact manifold, but not vice versa.

The subgroup, $SO(6)$, of the coset group corresponds to the rotational isometry of the five-sphere. By switching on the supergravity fields, the $SO(6)$ is broken down to a further subgroup. This corresponds to deforming the five-sphere. For the lift to be consistent, the symmetries of the two broken groups should match exactly.

There are only five solutions, γ_a, which preserve a subgroup of the original $SO(6)$ symmetry. The metric and warp factor for each of these solutions are given by

$$\begin{aligned} ds^2 &= \frac{1}{\sqrt{H}} dx^2_{//} - \sqrt{H} \sum_{i=1}^{6} dy_i^2 \ , \\ H &= \int_{|\vec{\omega}| \leq l} d^n \omega \sigma(\vec{\omega}) \frac{L^4}{|\vec{y} - \vec{w}|^4} \ . \end{aligned} \tag{6.10}$$

The form of γ_a for each of the five solutions, along with the symmetry that is preserved and the form of the distribution $\sigma(\vec{\omega})$, is given in table 6.1.

n	γ_a	symmetry	σ
1	$\frac{1}{\sqrt{15}}(1,1,1,1,1,-5)$	$SO(5)$	$\frac{2}{\pi l^2}\sqrt{l^2-\omega^2}$
2	$\frac{1}{\sqrt{6}}(1,1,1,1,-2,-2)$	$SO(4)\times SO(2)$	$\frac{1}{\pi l^2}\theta(l^2-\omega^2)$
3	$\frac{1}{\sqrt{3}}(1,1,1,-1,-1,-1)$	$SO(3)\times SO(3)$	$\frac{1}{\pi^2 l^2}\frac{1}{\sqrt{l^2-\omega^2}}$
4	$\frac{1}{\sqrt{6}}(2,2,-1,-1,-1,-1)$	$SO(4)\times SO(2)$	$\frac{1}{\pi^2 l^2}\delta(l^2-\omega^2)$
5	$\frac{1}{\sqrt{15}}(5,-1,-1,-1,-1,-1)$	$SO(5)$	$\frac{1}{\pi^3 l^2}\left(\frac{-\theta(l^2-\omega^2)}{2(l^2-\omega^2)^{\frac{3}{2}}}+\frac{\delta(l^2-\omega^2)}{\sqrt{l^2-\omega^2}}\right)$

Table 6.1: Geometries representing n-dimensional disk distributions with their supergravity field boundary conditions.

6.1.4 The Ten-Dimensional Solution

The solution of interest here has $n = 2$ (table 6.1), where a vev is switched on for the operator $\mathrm{Tr}\,\lambda^2$ of the form $diag(1,1,1,1,-2,-2)$. This vev preserves the $\mathcal{N} = 4$ symmetry (and therefore the $\mathcal{N} = 2$ symmetry when the probe is included). As explained in section 6.1.2, though the direction in the complex scalar field space is defined by γ_a, the size of the vev is a free parameter. The supersymmetry conditions, the superpotential and the warp factor are given by

$$\begin{aligned}
\frac{d\mu}{du} &= \frac{g}{2}\frac{\partial W}{\partial \mu}\,, \qquad \frac{dA}{du} = -\frac{g}{3}W\,,\\
W(\mu) &= -e^{\frac{2\mu}{\sqrt{6}}} - \frac{1}{2}e^{-\frac{4\mu}{\sqrt{6}}}\,,\\
A(\mu) &= \frac{1}{2}\log\left|\frac{e^{\frac{2\mu}{\sqrt{6}}}}{1-e^{\sqrt{6}\mu}}\right| + \log\left(\frac{l}{R}\right)\,,
\end{aligned} \tag{6.11}$$

where l is a constant of integration and R is the asymptotic AdS radius. At this point, a final reparametrisation is made before writing the metric for this

background. The supergravity field is rewritten as

$$\chi(u) = e^{-\frac{\mu(u)}{\sqrt{6}}} \ . \tag{6.12}$$

The metric for this background is then

$$ds^2 = \frac{\sqrt{X}}{\chi} e^{2A} dx^2 - \frac{\sqrt{X}}{\chi} \left(du^2 + \frac{R^2}{\chi^2} \left[d\theta^2 + \frac{\sin^2\theta}{X} d\phi^2 + \frac{\chi^6 \cos^2\theta}{x} d\Omega_3^2 \right] \right) \ , \tag{6.13}$$

where

$$X = \cos^2\theta + \chi^6 \sin^2\theta \ . \tag{6.14}$$

χ and A satisfy the differential equations

$$\frac{d\chi}{du} = \frac{1}{3R} \left(\frac{1}{\chi} - \chi^5 \right) \ , \qquad \frac{dA}{du} = \frac{2}{3R} \left(\frac{1}{\chi^2} + \frac{\chi^4}{2} \right) \ , \tag{6.15}$$

with solution

$$e^{2A} = \frac{l^2}{R^2} \frac{\chi^4}{\chi^6 - 1} \ . \tag{6.16}$$

There is also a non-zero four-form potential given by

$$C_{(4)} = \frac{e^{4A} X}{g_s \chi^2} dx^0 \wedge dx^1 \wedge dx^2 \wedge dx^3 \ . \tag{6.17}$$

Most of the following calculations are performed by solving equations 6.15 numerically, but it is interesting to note that u can be calculated analytically as a function of χ. There is a one-parameter family of solutions given by

$$u = const + \frac{R}{4} \left(I\sqrt{3} \log \left(\frac{1 + I\sqrt{3} + 2\chi}{1 - I\sqrt{3} + 2\chi} \right) + \log \left(\frac{1 + \chi^2 + \chi^4}{(\chi^2 - 1)^2} \right) \right) \ . \tag{6.18}$$

Figure 6.1 shows examples of some of the solutions for different values of the constant of integration.

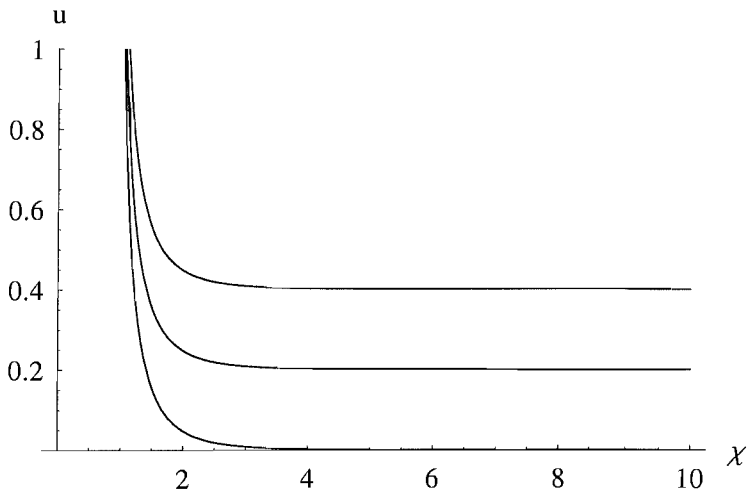

Figure 6.1: Analytic solutions to the first order equations of motion for the scalar field flow given by equation 6.18.

6.2 Adding Quarks to the $\mathcal{N} = 4$ Scalar Deformation

As in chapters 4 and 5, quarks are added to the field theory dual of this geometry by the introduction of a D7-brane probe. Before attempting to understand the excitations on the probe (corresponding to mesons), it is important to study the flow of a D7-brane from the UV (where the duality is understood) to the IR (where the chiral symmetry breaking may be triggered). This case differs from the dilaton flow geometry as there is no longer a natural Euclidean six-plane containing an undeformed five-sphere in which to embed. The most natural choice is to embed the D7-brane to lie in the $x_{//}, u, \Omega_3$ directions and study the profile of $\theta(u)$ at fixed ϕ. The embedding is illustrated in table 6.2. Fixing ϕ is equivalent to fixing a direction on the $U(1)$ circle (fixing Φ to be real in the

	x_0	x_1	x_2	x_3	u	θ	ϕ	Ω_1	Ω_2	Ω_3
D3	×	×	×	×	.	.	.	.	.	.
D7	×	×	×	×	×	.	.	×	×	×

Table 6.2: D3- and D7-brane embedding in the $\mathcal{N} = 4$ geometry. Filled dimensions are marked with crosses, those perpendicular to the world-volumes are denoted by a dot.

Constable-Myers D7 embedding). The DBI action for this embedding is

$$S_{DBI} = -T_7 \int d^8\zeta R^3 e^{4A(u)} |\cos^3\theta(u)| \sqrt{X}\chi(u)^2 \sqrt{1 + \frac{R^2\theta'(u)^2}{\chi(u)^2}} \ . \tag{6.19}$$

It is possible to plot the solutions for θ as a function of u, but to compare with the results which are understood in the Constable-Myers case, it is sensible to plot the brane flow in a similar coordinate system. In the large u limit, where the space returns to $AdS_5 \times S^5$, a change of coordinates given by

$$r^2 + v^2 = e^{2u} \ , \qquad \frac{v}{r} = \tan\theta \ , \tag{6.20}$$

transforms the circular coordinate system of equation 6.13 to Cartesian coordinates. However, it can be seen that by performing this coordinate transformation, the metric becomes

$$\begin{aligned} ds^2 \ = \ & \frac{\sqrt{X}}{\chi} e^{2A} dx_{//}^2 - \frac{\sqrt{X}}{\chi(v^2+r^2)^2} \left(dv^2 \left(v^2 + \frac{R^2 r^2}{\chi^2} \right) + dr^2 \left(r^2 + \frac{R^2 v^2}{\chi^2} \right) \right. \\ & \left. + 2\, r\, v\, dv\, dr \left(1 - \frac{1}{\chi} \right) + \frac{R^2(v^2+r^2)^2}{X^2} \left(\frac{1}{\chi^2 \left(\frac{r^2}{v^2} + 1 \right)} d\phi^2 + \frac{\chi^4}{\left(1 + \frac{v^2}{r^2} \right)} d\Omega_3^2 \right) \right) \ . \end{aligned} \tag{6.21}$$

This means that, though in the UV there is a Cartesian six-plane, in the IR of the theory the coordinates are not orthogonal and there is a deficit angle related to

χ. In this coordinate system, the D7-brane flow is given by v as a function of r, table 6.3. The existence of a deficit angle means that any plots in this coordinate

	x_0	x_1	x_2	x_3	r	v	ϕ	Ω_1	Ω_2	Ω_3
D3	×	×	×	×	.	.	.	.	.	.
D7	×	×	×	×	×	.	.	×	×	×

Table 6.3: D3- and D7-brane embedding in the pseudo-Cartesian $\mathcal{N} = 4$ geometry. Filled dimensions are marked with crosses, those perpendicular to the world-volumes are denoted by a dot.

system will be warped when drawn in flat-space.

The DBI action for a brane embedded in the coordinate system of table 6.3 is given by

$$\begin{aligned} S_{DBI} &= -T_7 \int d^8\zeta \frac{e^{4A} R^3 \chi^2 \sqrt{X}}{v^2 + r^2} \left(1 + \frac{v^2}{r^2}\right)^{\frac{3}{2}} \\ &\quad \cdot \sqrt{r^2 + \frac{R^2 v^2}{\chi^2} + 2rv\left(1 - \frac{R^2}{\chi^2}\right) v' + \left(v^2 + \frac{R^2 r^2}{\chi^2}\right) v'^2} \ , \end{aligned} \tag{6.22}$$

where

$$\chi = \chi[\log(\sqrt{v(r)^2 + r^2})] \ , \qquad A = A[\log(\sqrt{v(r)^2 + r^2})] \ , \tag{6.23}$$

and ' denotes the derivative with respect to r.

6.2.1 D7-Brane Flow in the Physical Coordinates

In this geometry, the correct, 'physical' coordinate system is known [98, 100]. In the physical coordinate system, the scalar and gauge fields living on a D3-brane in the background geometry are simultaneously canonically normalised.

The change of variables between the original coordinate system (6.13) and the physical coordinates is known in this case. Due to the supersymmetric nature of this geometry, the equations of motion are first order, and the action for the D3-brane can be manipulated using these first order equations of motion. The change of variables between the original coordinates and the physical coordinates $(\hat{u}, \alpha)$ is

$$\hat{u}^2 \cos^2\alpha = R^2 e^{2A(u)} \chi(u)^2 \cos^2\theta \ , \qquad \hat{u}^2 \sin^2\alpha = R^2 \frac{e^{2A(u)}}{\chi(u)^4} \sin^2\theta \ , \tag{6.24}$$

which gives the standard multi-centre D3-brane solution:

$$\begin{aligned} ds^2 &= H^{-\frac{1}{2}} dx_{//}^2 + H^{\frac{1}{2}} \sum_{i=1}^{6} d\hat{u}_i^2 \ , \\ C_{(4)} &= \frac{1}{H g_s} dx^0 \wedge dx^1 \wedge dx^2 \wedge dx^3 \ , \end{aligned} \tag{6.25}$$

where

$$H = \frac{\chi^2}{X e^{4A}} \ . \tag{6.26}$$

As explained in the formulation of this background, the introduction of the scalar field produces a distribution of D3-branes in a disk configuration. The physical coordinate system makes the distribution more explicit.

By writing the metric in the form of equation 6.25, it is clear that the DBI action for the UV/IR flow of the brane will be the same as the undeformed $AdS_5 \times S^5$ case. This is because the warp factors cancel in the determinant of the pullback and the D7-brane does not notice the distribution of the D3-branes.

The solution to the D7-brane equation of motion in the physical coordinates can be calculated analytically, just as in the $AdS_5 \times S^5$ case:

$$\alpha = \arcsin\left(\frac{m}{\hat{u}}\right) \ , \tag{6.27}$$

where m corresponds to the quark mass, and for a consistent flow there is no quark bilinear condensate.

This is the most important result of this chapter. As the D7-brane does not notice any difference between the current D3-brane distribution and the $AdS_5 \times S^5$ geometry, there is no chiral symmetry breaking. In the physical coordinates (where the solutions are the same as those for the undeformed geometry) it has been shown analytically in section 4.2.1, that no condensate forms.

If the meson spectrum were to be calculated in this geometry, the warp factors would not cancel out in the equations of motion and the mass spectrum would differ from that in the $AdS_5 \times S^5$ geometry. Though the meson spectrum has not be calculated for this geometry, this is an interesting route that will be investigated in the near future. It will be a useful exercise to compare the meson spectrum from this geometry with both the $AdS_5 \times S^5$ results and the Gell-Mann-Oakes-Renner relation. The expectation is that the results should coincide with the $AdS_5 \times S^5$ results.

6.2.2 The Supergravity Background in Physical Coordinates

The physical set of circular coordinates, $(\alpha, \hat{u})$, can be written in terms of a physical set of Cartesian coordinates, (c_1, c_2):

$$\begin{aligned} c_1^2 + c_2^2 &= \hat{u}^2 \ , \\ \frac{c_2}{c_1} &= \tan(\alpha) \ . \end{aligned} \tag{6.28}$$

The warp factor in the Cartesian coordinates is

$$H = \frac{2}{1+(c_1^2+c_2^2)^2-2(c_2^2-c_1^2)+(1+(c_1^2+c_2^2))\sqrt{1+(c_1^2+c_2^2)^2-2(c_2^2-c_1^2)}} \,. \tag{6.29}$$

This is plotted in figure 6.2 in the (c_1, c_2) plane. There are still singularities in the warp factor as expected. In fact, it is possible to see what happens in the coordinate transformation in more detail. At large v^2+r^2, the (v,r) and (c_1,c_2) coordinate systems are the same, and a circle in one is mapped to a circle in the other. As v^2+r^2 is reduced, a circle in the (v,r) coordinates is mapped to a deformed circle in the physical coordinates. As the singularity is a circle in the (v,r) system, it is possible to study what this is mapped to in the physical coordinates. The right hand side of figure 6.2 shows what happens to circles of different radii, mapped from (v,r) into (c_1,c_2). The inner ovals are mapped from the circles nearest to the singularity and it can be seen that the circular singularity is mapped to a line. The product of this line with the three-sphere gives the $SO(4)\times SO(2)$ symmetry expected from table 6.1.

It is also interesting to note that because both the solution in the physical coordinates, and the change of variables between the original and physical coordinates are known, the exact solution to the D7-brane flow in the original coordinate system is also known:

$$\theta = \arcsin\left(\frac{m\chi^4}{e^{2A}}\right) = \arcsin(m'\sqrt{\chi^6-1}) \,. \tag{6.30}$$

m and m' are not equal due to the constant of integration in $A(\chi)$.

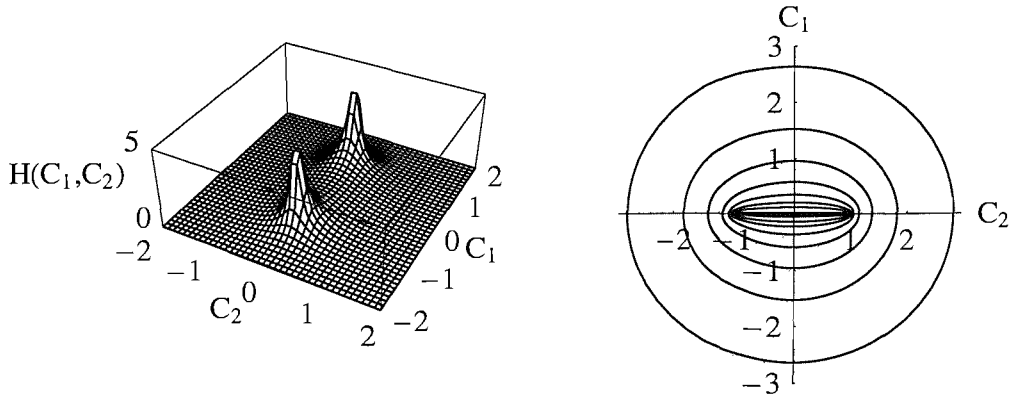

Figure 6.2: Singularity structure of the warp factor, H, in the physical coordinate system. The right hand plot demonstrates that the circular singularity is deformed to a disk singularity as expected from the D3-brane distribution.

6.2.3 The Unphysical Coordinates Revisited

It would be simple to conclude this investigation by stating that there is no chiral symmetry breaking in this background, as calculated in the physical coordinate system. However, in the next chapter, a very similar background to this one, which is not supersymmetric, is investigated for evidence of chiral symmetry breaking. Due to the absence of supersymmetry, there are no first order equations, with which to find the correct coordinate system. As the current geometry is well understood, it is useful to study it in the original, unphysical, coordinate system and discover what problems may be faced in the non-supersymmetric case.

Figure 6.3 illustrates solutions to the D7-brane equations of motion in the (v, r) plane. These look similar to the flows in the Constable-Myers geometry (figure 5.2). The numerical calculation to determine the D7-brane flows in the (v, r) plane can be performed in two ways. First, these flows can be calculated

using the pullback of the metric in the (v, r) coordinates onto the D7-brane (equation 6.22). The flow can then be calculated numerically from the equations of motion for $v(r)$. The second method is to use the analytical flow in the (c_1, c_2) coordinate system and the change of variables between (c_1, c_2) and (v, r). It is sensible to use both these methods to check the consistency of the numerical techniques (both of these methods are plotted in figure 6.3).

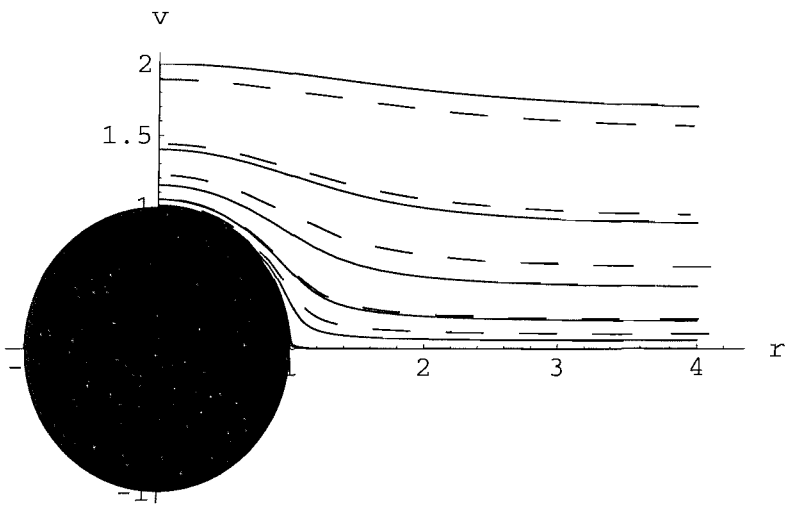

Figure 6.3: D7-brane flows in the scalar deformed geometry for different quark masses. The solid lines are the numerical solutions and the dashed lines, the coordinate transform of the full analytic solutions. This plot indicates that the numerical and analytical solutions to the DBI equations of motion for the D7-brane match well. The singularity of the geometry is shown as a black circle.

From the UV behaviour of these flows, the value of the mass and condensate for the quarks and quark bilinear can be calculated. In the physical coordinates, the D7-brane flows as if it were in $AdS_5 \times S^5$, so there is no condensate. Even before the physical coordinates were found, it was known that there would be

no condensate due to the supersymmetric nature of the background. The plot of mass against condensate calculated using the unphysical coordinates is shown in figure 6.4:

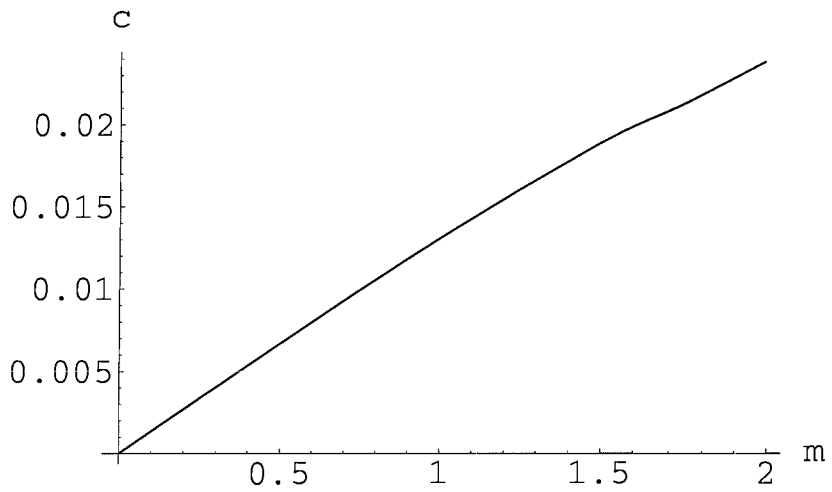

Figure 6.4: Apparent values of the quark mass and condensate extracted asymptotically from the flows in figure 6.3.

It appears that there is a small, but non-zero, condensate for non-zero quark mass, but it is known that this is not possible. This inconsistency is again due to the use of the incorrect coordinate system. The direction v, which has mass dimension one, has an asymptotic UV solution given by

$$v(r) \sim a + \frac{b}{r^2} + \frac{c}{r^4} \ldots \tag{6.31}$$

Whereas in the correct coordinate system, the solution contains only two terms (a and b), here it is not possible to extract the value of the mass and condensate. This means that the method by which the values m and c have been calculated for figure 6.4 is not the correct one for the unphysical coordinate system. In the

massless limit, where $v \to 0$, the action for the D7-brane in the AdS limit is given by

$$S_{D7} = -T_7 \int d^8\zeta r^3 \sqrt{1 + v'(r)^2} \ . \tag{6.32}$$

In this limit, the solution is exactly $v = m + \frac{c}{r^2}$, and the result of figure 6.4 can be trusted. Fortunately, the massless limit is the situation of interest for this investigation and so the result that there is no condensate is a useful one.

6.3 Brane Wrapping the $\mathcal{N} = 4$ Geometry

The original geometrical argument for the presence of chiral symmetry breaking now seems slightly misleading. In the current background, the flows in the massless limit appear to break the geometrical $SO(2)$ symmetry as they flow around the singularity (figure 6.3). However, it has now been shown that this is an artefact of using inappropriate coordinates.

In chapter 5, it was noted that in the massless quark limit there is a gap between the D7-brane and the Constable-Myers singularity. In this background, the gap is not present (see figure 6.3). There seems to be a qualitative difference in the force felt by the D7-brane, between this supersymmetric background and the Constable-Myers background.

The analytic techniques utilised at the end of chapter 5 to look at the potential of a brane wrapping around the singularity, can now be used. In the case of the Constable-Myers geometry, the embedding of the spherical wrapping brane was performed with r as a function of θ and it was shown that a constant radius brane satisfied the equations of motion. This was simple because the DBI action

was known analytically. In this case, the most natural embedding is with u as a function of θ. In this case, the DBI action is

$$S_{\text{wrapping brane}} \sim \int d^4x_{//} d\theta d\Omega_3 \sqrt{\cos^2\theta + \chi(u)^6 \sin^2\theta} \cdot \frac{\chi(u)^{10}}{(\chi(u)^6-1)^2} |\cos^3\theta| \sqrt{\frac{1}{\chi(u)^2} + \left(\frac{du(\theta)}{d\theta}\right)^2} . \quad (6.33)$$

At this stage, the action contains the numerical function $\chi(u)$, however, the dependent variable can be changed in order to write the action in a purely analytic form. Equation 6.15 provides an analytic expression which can be used to turn the derivative in equation 6.33 into a derivative purely in terms of χ and θ. All u-dependence is removed, thereby providing a fully analytic Lagrangian:

$$S_{\text{wrapping brane}} \sim \int d^4x_{//} d\theta d\Omega_3 \zeta \sqrt{\cos^2\theta + \chi^6 \sin^2\theta} \cdot \frac{\chi^{10}}{(\chi^6-1)^2} |\cos^3\theta| \sqrt{\frac{1}{\chi^2} + 9\frac{\chi^2}{(1-\chi^6)^2}\left(\frac{d\chi(\theta)}{d\theta}\right)^2} \quad (6.34)$$

Whereas, before the change of variables, the IR and UV limits were $u = -\infty$ and $+\infty$ respectively, now they correspond to the limits $\chi = +\infty$ and 1. The equation of motion for χ as a function of θ is now determined and the solution which minimises the action is found to be $\chi \to \infty$, corresponding to the brane falling onto the surface of the singularity. This is analytic proof that the brane feels no repulsive potential from the singular region. This result matches the result from 6.3 where the flow corresponding to massless quarks wraps onto the surface of the singularity. This is illustrated in figure 6.5.

In this background it has been possible to show, using several different techniques, that there is no chiral symmetry breaking. However, the numerical techniques are difficult to use to calculate the mass of the quarks and the condensate

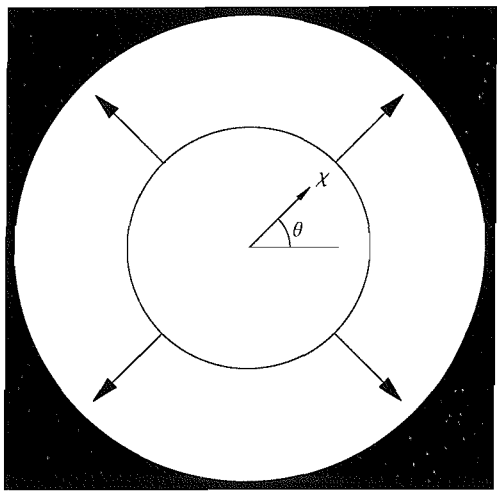

Figure 6.5: Wrapping D7-brane (central circle) falling onto singularity (outer circle) at $\chi = \infty$.

of the quark bilinear. It seems that the most reliable method for backgrounds in which the physical coordinates are not known is the brane wrapping technique. Using this method, an analytic calculation of the potential felt by a D7-brane in the massless limit can be performed. This will prove vital in the following chapters.

Chapter 7

A Non-Supersymmetric Scalar Deformation

Having studied the effects of quarks in a supersymmetric background where the metric is dependent on functions which are calculated numerically, a non-supersymmetric generalisation is investigated. Whereas, in chapter 6, chiral symmetry breaking was not permitted due to the supersymmetry, this generalised geometry may allow the induction of a chiral condensate.

7.1 The Background

As explained in section 6.1, there is a generalisation of the previous $\mathcal{N} = 4$ geometry [98] in which all the supersymmetry is broken by including a mass term for the scalars. This geometry has again been generated from a five-dimensional supergravity flow which was lifted to ten dimensions in [101].

As in the background discussed in chapter 6, a five-dimensional scalar field λ

in the **20** of $SO(6)$ is switched on. This has the potential

$$V = -e^{-\frac{4\lambda(u)}{\sqrt{6}}} - 2e^{\frac{2\lambda(u)}{\sqrt{6}}} \ . \tag{7.1}$$

The difference between the current and the previous geometry is that the scalar field, λ, acts as the source and vev for the field theory operator $\mathrm{Tr}\,(\phi_1^2+\phi_2^2+\phi_3^2+\phi_4^2-2\phi_5^2-2\phi_6^2)$. In the supersymmetric case, only the vev of this operator was switched on. Switching on a mass gives rise to an unbounded scalar potential so, as in the case of the Constable-Myers geometry, this is not a realistic field theory dual. However, as this background has a qualitatively different structure from the cases already studied, it may be able to provide an insight into the properties of a field theory necessary for chiral symmetry breaking to be triggered. Unlike the previous scalar deformed geometry, chiral symmetry breaking may be expected as there is no supersymmetry to prevent a chiral condensate from forming.

The relevant five-dimensional supergravity equations of motion are given by [102]

$$\begin{aligned} \lambda''(u) + 4\lambda'(u)\sqrt{\frac{1}{6}(\lambda'(u)^2 - 2V)} &= \frac{\partial V}{\partial \lambda(u)} \ , \\ A'(u) &= \sqrt{\frac{1}{6}(\lambda'(u)^2 - 2V)} \ . \end{aligned} \tag{7.2}$$

The solution to the large u limit of these equations is

$$\lambda = \mathcal{M}ue^{-2u} + \mathcal{C}e^{-2u} \ , \tag{7.3}$$

where, by studying the u-dependence, both $\mathcal{M}$ and $\mathcal{C}$ have dimension two. This is because both the source and condensate for this operator are of dimension two. In the supersymmetric case, only the $\mathcal{M} = 0$ solution exists and therefore

$\mathcal{M}$ is interpreted as the source for the field theory operator and $\mathcal{C}$ as the vev. This generalises the $\mathcal{N} = 4$ case where only the vev of the scalar operator is switched on. Equations 7.2 are solved numerically with boundary conditions set by equation 7.3 and some examples of these solutions are plotted in figure 7.1.

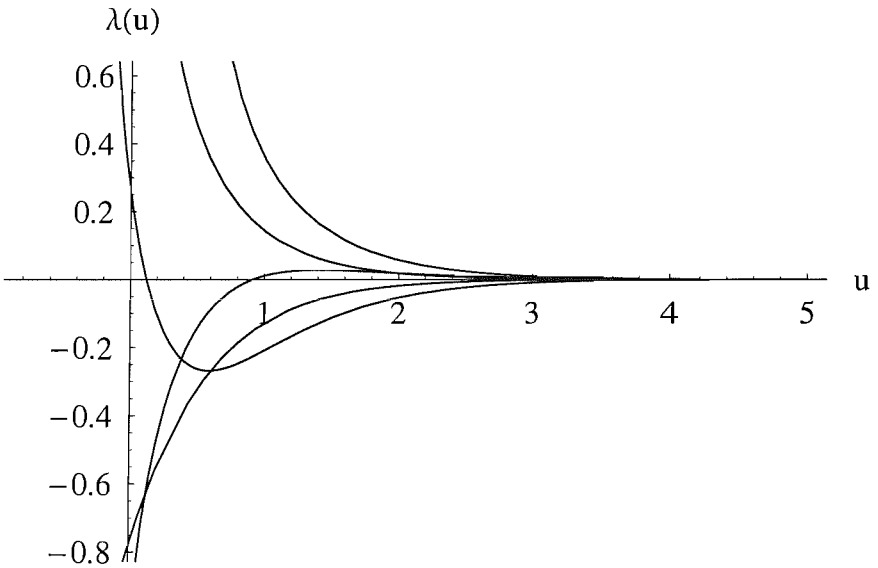

Figure 7.1: Plot of the scalar field $\lambda(u)$ for various values of $\mathcal{M}$ and $\mathcal{C}$.

Generically, the flows diverge in the IR with $\lambda \to \pm\infty$. It is interesting to study the IR behaviour and, in particular, how the different types of IR asymptotics relate to values of $\mathcal{M}$ and $\mathcal{C}$ which set the UV boundary conditions. Figure 7.2 shows a plot of the sign of the IR divergence as a function of the $\mathcal{M}$ and $\mathcal{C}$ boundary conditions.

The supersymmetric flows are given by the line $\mathcal{M} = 0$. There is a line of maximum stability between those solutions which asymptote to $\pm\infty$. The supersymmetric solutions lie on this line, but there is another set of solutions which are approximately the $\mathcal{M} = -\mathcal{C}$ flows.

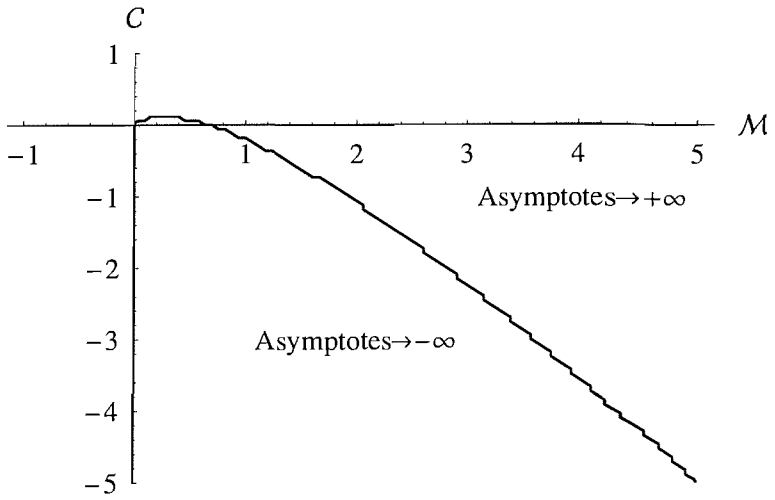

Figure 7.2: IR asymptotic behaviour of λ as a function of the mass and condensate defined by the boundary conditions in the UV. The supersymmetric line ($\mathcal{M} = 0$) is on the line of stability between those flows which diverge to $+\infty$ and $-\infty$. As seen from figure 6.1, these supersymmetric flows do diverge.

The ten-dimensional lift shares exactly the same form of the metric as the supersymmetric case:

$$ds^2 = \frac{\sqrt{X}}{\chi} e^{2A} dx^2 - \frac{\sqrt{X}}{\chi} \left(du^2 + \frac{R^2}{\chi^2} \left[d\theta^2 + \frac{\sin^2\theta}{X} d\phi^2 + \frac{\chi^6 \cos^2\theta}{X} d\Omega_3^2 \right] \right) , \quad (7.4)$$

where the parameters are defined in the same way as the $\mathcal{N} = 4$ case and

$$\chi = e^{\frac{\lambda(u)}{\sqrt{6}}} . \quad (7.5)$$

The four-form potential of the lift does not match the supersymmetric case but in neither case does it enter into the DBI action of the D7-brane probe.

7.2 Adding Quarks to the Non-Supersymmetric Scalar Deformation

It is important to note that there are masses and condensates for two different operators discussed in this section. One set (written in calligraphic text) defines the deformed geometry and is associated with the scalar bilinear operator. The second set is associated with the quark bilinear operator introduced with the D7-brane embedding and is always referred to by name rather than letter.

From chapter 6, it is known that the coordinates of equation 7.4 are not the physical ones in which to define the gauge theory living on a D7-brane. However, whereas in the supersymmetric case, the physical coordinates were found by using the first order equations of motion for the fields, this technique cannot be used in this case.

It was found in chapter 6 that, though the original coordinates were not physical for a non-zero quark mass, in the massless case the original and physical coordinates coincided. In the current geometry therefore, the D7-brane flow from the UV to the IR is used to discover whether, in the massless limit, a condensate is induced. As in the previous chapter, the brane is embedded in the $x_{//}, u, \Omega_3$ directions and the flow of θ as a function of r is calculated. The same change of variables used in the supersymmetric scalar deformation (equation 6.20) is utilised here. Using the symmetries of the background, the IR boundary conditions are set and the flow from the IR to the UV is calculated. By studying the UV behaviour, the values of the mass and condensate are calculated. A set of D7-brane flows is

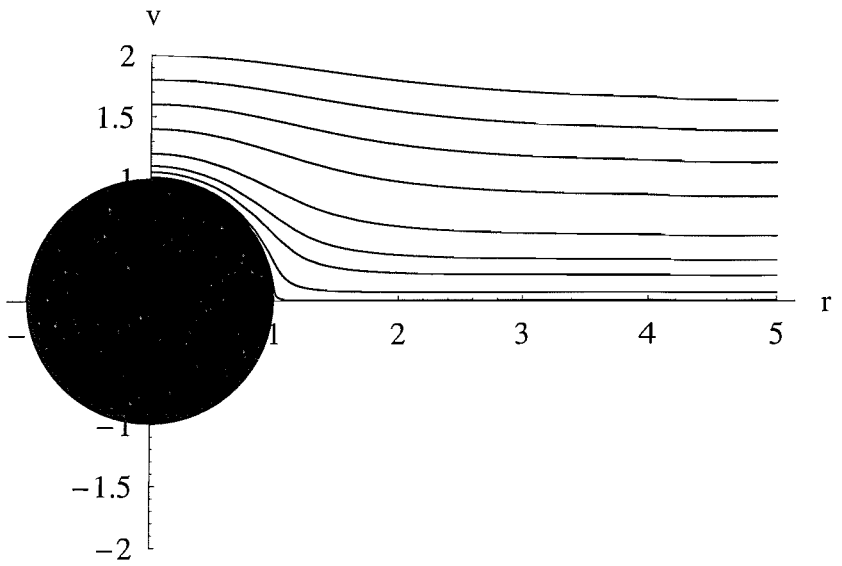

Figure 7.3: Sample solutions for a D7-brane embedding in the non-supersymmetric scalar deformation geometry showing the absence of a gap between the solutions and the singularity.

plotted in figure 7.3. In this example the scalar deformation has positive values of $\mathcal{M}$ and $\mathcal{C}$.

For all values of $\mathcal{M}$ and $\mathcal{C}$, defining the scalar deformation, in the massless quark limit the brane wraps onto the surface of the singularity (see figure 7.3). The quark bilinear condensate can be calculated numerically for this flow, and is always zero, indicating that in this geometry (as in the previous one) there is no chiral symmetry breaking.

In chapter 6, it was indicated that the numerical methods may not be reliable. It would be more persuasive if it were proved analytically that the singular region does not repel the brane, indicating that in the physical coordinate system, the

brane would flow in a straight line just as in figure 4.2.1. The next step is to study the IR region using the analytic techniques devised in the previous two chapters.

7.3 Analytic Search for Chiral Symmetry Breaking

Though the geometry is complicated as the solution of the scalar field, λ, is known only numerically, approximations can be made in the IR such that the limiting behaviour of the field can be calculated analytically. In the IR, the scalar field asymptotes to $\pm\infty$ meaning that the potential for the scalar field in this region can be approximated by

$$V = -2e^{\frac{\pm 2\lambda(u)}{\sqrt{6}}} = -2\chi(u)^{\pm 2} \ , \tag{7.6}$$

where the $\pm$ depends on whether the solution asymptotes to $\pm\infty$. When this potential is used in the equation of motion it can be solved analytically by inspection, assuming the form:

$$\lambda(u) = a\log(b(u-u_s)) \ , \qquad \chi(u) = (b(u-u_s))^{\frac{a}{\sqrt{6}}} \ . \tag{7.7}$$

By using this ansatz in the equation of motion, there are four possible solutions given by

$$\chi_1(u) = \sqrt{\tfrac{45}{2}}\tfrac{1}{(u-u_s)} \ , \qquad A_1(u) = 4\log(c(u-u_s)) \ , \tag{7.8}$$

$$\chi_2(u) = (\tfrac{2}{3}(u-u_s))^{\frac{1}{2}} \ , \qquad A_2(u) = \log(c(u-u_s)) \ , \tag{7.9}$$

$$\chi_3(u) = (b(u-u_s))^{\frac{1}{4}} \ , \qquad A_3(u) = \frac{1}{4}\log(c(u-u_s)) \ , \tag{7.10}$$

$$\chi_4(u) = (b(u-u_s))^{-\frac{1}{4}} \ , \qquad A_4(u) = \frac{1}{4}\log(c(u-u_s)) \ , \tag{7.11}$$

where b, and u_s are the free parameters of the second order equations of motion and c is a function of b, determined by matching onto the UV behaviour. The value of c is unimportant in all the following calculations. u_s corresponds to the value of u where the solution becomes singular. By studying the IR asymptotics of the supersymmetric equations of motion, it can be shown that the supersymmetric solution is given by equation 7.11 with $b = \frac{4}{3}$. This solution flows to the UV solutions with $\mathcal{M} = 0$ (figure 7.2).

Apart from the supersymmetric case (corresponding to the line $\mathcal{M} = 0$), there is no known analytic link between the UV and IR behaviour. Equations 7.8 and 7.9 appear to lie close to the ridge in figure 7.2. Equation 7.10 corresponds to the small quadrant which approximately corresponds to the lower right octant between the lines: $\mathcal{M} = 0$ and $\mathcal{C} = -\mathcal{M}$. Equation 7.11 corresponds to the majority of the plot where the field diverges to $+\infty$. This includes the supersymmetric flow.

7.4 Brane Wrapping the Non-Supersymmetric Scalar Deformation

Having found these solutions, the potential of a wrapped brane in the presence of the scalar potential can be calculated. The action for a D7-brane can be written with u and ϕ as perpendicular directions to the brane, with $u(\theta)$ and ϕ constant, giving

$$\begin{aligned} S_{DBI} &= -T_7 \int d^8\xi R^4 \sqrt{\cos(\theta)^2 + \chi(u(\theta))^6 \sin^2(\theta)} e^{4A(u(\theta))} \chi(u(\theta)) |\cos^3(\theta)| \\ &\cdot \sqrt{1 + \left(\frac{du(\theta)}{d\theta}\right)^2 \frac{\chi(u(\theta))^2}{R^2}} \, . \end{aligned} \tag{7.12}$$

Having calculated the analytic IR form of the scalar field, the potential can also be calculated analytically. This is the action with the variation of u with respect to θ set to zero. Care must be taken as the potential will vary for different values of θ. For instance the term $X = \sqrt{\cos^2\theta + \chi^6 \sin^2\theta}$ in the divergent χ limit has different behaviour for varying values of θ. The following gives the behaviour for $\theta \neq (0, \frac{\pi}{2})$ corresponding to the four solutions given by equations 7.8 to 7.11:

$$S_{DBI,1} \sim -\int d^8\xi (u_0 - u_s)^{12} |\sin(\theta)| |\cos^3(\theta)| \, , \tag{7.13}$$

$$S_{DBI,2} \sim -\int d^8\xi (u_0 - u_s)^{\frac{9}{2}} \cos^4(\theta) \, , \tag{7.14}$$

$$S_{DBI,3} \sim -\int d^8\xi (u_0 - u_s)^{\frac{5}{4}} \cos^4(\theta) \, , \tag{7.15}$$

$$S_{DBI,4} \sim -\int d^8\xi |\sin(\theta)| |\cos^3(\theta)| \, . \tag{7.16}$$

For $\theta = (0, \frac{\pi}{2})$, the potential in the IR is zero for all the analytic solutions.

Equations 7.13 to 7.15 are clearly minimised when $u_0 = u_s$ and the wrapped brane feels no repulsive potential. This means that a brane flowing from the UV

to the IR will wrap onto the surface of the singularity in the massless limit, and therefore there will be no chiral symmetry breaking.

Care must be taken with equation 7.16 which appears not to depend on u in the IR. The solution interpolates to e^{4r} in the UV. By performing the calculation numerically, a monotonically increasing potential for the brane, as a function of ρ, is found, indicating that for this solution, the brane also collapses onto the singularity just as in figure 6.5.

This non-supersymmetric deformation of $\mathcal{N} = 4$ super-Yang-Mills appears to preserve the chiral symmetry of the undeformed geometry. There is one major qualitative difference between this background and the Constable-Myers geometry – this background has a constant dilaton field in contrast to the flowing dilaton in Constable-Myers.

It may be that a dual gravity theory requires a running dilaton to trigger chiral symmetry breaking on the gauge theory side. This could be triggered when the magnitude of the dilaton reaches some critical value. It would be valuable to discover the generic properties of a background needed to trigger chiral symmetry breaking in a field theory dual.

As indicated in chapter 6, a further way to see if chiral symmetry is preserved in a geometry would be to calculate the meson spectrum. The Gell-Mann-Oakes-Renner relation (equation 3.11) indicates that in a model with chiral symmetry breaking, the meson mass is proportional to the square root of the quark mass, whereas the two masses are proportional in the case where chiral symmetry is preserved. The eigenvalues for the scalar field should not depend on the coordi-

nate system and therefore it should be possible to calculate the behaviour of the pion mass as a function of the quark mass even in the unphysical coordinates. Again, this is an interesting avenue for future research.

Chapter 8

An $\mathcal{N} = 2^\star$ Geometry

In chapter 9, a complicated deformation of $AdS_5 \times S^5$ that appears to be dual to a remarkably QCD-like theory, is studied. In order to understand some of the problems that are faced in this highly non-trivial deformation, another supersymmetric geometry is studied. In this chapter, quarks are added to the field theory dual to the $\mathcal{N} = 2^\star$ geometry. Though chiral symmetry breaking is not exhibited, studying this geometry proves a useful exercise before tackling the complicated background of chapter 9.

8.1 The Background

This background [99, 103] is a more complicated deformation of $AdS_5 \times S^5$ that is still supersymmetric, but does have a running dilaton. This geometry is complicated as the field equations have not been solved analytically, and because there are several R-R and NS-NS fields in the background that have not been switched on in the preceding geometries. There is also no simple three-sphere on which to

wrap a D7-brane as there has been in the previous examples.

This background is dual to the $\mathcal{N}=4$ geometry with the addition of a mass term for two of the adjoint chiral matter fields. This means that it contains the massless fields of $\mathcal{N}=2$ super-Yang-Mills, and therefore has a two-dimensional moduli-space (coming from the vev of the complex scalar field). The $\star$ in the name of this geometry indicates that this theory has a UV completion with a higher degree of supersymmetry ($\mathcal{N}=4$).

As in the geometries discussed in chapters 6 and 7, this background is derived from the lift of a five-dimensional supergravity solution to ten dimensions [99]. The solution to this lift in Einstein frame is given by

$$ds^2 = \Omega^2\left(e^{2A}dx_{//}^2 + dr^2\right) + \frac{R^2\Omega^2}{\chi^2}\left(\frac{d\theta^2}{c} + \chi^6\cos^2\theta\left(\frac{\sigma_1^2}{cX_2} + \frac{\sigma_2^2+\sigma_3^2}{X_1}\right) + \frac{\sin^2\theta}{X_2}d\phi^2\right) \tag{8.1}$$

In this metric

$$\begin{aligned}
\Omega^2 &= \frac{(cX_1X_2)^{\frac{1}{4}}}{\chi}\,, \\
c &= \cosh 2\zeta\,, \\
X_1 &= \cos^2\theta + \chi^6 c\sin^2\theta\,, \\
X_2 &= c\cos^2\theta + \chi^6\sin^2\theta\,, \\
C_{(4)} &= \frac{e^{4A}X_1}{4g_s\chi^2}dx^0\wedge dx^1\wedge dx^2\wedge dx^3\,,
\end{aligned} \tag{8.2}$$

where ζ , A and χ are the five-dimensional supergravity fields. The axion/dilaton

is

$$\begin{aligned}
\lambda &= i\left(\frac{1-B}{1+B}\right) = C_{(0)} + ie^{-\Phi} \ , \\
B &= e^{2i\phi}\left(\frac{b^{\frac{1}{4}} - b^{-\frac{1}{4}}}{b^{\frac{1}{4}} + b^{-\frac{1}{4}}}\right) \ , \\
b &= \frac{X_1}{X_2}\cosh 2\zeta \ .
\end{aligned} \tag{8.3}$$

Additionally, there is the anti-symmetric two-form, whose NS-NS and R-R parts are given respectively by

$$\begin{aligned}
B_{(2)} &= a_3 \cos\phi\, \sigma_1 \wedge \mathrm{d}\phi + a_1 \sin\phi\, \mathrm{d}\theta \wedge \sigma_1 - a_2 \sin\phi\, \sigma_2 \wedge \sigma_3 \ , \\
C_{(2)} &= -a_1 \cos\phi\, \mathrm{d}\theta \wedge \sigma_1 + a_2 \cos\phi\, \sigma_2 \wedge \sigma_3 + a_3 \sin\phi\, \sigma_1 \wedge \mathrm{d}\phi \ ,
\end{aligned} \tag{8.4}$$

where

$$\begin{aligned}
a_1 &= R^2 \tanh 2\zeta \cos\theta \ , \\
a_2 &= R^2 \frac{\chi^6 \sinh 2\zeta}{X_1} \sin\theta \cos^2\theta \ , \\
a_3 &= R^2 \frac{\sinh 2\zeta}{X_2} \sin\theta \cos^2\theta \ .
\end{aligned} \tag{8.5}$$

The supergravity fields ζ, A and $\chi = e^{\alpha}$ satisfy the equations of motion:

$$\begin{aligned}
\frac{d\alpha}{dr} &= \frac{1}{3R}\left(\frac{1}{\chi^2} - \chi^4 \cosh(2\zeta)\right) \ , \\
\frac{dA}{dr} &= \frac{2}{3R}\left(\frac{1}{\chi^2} + \frac{1}{2}\chi^4 \cosh(2\zeta)\right) \ , \\
\frac{d\zeta}{dr} &= -\frac{1}{2R}\chi^4 \sinh(2\zeta) \ .
\end{aligned} \tag{8.6}$$

These have solutions:

$$\begin{aligned}
e^A &= k\frac{\chi^2}{\sinh(2\zeta)} \ , \\
\chi^6 &= \cosh(\zeta) + \sinh^2(2\zeta)\left(\gamma + \log(\tanh\zeta)\right) \ ,
\end{aligned} \tag{8.7}$$

where γ is a free parameter which defines different forms of the deformation. In the large γ limit, these solutions deform into the $\mathcal{N}=4$ solutions of chapter 6. In this case, the vev is much larger than the supersymmetry breaking scale so the theory is effectively $\mathcal{N}=4$. The $\gamma=0$ geometry differs most from those studied in the previous chapters. This geometry can be probed with a D3-brane [104, 105]. Performing this embedding demonstrates that, when $\theta=\frac{\pi}{2}$, there is a moduli-space corresponding to the vanishing of the potential felt by the brane probe. It is possible to find the physical coordinates in which to describe the field theory and in particular these coordinates give the correct computation of the β-function. As in the $\mathcal{N}=4$ background, this coordinate change takes the spherical singularity to a disk.

The singular behaviour in this geometry comes from the supergravity fields ζ , A and χ, which asymptote to $\pm\infty$ in the IR. This asymptotic behaviour allows the limiting IR solutions to the equations of motion (equation 8.6) to be calculated analytically, just as in section 7.3. The solutions are given by

$$\begin{aligned}
\zeta(r) &= -\frac{3}{2}\log\left(\left(\frac{2}{3^5}\right)^{\frac{1}{3}}\frac{r-r_s}{R}\right) , \\
\chi(r) &= \frac{\sqrt{2}}{3}\sqrt{\frac{(r-r_S)}{R}} , \\
A(r) &= 4\log\left(\frac{(r-r_s)}{R}\right)+b , \qquad (8.8)
\end{aligned}$$

where $b=\log k+\log\left(\frac{8}{2187}\right)$ and k is a constant of integration fixed by the UV asymptotics. r_s, the radius of the singularity, is the single free parameter of the equations of motion.

8.2 Adding Quarks to the $\mathcal{N} = 2^\star$ Scalar Deformation

Quarks can now be added to the field theory by embedding a D7-brane in the $\mathcal{N} = 2^\star$ background. Whereas in all previous examples there has been an explicit three-sphere on which to wrap the D7-brane, in this geometry it is not obvious how to embed the brane. When quark fields are included, the chiral superfields have a superpotential coupling to the $\mathcal{N} = 4$ adjoint scalars of the form $\tilde{Q}AQ$, where the adjoint field is represented in the geometry by the two transverse directions to the D7-brane. In this geometry, the $\mathcal{N} = 4$ fields have already been broken to $\mathcal{N} = 2$ multiplets and care must be taken that the embedding does not break this symmetry further. To ensure this, the probe must lie perpendicular to the $\theta = \frac{\pi}{2}$ plane, because this plane corresponds to the massless scalar fields.

To calculate the potential of a D7-brane in this background, the three one-forms, $\sigma_{1,2,3}$, are written in terms of the spherical coordinates α, β, ψ which are taken from the parametrisation of an undeformed three-sphere:

$$\begin{aligned}
\sigma_1 &= \frac{1}{2}(d\alpha + \cos\psi d\beta) \ , \\
\sigma_2 &= \frac{1}{2}(\cos\alpha d\psi + \sin\alpha\sin\psi d\beta) \ , \\
\sigma_3 &= \frac{1}{2}(\cos\alpha\sin\psi d\beta - \sin\alpha d\psi) \ .
\end{aligned} \tag{8.9}$$

This converts the metric to the form:

$$\begin{aligned} ds^2 &= \Omega^2(e^{2A}dx_{//}^2 + dr^2) + \frac{R^2\Omega^2}{\chi^2}\left(\frac{1}{c}d\theta^2 + \frac{\sin^2\theta}{X_2}d\phi^2\right. \\ &\left. + \frac{\chi^6\cos^2\theta}{4}\left(\frac{d\psi^2}{X_1} + \frac{d\alpha^2}{cX_2} + d\beta^2\left(\frac{\sin^2\psi}{X_1} + \frac{\cos^2\psi}{cX_2}\right) + \frac{2d\alpha d\beta\cos\psi}{cX_2}\right)\right) . \end{aligned} \tag{8.10}$$

To study the D7-brane flow from the UV to the IR, the most natural embedding is in the $x_{//}$, r, α, β and ψ directions. From this, the DBI action can be calculated. However, it can be seen that the two perpendicular directions, θ and ϕ, will be dependent on both r and ψ making the equations of motion extremely difficult to solve. This contrasts with the previous examples where the perpendicular directions were dependent only on a single variable. This is discussed in more detail in chapter 9 where the Yang-Mills* geometry is investigated. Rather than attempting the UV/IR flow solution, for which no numerical calculation has yet been successfully performed, the wrapping techniques developed in the previous chapters are used to look at the potential felt by a D7-brane around the singularity. The wrapping brane has two perpendicular directions, r and ϕ, which are now functions of θ and ψ. ϕ is taken to be constant which, as before, corresponds to choosing a direction in the $SO(2)$ plane. This embedding is illustrated in table 8.1.

For simplicity, the brane is embedded with $\phi = n\pi$ where the axion vanishes and the dilaton is given by

$$e^{\Phi} = \sqrt{\frac{cX_1}{X_2}} , \tag{8.11}$$

and in this case, the NS-NS two-form is also zero. The DBI action for this

	x_0	x_1	x_2	x_3	r	θ	ϕ	α	β	ψ
D3	×	×	×	×	.	.	.	.	.	.
D7	×	×	×	×	.	×	.	×	×	×

Table 8.1: D3-brane and D7-brane embedding in the $\mathcal{N} = 2^*$ geometry. Filled dimensions are marked with crosses, those perpendicular to the world-volumes are denoted by a dot.

configuration is

$$S_{DBI} = \int d^8\xi \frac{R^4}{4} e^{4A} c X_1 \cos^2\theta |\sin\psi| \cdot \sqrt{\left(\frac{\chi^2\cos^2\theta}{4cX_1} + \frac{\chi^4\cos^2\theta}{4R^2X_1}\left(\frac{\partial r}{\partial\theta}\right)^2 + \frac{1}{cR^2\chi^2}\left(\frac{\partial r}{\partial\psi}\right)^2\right)} . \quad (8.12)$$

Whereas in the previous cases, it has been simple to see that the Wess-Zumino term is not important, more care must be taken here to show that it vanishes. The gauge fields living on the brane are order α' corrections so the Wess-Zumino term is given by

$$S_{WZ} = T_7 \int_{\mathcal{M}_8} (c_{(8)} + C_{(6)} \wedge B_{(2)}) . \quad (8.13)$$

However, due to the decision to set $\phi = n\pi$, the dual of the axion, $C_{(8)}$, vanishes. The second term is zero because the pullback onto the D7-brane world-volume of these two fields, when $\phi = n\pi$, also vanishes. As in the previous analysis, only the IR behaviour is of interest and so the exact solutions to the asymptotic equations of motion found in equation 8.8 can be used. The DBI potential of a spherical brane is then

$$V_{IR} \sim (r - r_s)^{15} |\cos^3\theta| |\sin\psi| \sqrt{5 + \cos 2\theta} . \quad (8.14)$$

This minimises the action when $r = r_s$. Note that the kinetic terms are important for all solutions, excluding those in the IR asymptotic region.

The D7-brane feels no repulsion from the singularity and so this test demonstrates that this background, as expected, does not induce chiral symmetry breaking. It must be noted that the particular embedding chosen is one which retains the original supersymmetry. It may be possible to find an embedding which does reproduce chiral dynamics though the analysis would be more complex. The main reason to study this background is as a preliminary exercise for the more complicated geometry studied in chapter 9.

Chapter 9

The Yang-Mills* Geometry

The final background studied for evidence of chiral symmetry breaking is the geometry whose dual most closely resembles QCD. It is also the most complicated deformation, and all the techniques developed from studying the previous geometries are crucial to gain insight into the phenomenology of the field theory that is dual to this background.

9.1 The Background

This background is another lift constructed from a five-dimensional supergravity in [106, 107]. Again, it is a deformation of $AdS_5 \times S^5$ so the field theory is deformed by a relevant operator. The supersymmetry is broken in this geometry by adding a scalar that corresponds to an equal mass and/or vev for the gaugino operator $\mathcal{O} = \sum_{i=1}^{4} \psi_i \psi_i$. Once the supersymmetry is broken, the masses of the scalars are no longer protected and these decouple from the low-energy theory. This means that the low-energy theory contains only gauge fields. Once quarks

are added to this geometry, the theory appears to be very similar to QCD. As all supersymmetry is removed, all equations of motion for the fields are second order, which must be solved numerically.

The five-dimensional background is constructed using the familiar ansatz for the metric:

$$ds^2 = e^{2A(r)} dx^\mu dx_\mu + dr^2 \ . \tag{9.1}$$

The scalar field Lagrangian can be written as

$$\mathcal{L} = \frac{1}{2}(\partial\lambda)^2 - V(\lambda) \ . \tag{9.2}$$

The scalar field of interest is in the **10** of $SO(6)$, which corresponds to a source and vev for the operator $\mathcal{O}$. This is the same operator as in the $\mathcal{N} = 1^*$ solution formulated in [108, 109, 110] which contains two supergravity scalars. These scalars are set equal to obtain the Yang-Mills* background. The potential for this scalar is given by

$$V = -\frac{3}{2}(1 + \cosh^2 \lambda) \ . \tag{9.3}$$

The equations of motion for this field are then the usual second order differential equations:

$$\begin{aligned} \lambda''(r) + 4A'(r)\lambda'(r) &= \frac{\partial V}{\partial \lambda(r)} \ , \\ 6A'(r)^2 &= \lambda'(r)^2 - 2V \ , \\ -3A''(r)6A'(r)^2 &= \lambda'(r)^2 + 2V \ . \end{aligned} \tag{9.4}$$

9.1.1 UV and IR Asymptotics of the Yang-Mills* Geometry

The AdS/CFT dictionary can be used to understand the UV behaviour of the field theory. For a supergravity scalar, the mass of the field is related to the conformal dimension of its dual field theory operator as explained in section 2.2.3:

$$m^2 = \Delta(\Delta - 4) \ . \tag{9.5}$$

This means that as the operator of interest is of dimension 3, $m^2 = -3$ so that in the UV, the potential is

$$V = -3 + \frac{m^2}{2}\lambda^2 \ . \tag{9.6}$$

In the UV, the space returns to $AdS_5 \times S^5$ as $\lambda \to 0$. The UV behaviour of the solution is

$$\lambda(r)|_{UV} = \mathcal{M}e^{-r} + \mathcal{K}e^{-3r} \ . \tag{9.7}$$

In this parametrisation of the metric, under conformal scaling $e^r \to \beta e^r$ as $x \to \frac{x}{\beta}$. Therefore, $\mathcal{K}$ and $\mathcal{M}$ have scaling dimensions three and one respectively, so they correspond to a vev and mass for the fermion bilinear operator. The scalar field solutions can be calculated numerically using these boundary conditions and, as before, some of the solutions asymptote to $-\infty$ and some to $+\infty$. An analysis, similar to the non-supersymmetric scalar deformation, carried out in chapter 7, can be performed by studying the IR asymptotics as a function of the UV boundary conditions, $(\mathcal{M}, \mathcal{K})$ (figure 9.1).

In section 9.2.2 the IR asymptotic solutions to the supergravity equations are calculated using the same methods as in chapters 7 and 8. From these solutions,

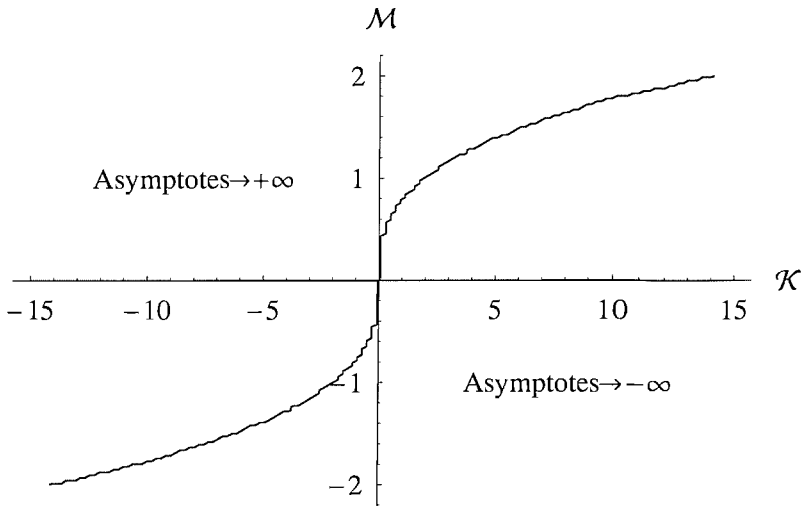

Figure 9.1: Plot of the IR asymptotic flow of the five-dimensional supergravity field corresponding to a fermion bilinear as a function of the UV boundary conditions. The lower half corresponds to flows which asymptote to negative infinity while those in the top half asymptote to positive infinity.

and figure 9.1, it is be possible to extract information about the near-singular potential for different UV scalar field boundary conditions.

9.1.2 The Ten-Dimensional Lift

The uplift to ten dimensions is described briefly here. In order to use Einstein's equation the stress-energy tensor for all the fields in the ten-dimensional bosonic spectrum must be known. Einstein's equation is

$$R_{MN} = T^{(1)}_{MN} + T^{(3)}_{MN} + T^{(5)}_{MN} \ , \tag{9.8}$$

where the indices are ten-dimensional curved-space indices and

$$\begin{aligned} T^{(1)}_{MN} &= P_M P^\star_N + P_N P^\star_M \ , \\ T^{(3)}_{MN} &= \frac{1}{8}\left(G^{PQ}{}_M G^\star_{PQN} + G^{\star PQ}{}_M G_{PQN} - \frac{1}{6} g_{mn} G^{PQR} G^\star_{PQR} \right) \ , \\ T^{(5)}_{MN} &= \frac{1}{6} F^{PQRS}{}_M F_{PQRSN} \ . \end{aligned} \tag{9.9}$$

These are the stress-energy tensors for the dilaton/axion, three-form and five-form field strengths respectively. The dilaton is written (in unitary gauge) in terms of a field B:

$$P_M = f^2 \partial_M B \ , \qquad Q_M = f^2 Im(B \partial_M B^\star) \ , \qquad f = \frac{1}{\sqrt{1 - BB^\star}} \ , \tag{9.10}$$

where the dilaton/axion combination is given by

$$\tau = a + ie^\Phi = i\frac{1-B}{1+B} \ . \tag{9.11}$$

This parametrisation is of the form $P_M = i\dfrac{\partial_M \tau}{2\mathrm{Im}\,\tau}$, as in section 5.1. The three-form field strength is written as

$$G_{(3)} = f(F_{(3)} - BF^\star_{(3)}) \ . \tag{9.12}$$

The equations of motion for the bosonic fields are then

$$\begin{aligned} (\Delta^R - iQ^R) G_{MNR} &= P^R G^\star_{MNR} - \frac{2}{3} i F_{MNQRS} G^{QRS} \ , \\ (\Delta^M - 2iQ^M) P_M &= -\frac{1}{24} G^{QRS} G_{QRS} \ . \end{aligned} \tag{9.13}$$

The self-duality condition for the five-form is imposed by hand: $F_{(5)} = \star F_{(5)}$. The Bianchi identities are given by

$$F_{(3)} = dA_{(2)} \ , \qquad dF_{(5)} = -\frac{1}{8}\mathrm{Im}\left(F_{(3)} \wedge F^\star_{(3)}\right) \ . \tag{9.14}$$

It is now necessary to find the operator which is dual to the gluino bilinear in the ten-dimensional theory. The lift of the five-dimensional scalar dual to the operator of interest is lifted to a two-form potential. The operator transforms in the $(\mathbf{4} \times \mathbf{4})_{sym} = \mathbf{10}$ of $SU(4)_R$. The three-form field strength must, therefore, have the correct rotational symmetry in the six-dimensional space perpendicular to the brane stack to make an $SU(4)_R$ singlet with the field theory operator. The six transverse directions are written in terms of three complex planes:

$$z_1 = \frac{w^1 + iy^1}{\sqrt{2}} , \qquad z_2 = \frac{w^2 + iy^2}{\sqrt{2}} , \qquad z_3 = \frac{w^3 + iy^3}{\sqrt{2}} . \tag{9.15}$$

It transpires that the three-form field strength with the correct symmetries is given by

$$\begin{aligned} F_{(3)} &= < \psi_1\psi_1 > dz^1 \wedge d\bar{z}^2 \wedge d\bar{z}^3 + < \psi_2\psi_2 > d\bar{z}^1 \wedge dz^2 \wedge d\bar{z}^3 \\ &+ < \psi_3\psi_3 > d\bar{z}^1 \wedge d\bar{z}^2 \wedge dz^3 + < \psi_4\psi_4 > dz^1 \wedge dz^2 \wedge dz^3 , \end{aligned} \tag{9.16}$$

where the $< \psi_a\psi_a >$ are the vevs of the gaugino bilinears. The operator of interest is the one in which all the gauginos are given the same mass and vev. This corresponds to a three-form:

$$F_{(3)} = dw^1 \wedge dw^2 \wedge dw^3 + dy^1 \wedge dy^2 \wedge dy^3 . \tag{9.17}$$

The final reparametrisation of this geometry is achieved by rewriting the six-plane in terms of a pair of two-spheres, a radial coordinate corresponding to the energy in the field theory, and an angle between the two-spheres. Each two-sphere is a spherical section in one of the three-dimensional spaces w and y. The metric for the two-spheres is parametrised as follows:

$$d\Omega_{\pm}^2 = d\theta_{\pm}^2 + \cos^2\theta_{\pm} d\phi_{\pm}^2 . \tag{9.18}$$

The two-form potential of the three-form field strength is

$$A_{(2)} = \cos^3\alpha \cos\theta_+ d\theta_+ \wedge d\phi_+ + \sin^3\alpha \cos\theta_- d\theta_- \wedge d\phi_- \quad . \tag{9.19}$$

The calculation of this two-form has been performed in the UV region where there is a quantitative link between the field theory and supergravity background. Though this has the correct symmetry properties for the operator in question, this does not give the correct five-dimensional truncation. In order to achieve the correct five-dimensional truncation this equation of motion for the two-form must reproduce the UV asymptotic behaviour of the five-dimensional field λ. This is given by

$$A_{(2)} = 2\lambda(i\cos^3\alpha \cos\theta_- d\theta_+ \wedge d\phi_+ + \sin^3\alpha \cos\theta_- d\theta_- \wedge d\phi_-) \ . \tag{9.20}$$

This solution then produces the full ten-dimensional flow of the two-form field strength.

The metric and dilaton are calculated using an ansatz formulated in [111, 112]. In [106], the lift of this deformation was calculated using the $\mathcal{N} = 1^\star$ lift [108, 109, 110] by equating the two scalars. The full ten-dimensional uplift solution is

$$
\begin{aligned}
ds_{10}^2 &= \xi^{\frac{1}{2}}(e^{2A}dx^2 + dr^2) + \xi^{-\frac{3}{2}}(\xi^2 d\alpha^2 + \sin^2\alpha F_+ d\Omega_+^2 + \cos^2\alpha F_- d\Omega_-^2), \\
d\Omega_\pm^2 &= d\theta_\pm^2 + \sin^2\theta_\pm d\phi_\pm^2 \ , \\
\xi^2 &= \cosh^4\lambda(r) + \sinh^4\lambda(r)\cos^2 2\alpha \ , \\
F_\pm &= \cosh^2\lambda(r) \pm \sinh^2\lambda(r)\cos 2\alpha \ , \\
A\pm &= \frac{\sinh 2\lambda(r)}{\cosh^2\lambda(r) \pm \cos 2\alpha \sinh^2\lambda(r)} \ , \\
B &= \frac{\sinh^2\lambda(r)\cos 2\alpha}{\cosh^2\lambda(r) + \xi} \ , \\
e^{-\Phi} &= \frac{1-B}{1+B} \ , \\
A_{(2)} &= iA_+(\lambda(r),\alpha)\cos^3\alpha\cos\theta_+ d\theta_+ \wedge d\phi_+ - A_-(\lambda(r),\alpha)\sin^3\alpha\cos\theta_- d\theta_- \wedge d\phi_- \ , \\
C_{(4)} &= \omega(r,\alpha) dx^0 \wedge dx^1 \wedge dx^2 \wedge dx^3 \ , \\
\omega(r) &= e^{4A(r)}A'(r) \ .
\end{aligned}
\tag{9.21}
$$

9.2 D3-Brane Probing the Yang-Mills* Geometry

9.2.1 UV Asymptotics

Prior to adding quarks, it is interesting to study the stability of various solutions parametrised by different values of the mass of the gauginos and the gaugino bilinear condensate ($\mathcal{M}$ and $\mathcal{K}$ respectively). To study the stability, the probe potential of a D3-brane is calculated. In this case, the DBI action is given by

$$
S_{probe} = -\tau_3 \int_{\mathcal{M}_4} dx^4 \sqrt{|G_{ab}^E + 2\pi\alpha' e^{-\Phi/2} F_{ab}|} + \mu_3 \int_{\mathcal{M}_4} C_{(4)} \ , \tag{9.22}
$$

with $\mu_3 = g_s\tau_3$. Calculating the pullback, the probe potential is

$$V_{probe} = e^{4A}(\zeta - A'(r)) \ . \tag{9.23}$$

The region of interest is the UV of the potential and if this is unbounded, the field theory will not be well behaved. The UV behaviour for this potential can be calculated and is given by

$$V_{UV} = \frac{1}{9}\mathcal{M}(9\mathcal{K} + 5\mathcal{M}^2) + \frac{1}{4}\mathcal{M}^4\cos 4\alpha + \frac{2}{3}\mathcal{M}^2 e^{2r} \ . \tag{9.24}$$

Therefore, the condensate-only solution is unbounded. A gaugino mass must be present to produce a well-defined field theory.

9.2.2 IR Asymptotics

The IR asymptotic solutions to the equations of motion for λ and A can be calculated using the techniques employed in the previous examples. The solutions are

$$\lambda_{IR,1}(r) = -\log\left(\sqrt{\tfrac{9}{20}}(r - r_s)\right) \ , \qquad A = 2/3\log(r - r_s) \ , \tag{9.25}$$

$$\lambda_{IR,2}(r) = \log\left(\sqrt{\tfrac{9}{20}}(r - r_s)\right) \ , \qquad A = 2/3\log(r - r_s) \ , \tag{9.26}$$

$$\lambda_{IR,3}(r) = -\tfrac{\sqrt{6}}{4}\log(a(r - r_s)) \ , \qquad A = 1/4\log(r - r_s) \ , \tag{9.27}$$

$$\lambda_{IR,4}(r) = \tfrac{\sqrt{6}}{4}\log(a(r - r_s)) \ , \qquad A = 1/4\log(r - r_s) \ , \tag{9.28}$$

where a and r_s are free parameters, the latter setting the size of the singularity. This IR behaviour cannot be linked analytically with the UV boundary conditions. However, each IR flow can be numerically solved into the UV to establish where in the $(\mathcal{M}, \mathcal{K})$ phase-space each IR solution flows to.

Equations 9.25 and 9.26 appear to lie very close to the critical line in figure 9.1 between those solutions that asymptote to $\pm\infty$ in the IR. In particular, equation 9.25 flows to positive mass and positive condensate solutions and lies just above the critical line, while equation 9.26 flows to negative mass and negative condensate solutions and lies just below the critical line.

Equation 9.27 appears to fill the remaining positive $\mathcal{K}$ region of figure 9.1, and equation 9.28 completes the negative $\mathcal{K}$ region. In particular, the $\mathcal{M} = 0$ solutions are given by equations 9.27 and 9.28 with $a = 1.42$, and the $\mathcal{K} = 0$ solutions are given by $a = 3.64$.

Using equations 9.25 to 9.28 the D3-brane potential can be recalculated. Due to the nature of the scalar potential, V, the sign of λ is unimportant (specifically because the potential depends only on the square of hyperbolic functions of λ). This means that, though there appear to be four separate forms of the IR boundary behaviour, in fact equations 9.25 and 9.26 produce exactly the same D3-brane IR potential, as do equations 9.27 and 9.28. For the first two solutions, the potential in the IR is given by

$$V_{IR,(1,2)} = \frac{10\sqrt{1+\cos^2 2\alpha}\log(r-r_s)}{27(r-r_s)} \ , \tag{9.29}$$

while for the second two solutions it is

$$V_{IR,(3,4)} = -\frac{\log(r-r_s)}{16(r-r_s)} \ . \tag{9.30}$$

Therefore, independent of the parameters r_s and a, the first two solutions asymptote to $-\infty$ while the second two asymptote to $+\infty$.

From these investigations of the UV and IR behaviour, it can be seen that only the boundary behaviour set by equations 9.27 and 9.28 give a bounded potential

in the IR, while in the UV any solution with a mass will give a bounded potential. Therefore, the well-behaved solutions are given by:

$$\lambda_{IR,(3,4)}(r) = -\frac{\sqrt{6}}{4}\log(a(r-r_s)) \ , \qquad A = \frac{1}{4}\log(r-r_s), \qquad a \neq 1.42 \ . \quad (9.31)$$

9.3 Glueballs in the Yang-Mills* Geometry

A detailed calculation of the glueball potential [107] is not provided in this section as it is covered fully in chapter 10. However, some general remarks about analytic solutions which produce bounded glueball potentials are made.

From the AdS/CFT correspondence, the field dual to the operator $\mathrm{Tr}\, F^2$ is given by the dilaton, a massless scalar field. x-dependent excitations of this scalar correspond to x-dependent excitations of the square of the gauge field, corresponding to glueballs. The equation of motion for the dilaton in a supergravity background can be calculated, and using the same plane-wave ansatz as used in the previous meson spectrum calculations, the mass eigenstates of the glueball can be determined. This procedure is covered in detail in chapter 10. The potential felt by the dilaton can be calculated and its dependence on the UV and IR boundary conditions established. In particular, the existence of a discrete glueball spectrum depends on the gradient of the potential in the UV and the IR.

To calculate the potential, the equation of motion for the scalar is rewritten in a Schrödinger form. A change of variables is performed, given by

$$\frac{dz}{dr} = e^{-2A(r)} \ . \quad (9.32)$$

Having implemented this change of variables, the Schrödingerpotential is given

by

$$U(z) = \frac{3}{2}A''(r) + \frac{9}{4}(A'(r))^2 \ . \tag{9.33}$$

In the UV, $A(r) \to r$ meaning that $z = e^{-r}$, and therefore $A(r) \to -\log(-z)$. Therefore the Schrödinger potential in the UV is

$$U(z)|_{uv} = \frac{15}{4z^2} \ , \tag{9.34}$$

As $z \to 0_-$, $U(z)|_{uv} \to \infty$ meaning that the UV of the glueball potential is bounded independent of the value of $\mathcal{M}$ and $\mathcal{K}$.

Next, the IR behaviour is calculated using a general IR form for A (of which the true solutions given by equations 9.25 to 9.28 form a subset):

$$\begin{aligned} A(r) &= c\log(r - r_s) + b \ , \\ z - z_s &= \frac{e^{-b}(r - r_s)^{1-c}}{1-c} \ , \\ A(z) &= \frac{c}{1-c}\log((1-c)e^b(z - z_s)) + b \ , \\ U(z) &= \frac{3}{2(z-z_s)^2}\frac{c}{1-c}\left(\frac{3}{2}\frac{c}{1-c} - 1\right) \ . \end{aligned} \tag{9.35}$$

For quantum mechanical, potential-well problems, there is a bound on the gradient of the potential, which produces a discrete mass spectrum [113]. This is

$$U(z - z_s) \sim \frac{k}{z^2} \ , \qquad k \geq -\frac{1}{4} \tag{9.36}$$

ensures the existence of a discrete spectrum. From $U(z)$ in equation 9.35, for this bound to be satisfied, the value of c must be $\geq \frac{1}{4}$. This bound is exactly saturated for equations 9.27 and 9.28 which fill most of the $(\mathcal{M}, \mathcal{K})$ phase-space. Equations 9.25 and 9.26 also satisfy the inequality, so all possible boundary conditions for the Yang-Mills* geometry exhibit a discrete glueball spectrum. This result is in

contrast to the conclusions drawn in [107] where it appeared that only the $\mathcal{K} = 0$ solutions produced a discrete spectrum. The link between the IR solutions and the UV boundary conditions is illustrated in figure 9.2

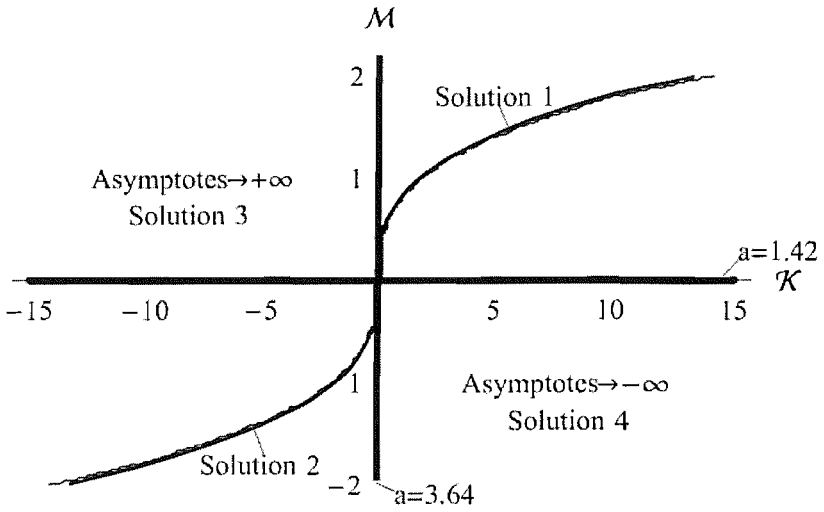

Figure 9.2: Plot indicating the link between the IR asymptotic behaviour of the supergravity scalar, $\lambda(r)$, and the UV boundary conditions defined by $\mathcal{M}$ and $\mathcal{K}$.

The conclusions from section 9.2 and 9.3 are that, provided the gauginos are not massless, the field theory dual to the Yang-Mills* geometry will be stable and have a discrete glueball spectrum.

9.4 Adding Quarks to the Yang-Mills* Geometry

As in the previous chapters, quarks can be added by the introduction of D7-branes. In this case, the brane is embedded in the direction illustrated in table 9.1. The DBI action for this embedding can be calculated and is given by equation

	x_0	x_1	x_2	x_3	r	α	θ_+	ϕ_+	θ_-	ϕ_-
D3	×	×	×	×	.	.	.	.	.	.
D7	×	×	×	×	×	×	.	.	×	×

Table 9.1: D3- and D7-brane embedding in the Yang-Mills* geometry. Filled dimensions are marked with crosses, those perpendicular to the world-volumes are denoted by a dot.

9.37.

In contrast to the actions calculated in chapters 4 to 8, the two-form potential is important. The embedding is chosen such that the directions on the two-sphere, (θ_+, ϕ_+), are perpendicular to the D7-brane, so these correspond to the scalar fields living on the brane. The DBI action is given by

$$S_{DBI} = -T_{D7}\int d^8\zeta e^{\Phi}e^{4A}\sqrt{F_-^2\sin^2\theta_-\cos^4\alpha+\frac{\zeta^3}{4}(A_-\sin^3\alpha\cos\theta_-)^2}$$
$$\sqrt{1+((\partial_r\theta_+)^2+(\partial_\alpha\theta_+)^2)\frac{\sin^2\alpha}{F_-}+((\partial_r\phi_+)^2+(\partial_\alpha\phi_+)^2)\frac{\sin^2\theta_+\cos^2\alpha}{F_-}}\,, \tag{9.37}$$

where the ansatz $\theta_+ = \theta_+(r,\alpha)$, $\phi_+ = \phi_+(r,\alpha)$ is used. The above action includes a term from the NS-NS two-form. The Wess-Zumino term is

$$S_{WZ} = T_{D7}\int C^{(8)} + C^{(6)} \wedge B_{(2)}^{NS-NS}\,. \tag{9.38}$$

However, the eight-form is dual to the axion which is zero in this background. The six-form is dual to the two-form by the relation $dC^{(6)} = \star B_{(2)}^{(R-R)}$. Therefore,

$$\star dB^{RR} \sim \frac{\partial f}{\partial r}dx^0\wedge dx^1\wedge dx^2\wedge dx^3\wedge d\alpha\wedge d\theta_-\wedge d\phi_- + \frac{\partial f}{\partial \alpha}dx^0\wedge dx^1\wedge dx^2\wedge dx^3\wedge dr\wedge d\theta_-\wedge d\phi_- \tag{9.39}$$

When the wedge product of the NS-NS two-form is taken with the six-form, each term contains two copies of at least one of the Ω_- directions giving a total antisymmetric product of zero. This means that in this case, the Wess-Zumino term vanishes.

As in the previous examples, a constant value in one of the perpendicular directions to the D7-brane is chosen corresponding to picking a direction in the $U(1)$ chiral plane. In this case, the direction is given by $\phi_+ = const.$ To calculate the equation of motion for θ_+ the two directions in the action on which θ_+ is independent must be integrated out. Integrating over ϕ_- is trivial and produces a numerical prefactor in the action. However, integrating over θ_- produces an elliptic integral, giving a DBI action of the form

$$S_{DBI} = -T_{D7}\int d^6\zeta e^{\Phi}e^{4A}4\pi F_- \cos^2\alpha EllipticE\left(1-\frac{A_-^2\sin^6\alpha\zeta^3}{4\cos^4\alpha F_-^2}\right) \sqrt{1+((\partial_r\theta_+)^2+(\partial_\alpha\theta_+)^2)\frac{\sin^2\alpha}{F_-}+((\partial_r\phi_+)^2+(\partial_\alpha\phi_+)^2)\frac{\sin^2\theta_+\cos^2\alpha}{F_-}}\,. \tag{9.40}$$

9.4.1 D7-Brane Solutions in the Yang-Mills* Coordinates

It is now possible to calculate the equation of motion for θ_+ which is a second order partial differential equation in r and α:

$$\frac{\partial}{\partial r}\left(\frac{e^{\Phi}e^{4A}EllipticE\left(1-\frac{A_-^2\sin^6\alpha\zeta^3}{4\cos^4\alpha F_-^2}\right)\partial_r\theta_+}{\sqrt{1+\frac{\sin^2\alpha}{F_-}((\partial_\alpha\theta_+)^2+(\partial_r\theta_+)^2)}}\right)\sin^2\alpha\cos^2\alpha + \frac{\partial}{\partial\alpha}\left(\frac{e^{\Phi}e^{4A}EllipticE\left(1-\frac{A_-^2\sin^6\alpha\zeta^3}{4\cos^4\alpha F_-^2}\right)\sin^2\alpha\cos^2\alpha\partial_\alpha\theta_+}{\sqrt{1+\frac{\sin^2\alpha}{F_-}((\partial_\alpha\theta_+)^2+(\partial_r\theta_+)^2)}}\right)=0\,. \tag{9.41}$$

This equation is clearly not analytically solvable, but it may be possible to gain some insight by studying it in the large r limit, where the space returns to

$AdS_5 \times S^5$. It is critical that even in this limit, though it can be solved analytically, it cannot be solved numerically due to the nature of the boundary conditions. In the AdS limit, the metric becomes

$$ds^2 = e^{2r} dx_{//}^2 + dr^2 + d\alpha^2 + \sin^2\alpha(d\theta_+^2 + \sin^2\theta_+ \mathrm{d}\phi_+^2) + \cos^2\alpha(d\theta_-^2 + \sin^2\theta_- \mathrm{d}\phi_-^2) \,. \tag{9.42}$$

The dilaton and five-form field strength are constant and the three-form field strength vanishes. The pullback of this metric onto a D7-brane, embedded with orthogonal direction θ_+ and ϕ_+ and the latter set as a constant, produces an action of the form

$$S_{DBI} = -T_7 \int d^8\zeta e^{4r} \cos^2\alpha \sin\theta_- \sqrt{1 + \sin^2\alpha((\partial_\alpha\theta_+)^2 + (\partial_r\theta_+)^2)} \,. \tag{9.43}$$

Though in the deformed case, the integral over θ_- gave an elliptic integral, in this case it simply gives a numerical prefactor which is ignored as it does not alter the solutions. The equation of motion is given by

$$\frac{\partial}{\partial r}\left(\frac{e^{4r}\sin^2\alpha\cos^2\alpha\partial_r\theta_+}{\sqrt{1+\sin^2\alpha((\partial_\alpha\theta_+)^2+(\partial_r\theta_+)^2)}}\right) + \frac{\partial}{\partial\alpha}\left(\frac{e^{4r}\sin^2\alpha\cos^2\alpha\partial_\alpha\theta_+}{\sqrt{1+\sin^2\alpha((\partial_\alpha\theta_+)^2+(\partial_r\theta_+)^2)}}\right) = 0 \,. \tag{9.44}$$

Unsurprisingly, this second order, non-linear, partial differential equation cannot be solved using the normal methods in Mathematica. However, because the solution is known in the usual parametrisation of $AdS_5 \times S^5$ (equation 9.45) and the change of variables between the current coordinate system and the canonical one is known, the solution to this equation can be found with some effort. The

canonical metric is

$$\begin{aligned} ds^2 &= (\rho^2 + x_8^2 + x_9^2)^2 dx_{//}^2 \\ &+ \frac{1}{(\rho^2 + x_8^2 + x_9^2)^2} \left(\rho^2 + \rho^2(d\chi_1^2 + \cos^2\chi_1^2 d\chi_2^2 + \cos^2\chi_1 \sin^2\chi_2 d\chi_3^2) + dx_8^2 + dx_9^2\right) , \end{aligned} \tag{9.45}$$

the solution to the D7-brane action in this coordinate system is

$$x_8 = m + \frac{c}{\rho^2} , \qquad x_9 = 0 , \tag{9.46}$$

and the change of variables between the two coordinate systems is

$$\begin{aligned} \rho \sin\chi_1 &= e^r \cos\alpha \cos\theta_- , \\ \rho \cos\chi_1 \cos\chi_2 &= e^r \cos\alpha \sin\theta_- \cos\phi_- , \\ \rho \cos\chi_1 \sin\chi_2 \cos\chi_3 &= e^r \cos\alpha \sin\theta_- \sin\phi_- , \\ \rho \cos\chi_1 \sin\chi_2 \sin\chi_3 &= e^r \sin\alpha \cos\theta_+ , \\ x_8 &= e^r \sin\alpha \sin\theta_+ \cos\phi_+ , \\ x_9 &= e^r \sin\alpha \sin\theta_+ \sin\phi_+ . \end{aligned} \tag{9.47}$$

At this stage, the choice to set $\phi_+ = 0$ is made. It is possible to rewrite x_8 in equation 9.46 in terms of θ_+:

$$\begin{aligned} x_8 &= e^r \sin\alpha \sin\theta_+ \\ &= m + \frac{c}{\rho^2} = m + \frac{c}{e^{2r}(1 - \sin^2\alpha \sin^2\theta_+)} . \end{aligned} \tag{9.48}$$

The solution to this cubic is very complicated and demonstrates why the equation cannot be solved analytically using Mathematica. The solution to equation 9.48,

describing the flow of a D7-brane in pure $AdS_5 \times S^5$ in the Yang-Mills* coordinate system, can be written as a series expansion and the first two terms are

$$\theta_+ = \arcsin\left(\frac{m}{e^r \sin\alpha} + \frac{c}{e^{3r}\sin\alpha}\right) . \tag{9.49}$$

From equation 4.8 it is known that the well-behaved solution is given by the $c = 0$ branch of equation 9.48. This makes the analytic form of the equation much more simple:

$$\theta_+ = \arcsin\left(\frac{m}{e^r \sin\alpha}\right) . \tag{9.50}$$

9.4.2 Boundary Value Problems for PDEs

In the Yang-Mills* coordinate system, it is very difficult to calculate the solution to equation 9.44 numerically. This should be a simple question of how the D7-brane flows in an $AdS_5 \times S^5$ geometry and therefore it is surprising that it is so complicated. This is due to the nature of the boundary conditions for this partial differential equation. In the UV, the solution is known to be equation 9.49 where the UV is the large r limit. Ideally, the boundary conditions for all values of α would be set, however, this means that the largest value of r in the domain of the arcsin function is given by the solutions of

$$\frac{c}{e^{3r}} + \frac{m}{e^r} < \sin\alpha . \tag{9.51}$$

As $\alpha \to 0$, r must $\to \infty$ for this condition to be satisfies. This analysis indicates that the boundary values for α and r cannot be set independently. For a non-linear, partial differential equation, such as 9.44, Mathematica will not attempt a numerical solution with this sort of boundary condition and so another method

must be sought. The method attempted for this problem was the relaxation method [114].

9.4.3 D7-Brane Solutions using the Relaxation Method

A relaxation method can most easily be explained using a simpler example of a differential equation. The example given here is the equation of motion for a D7-brane in the canonical $AdS_5 \times S^5$ coordinates (equation 9.45). This is simpler because, though it is still non-linear, the function is dependent only on a single variable. First, the action for the D7-brane is written as in section 4.1:

$$S_{DBI} = -T_7 \int d^8\zeta \rho^3 \sqrt{1 + (\omega'(\rho))^2} \ . \tag{9.52}$$

In this case, because the action is clearly negative, the function $\omega(\rho)$ which maximises the action is sought. This action can then be discretised (having already integrated over $x_{//}$ and the three-sphere and discarded all numerical factors). To perform this discretisation, a $2 \times N$ array is defined, where the first column is the discretised values of ρ and the second column is the corresponding values of ω. The UV boundary condition is given by fixing the value of ω for the largest value of ρ. The other values are then allowed to vary. To initialise, the values of ω are set as random numbers (in a sensible range) in all of the array entries apart from the boundary value. The discretised action is then written in terms of these array elements as

$$S_{discrete} = \sum_{i=1}^{N-1} (\rho_{(i+1)} - \rho_i)\rho_i^3 \sqrt{1 + \left(\frac{\omega_{(i+1)} - \omega_i}{\rho_{(i+1)} - \rho_i}\right)^2} \ . \tag{9.53}$$

Note that, for simplicity, the sign of the action has been changed so the minimising action solution is sought. For the current values in the array, the action

is calculated. The next stage is a loop algorithm by which one of the ω_i values is adjusted randomly, followed by a recalculation of the action. If the action is closer to zero than the previous action, the new value of ω_i is kept, and if not, it is returned to its initial value. There are many possible algorithms for this procedure. One algorithm chooses the value of i randomly, then the derivative of the action with respect to ω_i is evaluated to find the action minimising value of ω_i.

Given a random starting array, it should be possible to find the minimising solution (provided there are no local minima). This is illustrated in figure 9.3

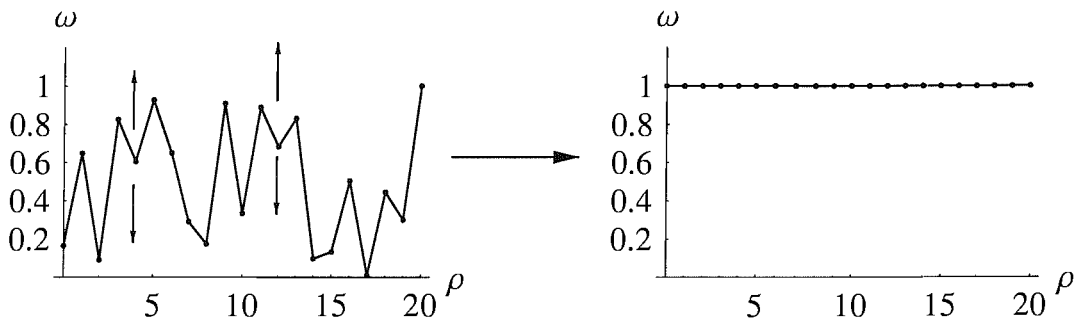

Figure 9.3: Plots illustrating the relaxation method for a D7-brane flow in the canonical $AdS_5 \times S^5$ coordinates. Starting from a random discretised brane flow with a fixed UV boundary point ($\rho = 20$), it is possible to find the action minimising solution using the relaxation method.

The values of the mass and condensate corresponding to this solution can be calculated by studying the UV behaviour and matching onto $m + \frac{c}{\rho^2}$. Indeed, in this very simple case, the analysis does work and obtains the correct answer $\omega_i = m$, $\forall i$. Unfortunately, though many months were spent attempting to

solve the partial differential equation in the Yang-Mills* coordinate system, the problems with singularities in the supergravity fields, as well as a lack of an efficient discretisation procedure, meant that a successful solution has not yet been found.

Chronologically, this was the point that the wrapping method was first developed. In chapters 5 to 8, spherical solutions were found which minimised the action. In the Constable-Myers case, due to the symmetries of the problem, the solution to the brane wrapping action was reduced to solving an algebraic equation analytically. In the current case, it is possible to reduce the partial differential equation to an ordinary differential equation which can be solved using the relaxation method.

9.5 Brane Wrapping the Yang-Mills* Geometry

It has not been possible to study the flow of a brane from the UV to the IR in this geometry, however, the methods developed in chapter 5 to study the near-singular behaviour can be investigated. A D7-brane wraps the singularity with two directions orthogonal to its world-volume, r and ϕ_+, and the functional ansatz for these directions are $\phi = 0$ and $r(\alpha\ , \theta_+)$. As in the case of the UV/IR flow, the Wess-Zumino term is zero. The action for the D7-brane in this wrapping configuration is

$$\begin{aligned} S_{DBI} &= -T_{D7} \int d^7\xi\ e^{\Phi} e^{4A} 2F_- cos^2\alpha\ EllipticE\left(1 - \frac{A_-^2 sin^6\alpha\zeta^3}{4F_-^2 \cos^4\alpha}\right) \\ &\quad \cdot \sqrt{(\partial_{\theta_+} r)^2 + (1 + (\partial_\alpha r)^2)\frac{sin^2\alpha}{F_-}}\ . \end{aligned} \tag{9.54}$$

The simplest possible solution would be one in which the brane is perfectly spherical (has no α or θ dependence). For this to be a solution, there must be no repulsive potential to this configuration. To calculate the potential, the asymptotic IR solutions (equations 9.25 to 9.28) are used. The signs of the IR asymptotics of the field equations are unimportant for this action, so there are two different forms of IR behaviour. The potentials for these solutions are given by

$$V_{sphere,(1,2)} = \int d^7\xi \, (r_c - r_0)^{\frac{2}{3}} \, EllipticE\left(1 - \frac{18}{5}(r_c - r_0)^2 |\cot\alpha|\right) \sqrt{|\cos^5\alpha \sin^3\alpha|}\,, \tag{9.55}$$

corresponding to $\lambda_{IR,1}$ and $\lambda_{IR,2}$ and

$$V_{sphere,(3,4)} = \int d^7\xi \, (a(r_c - r_0))^{1-\sqrt{\frac{3}{2}}} \, EllipticE\left(1 - 8(a(r_c - r_0))^{\sqrt{\frac{3}{2}}} |\cot\alpha|\right) \cdot \sqrt{|\cos^5\alpha \sin^3\alpha|}\,, \tag{9.56}$$

corresponding to $\lambda_{IR,3}$ and $\lambda_{IR,4}$.

It is important to understand the nature of the elliptic integrals in the IR limit. As $r_c \to r_0$, the asymptotics of the cot function can cause the argument of the elliptic integral to blow up. For equation 9.55, for $\alpha << \arctan(r_c - r_0)^2$ the elliptic integral is given by

$$EllipticE\left(1 - \frac{18}{5}(r_c - r_0)^2 |\cot\alpha|\right) \to \sqrt{\frac{18}{5}}(r_c - r_0)\sqrt{|\cot\alpha|}\,, \tag{9.57}$$

so the potential in this limit is

$$V_{sphere} \sim (r_c - r_0)^{\frac{5}{3}} \sqrt{\cos^6\alpha \sin^2\alpha}\,. \tag{9.58}$$

For equation 9.56, when $\alpha \ll \arctan(r_c - r_0)^{\sqrt{\frac{3}{2}}}$, the elliptic integral goes like

$$EllipticE\left(1 - 8(a(r_c - r_0))^{\sqrt{\frac{3}{2}}} |\cot\alpha|\right) \to \sqrt{8}(r_c - r_0)^{\sqrt{\frac{3}{8}}}\sqrt{|\cot\alpha|}\,, \tag{9.59}$$

so the potential is

$$V_{sphere} \sim (r_c - r_0)^{1-\sqrt{\frac{3}{2}}} \sqrt{\cos^6\alpha \sin^2\alpha} \ . \tag{9.60}$$

Therefore, for this small α limit, neither of the potentials are repulsive. However, it is significant that, as $r_c \to r_0$, the range of α for which this limit holds is vanishingly small.

In the opposite limit, $\alpha >> \arctan(r_c - r_0)^{\sqrt{\frac{3}{2}}}$, equation 9.55 goes like

$$V_{sphere} \sim (r_c - r_0)^{\frac{2}{3}} \sqrt{|\cos^5\alpha \sin^3\alpha|} \ , \tag{9.61}$$

while equation 9.56 goes like

$$V_{sphere} \sim (a(r_c - r_0))^{1-\sqrt{\frac{3}{2}}} \sqrt{|\cos^5\alpha \sin^3\alpha|} \ , \tag{9.62}$$

This contrasts with the small α limit where neither potential was repulsive. In this case, the second potential is repulsive. It can be seen that the first potential will always be minimised for small r,independent of α. This suggests that for this set of solutions, there is a brane configuration where the brane does wrap onto the surface of the singularity.

From the analysis of chapters 5 and 6, the conclusion is that the field theory dual to the geometry with IR boundary behaviour given by equations 9.25 and 9.26 does not exhibit chiral symmetry breaking. The Yang-Mills* geometry with IR boundary behaviour given by equations 9.27 and 9.28 does produce a repulsive potential in the IR limit. This suggests that for a D7-brane flowing from the UV to the IR, the brane will be repelled inducing chiral symmetry breaking in the field theory. It would be extremely interesting to find the D7-brane flow solution from the UV to the IR of the gauge theory and show explicitly by studying the

quark mass and bilinear condensate that chiral symmetry breaking is induced in this region.

9.5.1 Dilaton Behaviour in the IR

It has been postulated in this thesis that a running dilaton may be necessary to trigger chiral symmetry breaking. In the region between the UV and the IR of the Yang-Mills* geometry, the dilaton is dependent on the radial-direction, r. However, in the IR limit, the dilaton is purely a function of α:

$$\begin{aligned} e^{\Phi} &= \frac{\cosh^2\lambda + \sinh^2\lambda\cos 2\alpha + \sqrt{\cosh^4\lambda + \sinh^4\lambda\cos^2 2\alpha}}{\cosh^2\lambda - \sinh^2\lambda\cos 2\alpha + \sqrt{\cosh^4\lambda + \sinh^4\lambda\cos^2 2\alpha}} \\ &\lim_{\lambda\to\infty} \quad \cos 2\alpha + \sqrt{1+\cos^2 2\alpha}\ . \end{aligned} \tag{9.63}$$

This is in contrast to the Constable-Myers dilaton which asymptotes to infinity in the IR. The α dependence of the dilaton, given by equation 9.63, is shown in figure 9.4.

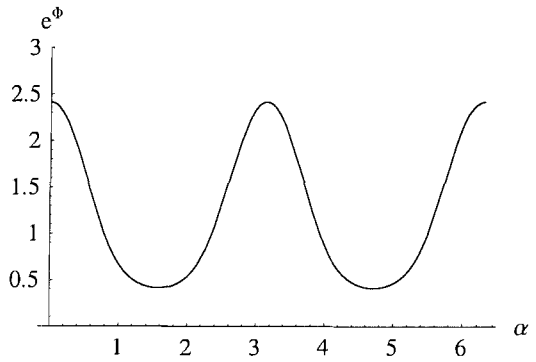

Figure 9.4: Asymptotic behaviour of the dilaton as a function of α. The dilaton is independent of r in the IR of the gauge theory.

9.5.2 D7-Brane Wrapping in a Repulsive Potential

The IR behaviour defined by equations 9.27 and 9.28 appears to produce a repulsive potential for the D7-brane wrapping the singularity. In the analysis to calculate the potential, a spherical ansatz for the brane was postulated. By studying the symmetries of the action for the brane, a spherically symmetric configuration appears impossible. However, the symmetries of the action do allow a solution for which there is no θ_+-dependence in r. This reduces the problem of finding a solution from a partial to an ordinary differential equation. This problem is the equivalent of calculating the configuration of a charged elastic band, stretched about a non-spherical charge distribution. The tension of the band pulls it in, while the charge distribution repels it. Due to the symmetries of the charge distribution, the band will not lie in a circular configuration.

The simplest way to set the boundary conditions for the solution would be to state that the rubber band is both continuous and smooth: $r[0] = r[2\pi]$ and $r'[0] = r'[2\pi]$. To be able to use Mathematica to solve a problem numerically with boundary conditions of this form, the equation must be linear which is not the case for the wrapping D7-brane. If instead, the value and gradient of r at some fixed value of α are set, Mathematica will not find a solution which is continuous. Figure 9.5 illustrates the answer when these boundary conditions are used.

Mathematica's algorithms are clearly not suitable for this problem so the relaxation method is used instead. There is more freedom in how to define the boundary values in the relaxation method.

In this case the boundary values are set such that the value of r at some fixed α'

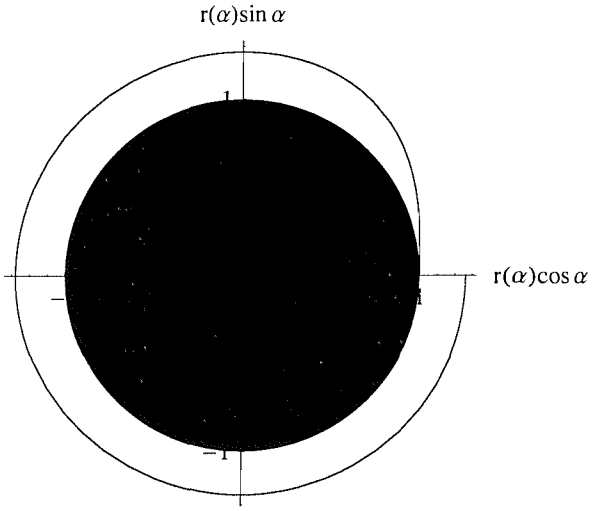

Figure 9.5: Attempts to solve the differential equation for a wrapped brane using the usual boundary condition methods (plot calculated using the IR asymptotic form of λ).

and $\alpha' + 2\pi$ are equated. This value of r is then allowed to vary and the relaxation algorithm is run. To obtain a smooth function in the highly singular region, a large number of points are needed on the curve, which consequently takes a long time to run. Having calculated the function $r(\alpha)$, the two dimensional surface $r(\alpha, \theta_+)$ can be drawn. This is shown in figure 9.6.

The field theory dual to the Yang-Mills* geometry does exhibit chiral symmetry breaking for almost all of the parameter space defined by the supergravity field UV boundary conditions. It would be a major achievement if the UV/IR flow of a D7-brane could be calculated in this geometry.

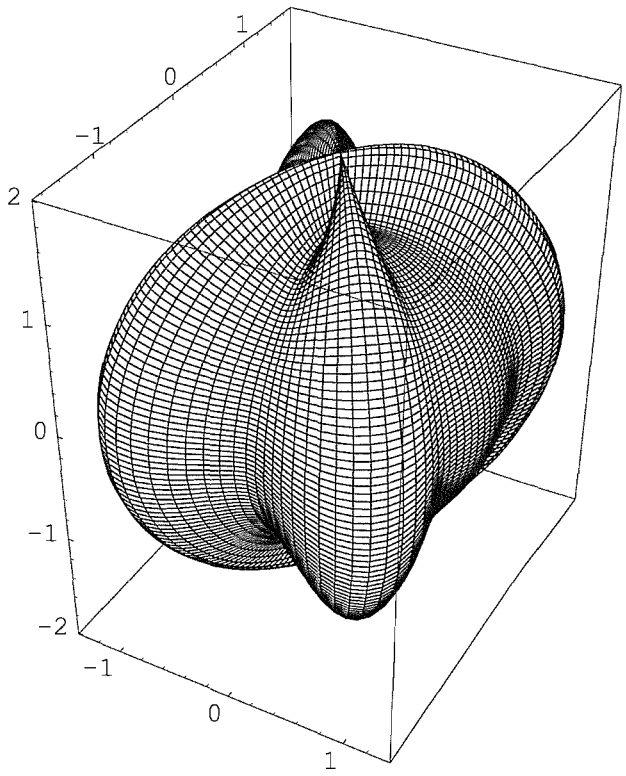

Figure 9.6: Three-dimensional brane wrapping solution about a spherical singularity. This plot is generated using the ansatz that r is a function of α, but independent of θ_+. The function r is then found using the relaxation method and the three-dimensional plot generated from this function. The distance between the brane and the singularity has been exaggerated in order to see the deviation of the brane from a perfect sphere.

Chapter 10

Glueballs and Perfect Actions

10.1 Glueballs from Eleven-Dimensional Supergravity

This chapter is conceptually different from the previous ones, however, the motivation is similar. In chapters 4 to 9, the inclusion of relevant operators to the IR of the gauge theory has been studied [102, 108, 99, 109]. This process was used to remove some or all of the unrealistic symmetries from the low-energy limit of the field theory, while in the UV, the theory returned to the superconformal phase. These operators were included in an attempt to construct a realistic model of QCD. At low-energy in QCD, the theory is non-supersymmetric, non-conformal and appears to have an induced quark bilinear condensate. All of these properties have been investigated in chapters 4 to 9. The aim of this chapter is to study the UV of the field theory in an attempt to make it more QCD-like.

10.2 A UV Cutoff in the AdS/CFT Correspondence

The AdS/CFT correspondence is perturbatively controlled on the supergravity side when the gauge theory coupling, $\lambda = g_s N$, is large. This condition is satisfied for low-energy QCD, but not in the high-energy regime. In the examples in previous chapters, the UV of the theory has been conformal and strongly-coupled. It is interesting to investigate whether this discrepancy from QCD can be removed. Figure 10.1 illustrates the discrepancy between the QCD coupling and the coupling studied previously.

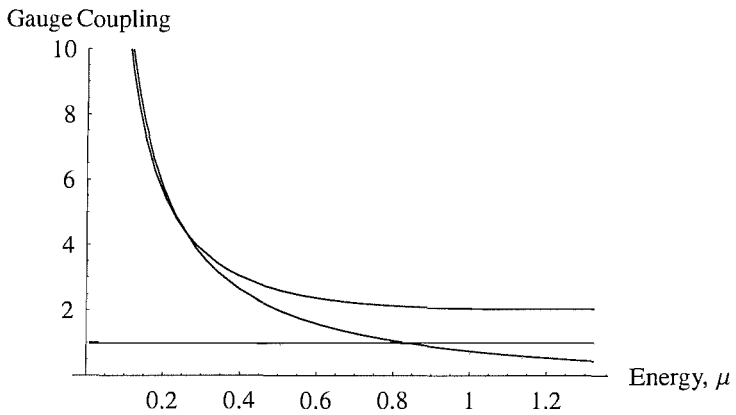

Figure 10.1: Comparison of the QCD gauge coupling (lower curve) and the gauge coupling of the field theory dual to the supergravity backgrounds in the applicable regimes (upper curve). The plots match well in the IR, but not in the UV.

The supergravity approximation to string theory is an inaccurate description of the physics in the small 't Hooft coupling limit of the AdS/CFT correspondence. In this limit, the radius of curvature is smaller than the string length and

so stringy effects are important. It appears that, if the AdS/CFT correspondence is to describe QCD with a supergravity theory, the UV of the field theory must somehow be removed.

By defining the boundary conditions for the couplings and vevs in a field theory at an energy scale, Λ, a cutoff is automatically imposed. By the string-gauge duality, supergravity fields correspond to sources and vevs for field theory operators, so, setting the supergravity field boundary conditions in the large r limit corresponds to defining a high-energy UV cutoff in the field theory. In previous examples, this cutoff was sent to infinity because in the deformed geometries it is only at $r = \infty$ (where the space returns to $AdS_5 \times S^5$) that the field-operator correspondence is quantitatively understood. If a cutoff is defined such that the boundary conditions for operators are set in the IR, quantum corrections change the scaling dimensions for the field theory operators and full control over the duality is lost.

As illustrated in figure 10.1, the high-energy limit of the field theories formulated in the previous chapters has not been QCD-like. The boundary conditions for the supergravity fields can be set further into the IR (where the field theory does exhibit QCD-like behaviour) thereby defining a field theory with a UV cutoff. This field theory will then include only the QCD-like region.

When a finite UV cutoff is introduced into a field theory, an infinite number of higher dimension operators are switched on to take account of the high-energy degrees of freedom that are integrated out. These operators are non-renormalisable as the field theory now has a cutoff. As the cutoff is lowered, the higher di-

mension operators become increasingly important, and to provide an accurate description of the physics, more of these operators must be included in perturbative calculations. This same process can be employed in the AdS/CFT correspondence. When the UV cutoff is lowered from infinity to a finite value of r, non-renormalisable operators can be introduced. This idea is motivated directly by lattice QCD [115, 116] in which, due to the finite lattice spacing, there is automatically a UV cutoff. A perfect lattice action has, in addition to the usual QCD terms (equation 1.3), the most important higher-dimensional operators switched on to take account of this cutoff. By using the exact renormalisation group [117, 118], the renormalisation of the coupling constants for these higher-dimensional operators can be studied.

10.2.1 Non-Renormalisable Operators in the AdS/CFT Correspondence

This preliminary investigation aims to introduce a UV cutoff to the field theory and add a single, higher-dimensional operator to take account of the integration over the high-energy modes. The higher dimension operator has a coupling constant that is free to be tuned. By calculating some physical, measurable quantity using this field theory with a cutoff, the coupling constant can be tuned to match the AdS/CFT results with experimental results.

In this example, the AdS/CFT results to be compared to experiment are the masses of glueball bound-states in a four-dimensional large N field theory. Unfortunately, glueballs have yet to be seen, conclusively, in any experiments. For

this reason, results from lattice QCD simulations [119, 120, 121, 122, 123, 124, 125] are used to compare to the AdS/CFT results. Even using lattice results, there are only a very small number of data points available for large N field theories. Therefore, it is difficult to draw confident conclusions from this preliminary study of the effects of defining the gauge-gravity duality with a cutoff.

The aim is to tune the free parameter (the coupling constant) so that the ratio of two glueball masses match the lattice results. Then, using the value for the parameter which gives the correct ratio, the rest of the glueball spectrum is calculated and compared with both the lattice data, and the results of AdS/CFT calculations without the inclusion of the higher-dimensional operator. The overall scale of the spectrum is set by tuning the AdS radius, R, such that the first glueball mass matches the lattice data.

10.3 The AdS-Schwarzschild Black-Hole Solution

It was proposed by Ed Witten in [53] that the Schwarzschild black-hole solution in ten-dimensional AdS space is dual to three-dimensional, non-supersymmetric Yang-Mills theory at finite temperature. The AdS-Schwarzschild background [36] is given by

$$ds^2 = \frac{r^2}{b^2}\left(\left(1-\frac{b^4}{r^4}\right)dt^2 + b^2\sum_{i=1}^{4}dx_i^2\right) + \frac{b^2}{r^2}\left(\frac{dr^2}{1-\frac{b^4}{r^4}} + r^2 d\Omega_5^2\right) , \qquad (10.1)$$

where b is the inverse temperature of the dual field theory. The near-horizon solution to this geometry is

$$\begin{aligned} ds^2 &= H^{-\frac{1}{2}}\left(\left(1-\frac{b^4}{r^4}\right)dt^2 + b^2\sum_{i=1}^{4}dx_i^2\right) + H^{\frac{1}{2}}\left(\frac{dr^2}{1-\frac{b^4}{r^4}} + r^2 d\Omega_5^2\right) , \\ H &= \lim_{r\to 0} a + \frac{b^4}{r^4} . \end{aligned} \tag{10.2}$$

The theory is non-supersymmetric as the fermions, with anti-periodic boundary conditions around the compactified direction, have a different mass from the lowest mass bosonic states. The broken supersymmetry allows quantum corrections to the scalar masses which are driven to the fermion mass scale. At low energy ($\mu < b$), the gauge theory is left with pure glue.

It is simple to add a higher dimension operator to the field theory dual to this background. The operator must be constructed from the gauge field only and have dimension higher than four. The first two options are $\mathrm{Tr}\, F^3$ and $\mathrm{Tr}\, F^4$ [126, 127, 128, 85]. The simplest operator to add in this case is the dimension eight operator, $\mathrm{Tr}\, F^4$. At high energy, large r, the field theory is actually four-dimensional. Switching on this operator adds the following term to the action:

$$S_{HD} = \int d^4x\ G \cdot \mathrm{Tr}\, F^4 . \tag{10.3}$$

G has scaling dimension four and zero R-charge, meaning that the background must be deformed by adding a dimensionless term ar^4. This term is dual to an R-symmetry scalar because it has no dependence on the coordinates of the five-sphere. In this case, the operator is easy to find as the harmonic warp factor, H, away from the near-horizon limit already contains this field:

$$H = r^{-4}(b + ar^4) . \tag{10.4}$$

The new supergravity field is part of the s-wave component of the graviton. The addition of this higher-dimensional operator corresponds to leaving the near-horizon (extremal) limit of the black-hole geometry. By performing this deformation, the geometry asymptotes to flat-space instead of $AdS_5 \times S^5$. It can be seen from equation 10.4 that this term becomes less important in the IR and more important in the UV. This equates with the fact that it corresponds to a non-renormalisable operator.

10.4 The Eleven-Dimensional Black-Hole Solution

Though the field theory dual to the geometry defined by equation 10.2 is four-dimensional in the UV, it is only three-dimensional in the IR. In order to compare it with QCD, a four-dimensional IR background must be studied. The background dual to a finite temperature, four-dimensional field theory in the IR is the M5-brane solution of eleven-dimensional Euclidean supergravity with a compactified time direction. An M5-brane is a solitonic object, believed to exist in M-theory of which eleven-dimensional supergravity is the classical field theory limit. This metric for the M5-brane solution is

$$\begin{aligned} ds_{11}^2 &= h^{-\frac{1}{3}} \left(\left(1 - \frac{b^6}{\rho^3} \right) d\tau^2 + \sum_{i=1}^{5} dx_i^2 \right) + h^{\frac{2}{3}} \left(\left(1 - \frac{b^6}{\rho^3} \right)^{-1} d\rho^2 + \rho^2 d\Omega_4^2 \right), \\ h &= \rho^{-3}(1 + \alpha\rho^3) , \end{aligned} \tag{10.5}$$

where $\rho = r^2$. r has mass dimension one, meaning that the parameter α has mass dimension -6. This is consistent because in the UV, the dual of this background

is actually a six-dimensional field theory given by the action

$$S_{FT} = \int d^6x \left[\frac{1}{g^2} \mathrm{Tr}\, F^2 + \alpha \mathrm{Tr}\, F^4 \right] , \tag{10.6}$$

where the coupling α is six-dimensional. Finite temperature QCD_4 (the subscript four denoting the number of dimensions) is dual to the low-energy limit of type IIA string theory on the AdS-Schwarzschild black-hole background [18, 129]. The IIA metric is obtained by compactifying the eleventh dimension and taking the limit as the radius of that dimension goes to zero. The metric is then rescaled by a factor $e^{\frac{2\phi}{3}} = h^{-\frac{1}{6}}$ to obtain

$$ds^2_{IIA} = h^{-\frac{1}{2}} \left(\left(1 - \frac{b^6}{\rho^3} \right) d\tau^2 + \sum_{i=1}^{4} dx_i^2 \right) + h^{\frac{1}{2}} \left(\left(1 - \frac{b^6}{\rho^3} \right)^{-1} d\rho^2 + \rho^2 d\Omega_4^2 \right) . \tag{10.7}$$

This solution has a non-constant dilaton related to the moduli-space of the compactification of the eleventh dimension given by $e^{\phi} = h^{-\frac{1}{4}}$. The function h is a solution of the five-dimensional Laplace equation

$$\frac{d}{d\rho} \left(\sqrt{\tilde{g}} \tilde{g}^{\rho\rho} \frac{dh}{d\rho} \right) = 0 , \tag{10.8}$$

where

$$\begin{aligned} \tilde{ds}^2 &= d\rho^2 + \rho^2 d\Omega_4^2 \\ \frac{d}{d\rho} \left(\rho^4 \frac{dh}{d\rho} \right) &= 0 , \end{aligned} \tag{10.9}$$

with solution

$$h(\rho) = c_1 + c_2 \rho^{-3} . \tag{10.10}$$

This solution is a very specific case which depends only on ρ, and not on the five-sphere coordinates. There are an infinite number of other solutions that depend

on the spherical coordinates and correspond to R-charged operators. There are also solutions which fall off faster than ρ^3 corresponding to operators of the form $\mathrm{Tr}\,\phi^n$ [130, 100].

10.5 Calculating the 0^{++} Glueball Spectrum

To calculate the glueball spectrum, the equation of motion for a scalar field with mass zero ($m = \Delta(\Delta - 4)$), with x- and ρ-dependence but no five-sphere-dependence, must be calculated. This field corresponds to excitations of the operator $\mathrm{Tr}\,F^2$. This operator has scaling dimension four, so if the geometry were undeformed, the UV behaviour of the scalar field would be $\frac{a}{\rho^4}$. This equation of motion for the scalar field is

$$\partial_\mu[\sqrt{g}g^{\mu\nu}e^{-2\phi}\partial_\nu\Phi] = 0 \ , \tag{10.11}$$

where the metric is given in the string frame background (equation 10.7). The scalar field is taken as a small perturbation so the plane wave ansatz is used:

$$\Phi = f(\rho)e^{ik.x} \ , \tag{10.12}$$

leading to

$$\begin{aligned} \frac{1}{\rho}\frac{d}{d\rho}\left[(\rho^4-\rho)\frac{df}{d\rho}\right] &= k^2(1+\alpha\rho^3)f(\rho) \ , \\ \frac{4\rho^3-1}{\rho^4-\rho}\frac{df}{d\rho} + \frac{d^2f}{d\rho^2} &= k^2\frac{1+\alpha\rho^3}{\rho^3-1}f \ . \end{aligned} \tag{10.13}$$

The radius of the black-hole, b, is set to 1 and the mass of the dilaton, $m^2 = -k^2$, is in units of b. By changing b, the entire glueball spectrum can be scaled so that the first glueball mass matches the lattice result. The second free parameter, α,

can then be tuned such that the second glueball mass also coincides with that calculated on the lattice. The inclusion of a single higher-dimensional operator has added one extra degree of freedom compared with the AdS/CFT result with the operator absent. It is hoped that this extra degree of freedom will give results which match the lattice results to higher accuracy than those obtained previously.

To study the potential felt by the scalar field, the equation of motion (equation 10.13) is translated into the Schrödinger form. This involves performing a change of variables, from ρ to z, so that the right hand side of equation 10.13 takes the form $k^2 f$. The change of variables is given by

$$\frac{dz}{d\rho} = \sqrt{\frac{1+\alpha\rho^3}{\rho^3-1}} = \beta \ . \tag{10.14}$$

Therefore

$$\begin{aligned}
\frac{df}{d\rho} &= \frac{dz}{d\rho}\frac{df}{dz} = \beta\frac{df}{dz} \ , \\
\frac{d^2 f}{d\rho^2} &= \beta^2\frac{d^2 f}{dz^2} + \frac{d\beta}{d\rho}\frac{df}{dz} \ , \\
\beta^2 f'' + \left(\frac{d\beta}{d\rho} + \frac{4\rho^3-1}{\rho^4-\rho}\beta\right) f' &= k^2\beta^2 f \ , \\
f'' + \frac{1}{\beta^2}\left(\frac{d\beta}{d\rho} + t\beta\right) f' &= k^2 f \ , \\
t &= \frac{4\rho^3-1}{\rho^4-\rho} \ ,
\end{aligned} \tag{10.15}$$

where $'$ is derivative with respect to z. The function f is then rewritten as $f = gh$:

$$\begin{aligned}
g''h + 2g'h' + gh'' + \left(\frac{1}{\beta^2}\frac{d\beta}{d\rho} + \frac{t}{\beta}\right)(gh' + hg') &= k^2 gh \ , \\
g''h + 2g'h' + gh'' + P(gh' + hg') &= k^2 gh \ .
\end{aligned} \tag{10.16}$$

To get the equation into a Schrödinger form, all terms in g' must be removed. Its

coefficient must therefore be zero:

$$\begin{aligned} 2h' + Ph &= 0 \ , \\ \frac{h'}{h} &= -\frac{P}{2} \ , \\ h'' &= -\frac{P'h - Ph'}{2} = h\left(\frac{P^2}{4} - \frac{P'}{2}\right) \ , \end{aligned} \tag{10.17}$$

which gives

$$\begin{aligned} -g'' + \left(\frac{P'}{2} + \frac{P^2}{4}\right) g &= m^2 g \ , \\ -g'' + Vg &= m^2 g \ , \end{aligned}$$

$$\begin{aligned} V &= \frac{1}{2}\sqrt{\frac{\rho^3 - 1}{1 + \alpha^3}}\frac{dP}{d\rho} + \frac{1}{4}P^2 \\ &= \frac{-4 + 8(2\alpha - 5)\rho^3 + (35 - \alpha(146 + 25\alpha))\rho^6 - 16(\alpha - 7)\alpha\rho^9 + 32\alpha^2\rho^12}{16\rho^2(\rho^3 - 1)(1 + \alpha\rho^3)^3} \ . \end{aligned} \tag{10.18}$$

The equation of motion is now in the Schrödinger form so the potential felt by the scalar field can be studied. The potential is plotted as a function of ρ for various values of α in figure 10.2.

For $\alpha \neq 0$ the potential is unbounded in the UV. Though it has been stated previously that the addition of this new operator introduces only a single extra free parameter, this is not strictly true. In reality there are two new free parameters. As well as the value of α, there is a free choice of the value of ρ at which to set the boundary conditions for the scalar field. This corresponds to choosing the UV cutoff in the dual field theory. In fact, the value of α that will give the correct second glueball mass will depend on the cutoff. As the cutoff is lowered, the value of the coupling constant of this higher-dimensional operator is expected

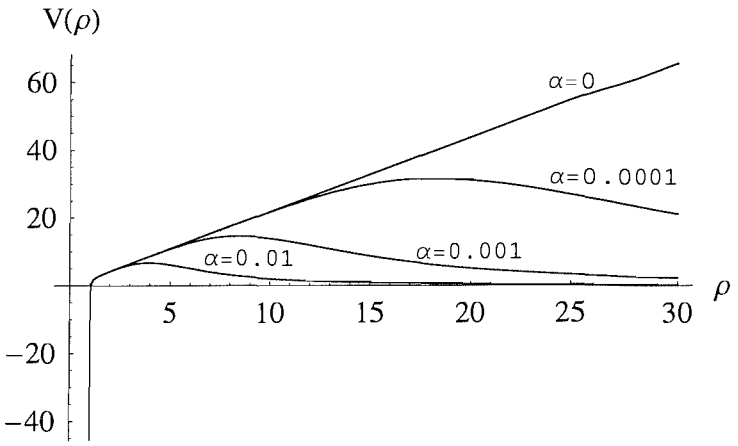

Figure 10.2: Graph of the potential felt by the scalar field in the non-extremal, AdS-Schwarzschild black-hole background for different values of α. α is the coupling constant for the higher-dimensional operator $\mathrm{Tr}\, F^4$.

to increase. The aim, however, was to introduce a single free parameter and to show that, with this single new degree of freedom, the second glueball mass could be tuned onto the lattice data. It is possible to restrict artificially the second degree of freedom to prove that, in this restricted regime, it is still possible to get the correct answer. The cutoff radius is chosen to correspond to the peak position in the potential. This is a function of α and is plotted in figure 10.3.

The cutoff is no longer free but is tied to the value of α. The peak position is chosen as the cutoff, because, with finite α, as the geometry returns to flat-space, the glueball potential becomes flat. A flat potential in the UV does not produce a discrete spectrum. By choosing the cutoff to be at the peak position of the potential, the discrete spectrum will contain the maximum number of states (discrete masses up to the height of the potential).

Having found the cutoff for a particular value of α, the glueball spectrum

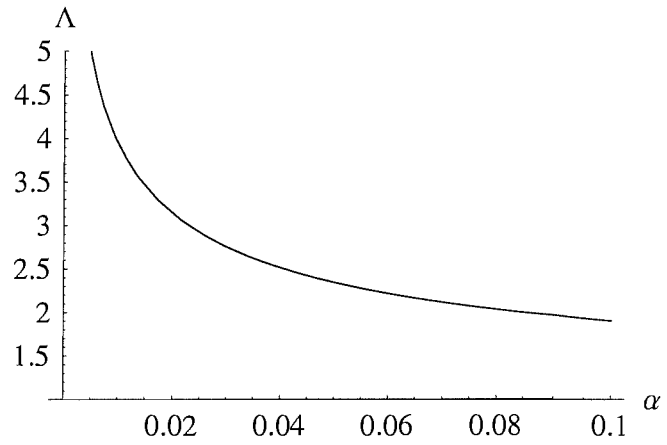

Figure 10.3: Peak position of the potential plotted in figure 10.2 as a function of α. This sets the value of the field theory cutoff, Λ.

can be calculated. To do this, the boundary value behaviour for the scalar field must be known in order to set up the boundary conditions correctly. However, in lowering the cutoff and adding the new operator, the $AdS_5 \times S^5$ region has been removed. This is the only region where the gauge-gravity duality is known quantitatively. The large ρ region of the current geometry is flat-space. In flat-space, the solution to the equation of motion is given by $a \sin \rho + b \cos \rho$. This solution is not normalisable unlike the solutions for the $AdS_5 \times S^5$ region. In addition, because the gauge-gravity duality is not understood in this region, it is unknown what sort of field theory operator each solution corresponds to. At this point, the quantitative control becomes more speculative. In $AdS_5 \times S^5$, there are two solutions to the large ρ behaviour of the scalar field, given by

$$f(\rho) = a + b\rho^{-3}. \tag{10.19}$$

Only the solution $a = 0$ is normalisable, so this is chosen to be the boundary

behaviour of the field. This means that b has the conformal scaling of r^6 which corresponds, as expected, to the six-dimensional operator $\mathrm{Tr}\, F^2$. Ideally, the dimension of the operator $\mathrm{Tr}\, F^2$ would be calculated at the cutoff, however, this will be renormalised and its dimension is unknown for an arbitrary cutoff value. Unfortunately, the least naive procedure is to use the $\mathrm{AdS}_5 \times \mathrm{S}^5$ UV boundary conditions to set the behaviour of the scalar field at the cutoff. As α increases and the cutoff lowered, the dimensions of $\mathrm{Tr}\, F^2$ will change and might be expected to become dimension four in the four-dimensional IR. The calculation is therefore also performed with an alternative set of boundary conditions:

$$\begin{aligned} f(\Lambda) &= \Lambda^{-(3+\epsilon)} , \\ f'(\Lambda) &= -(3+\epsilon)\Lambda^{-(4+\epsilon)} , \end{aligned} \tag{10.20}$$

with $-1 < \epsilon < 1$, which includes the speculative four-dimensional value. It is hoped that, through this range, the spectrum will not change dramatically, indicating that the naive boundary conditions do not alter the results significantly.

The algorithm to calculate the glueball spectrum is the same as that used in the previous chapters to calculate any other mass spectrum. The mass in the equation of motion is altered until a well-behaved IR behaviour is found. This procedure is performed for different values of α and for each value, the ratio $m(0^{++*})/m(0^{++})$ is calculated. The lattice result [131, 132] for this ratio is 1.9. The variation of this ratio is plotted as a function of α for $\epsilon = 0$ in figure 10.4.

The correct value of the ratio is obtained for $\alpha = 0.0855$ (in units of b). The peak position of the potential is at $\Lambda = 1.99$. Λ is of scaling dimension mass^2 and, therefore, the cutoff is actually at $\Lambda_{cutoff} = \sqrt{1.99} = 1.41$.

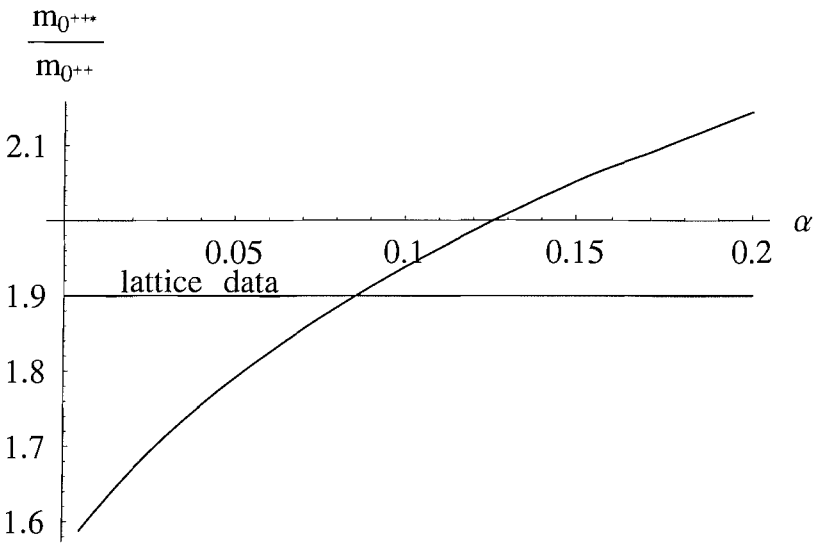

Figure 10.4: Ratio of the first two glueball masses as a function of the parameter α. The lattice value [131, 132] 1.9 is indicated in the diagram.

As the boundary conditions are altered, by varying ϵ, The stability of these results is now calculated. In the range $-1 < \epsilon < 1$, the glueball mass ratio changes by only 6%.

To find the correct glueball mass ratio, the value of α is such that there is a field theory description only between the IR scale $b = 1$ and the UV scale $\Lambda_{cutoff} = 1.41$. This means that the AdS-like (conformal) region has almost entirely been removed from the description. This matches the expectations of a realistic model of QCD for which the region between the mass gap and the perturbative regime is indeed small.

The full glueball spectrum from the supergravity calculation with $\alpha = 0.0855$ and with $\alpha = 0$ can be compared with those from the lattice data. This is not a remarkable result as there are only two lattice values to compare to and there are

Glueball State	*Improved Geometry*	$\alpha = 0$	$N = 3$ *Lattice*	$N = \infty$ *Lattice*
0^{++}	1.00	1.00	1.00	1.00
0^{++*}	1.90	1.58	1.74	1.90
0^{++**}	3.05	2.15	-	-
0^{++***}	4.27	2.72	-	-
0^{++****}	5.52	3.33	-	-

Table 10.1: QCD_4 0^{++} glueball masses from AdS ($\alpha = 0$) and Improved ($\alpha = 0.0855$) geometries along with lattice data [131, 132] . All states are normalised to the 0^{++} ground state.

two free parameters (b and α) in the supergravity theory. It is interesting that the spectra can be tuned to match exactly. However, more impressive matching is possible.

The 0^{-+} glueball spectrum can be calculated using the same values of b and α that were used to match onto the 0^{++} spectrum. This provides more data values to investigate whether the addition of a cutoff improves previous supergravity calculations.

10.6 Calculating the 0^{-+} Glueball Spectrum

The 0^{-+} glueball is dual to the operator $\mathrm{Tr}\, F\tilde{F}$, as this is the lowest dimension operator with the correct quantum numbers. On the supergravity side, the dual of this operator is given by the R-R one-form A_μ. The equation of motion for

this field is

$$\partial_\nu[\sqrt{g}g^{\mu\delta}g^{\nu\sigma}(\partial_\delta A_\sigma - \partial_\sigma A_\delta)] = 0 \ . \tag{10.21}$$

The component of interest of this one-form can be found by studying the action for N D4-branes. The $\mathrm{Tr}\, F\tilde{F}$ term comes from the WZ part of the action, given by

$$\frac{1}{16\pi^2}\int d^5x\epsilon^{\rho\alpha\beta\gamma\delta}A_\rho \mathrm{Tr}\left(F_{\alpha\beta}F_{\gamma\delta}\right) \ . \tag{10.22}$$

Compactifying the τ-direction, the θ-angle is related to the integral of the one-form on the compactified direction:

$$\theta = \int d\tau A_\tau \ . \tag{10.23}$$

The θ-angle is the source for $F\tilde{F}$ so it is this component of the field A that is of interest. Using the plane-wave ansatz for this component, $A_\tau = f(\rho)e^{ik.x}$, gives the equation of motion

$$\frac{1}{\rho^4}(\rho^3 - 1)\frac{d}{d\rho}\left[\rho^4\frac{df}{d\rho}\right] = k^2(1+\alpha\rho^3)f(\rho) \ . \tag{10.24}$$

Setting $\alpha = 0.0855$ and $\Lambda = 1.99$, the spectrum for these states can be calculated in the same way as for the 0^{++} glueball states. Unfortunately, there are no lattice data available for the large N limit of the 0^{-+} glueball spectrum, so a comparison can be drawn only to the $N = 3$ data. The results of the 0^{-+} glueball spectrum along with previous supergravity calculations and the $N = 3$ lattice data are provided in table 10.2. There seems to be a large mismatch between the AdS/CFT calculations and the data. However, in the literature, for the $\alpha = 0$ results, the first data point always appears to be omitted, though the reasoning for this seems to have been forgotten. Whether this point is omitted or not, the results with

Glueball State	*Improved Geometry*	$\alpha = 0$	$N = 3$ *Lattice*
0^{-+}	0.35	0.29	1.61
0^{-+*}	1.38	1.24	2.26
0^{-+**}	2.48	1.84	n/a
0^{-+***}	3.71	2.42	n/a

Table 10.2: QCD_4 0^{-+} glueball masses from AdS ($\alpha = 0$) and improved ($\alpha = 0.0855$) geometries along with lattice data [131] . All states are normalised to the 0^{++} ground state.

a small UV cutoff are better than those with the cutoff at ∞ (by 10% or 4% depending on whether the first mass is, or is not, left in). It would be interesting to compare to large N lattice data and to understand the reasoning behind the mismatch in the first data point.

Chapter 11

Conclusions

QCD still holds many mysteries, from confinement and asymptotic freedom [133] to chiral symmetry breaking and the nature of glueballs. Some of these phenomena have been studied experimentally, but others remain speculative. The AdS/CFT correspondence has proved to be a valuable tool in our understanding of strongly-coupled gauge theories and may one day give significant insight into the real structure of the strong force. This will take considerable time and effort, but an attempt has been made here to progress in this endeavour.

Chapters 1 to 3 provided an introduction to large N gauge theories, string theory and chiral perturbation theory, as well a detailed look at the AdS/CFT correspondence.

In chapter 4, quarks were introduced into the AdS/CFT correspondence in the simplest manner possible, via a D7-brane probe. By studying the action of D7-branes in an $AdS_5 \times S^5$ background, many properties of the field theory living on the brane surface were investigated. By studying the relationship between the

quark mass and quark bilinear condensate, it was shown that chiral symmetry breaking was not induced. The relationship between the quark mass and the mass of the scalar fields living on the D7-brane, corresponding to mesons, was calculated both analytically and numerically to ensure that the numerics were understood. The $AdS_5 \times S^5$ background was studied to gain insight into the sort of results that may be expected in the deformed geometries corresponding to more QCD-like theories.

In chapter 5, a singular, non-supersymmetric supergravity background was studied. This geometry has been investigated in the past and was the first background in which chiral symmetry breaking was found. This background is particularly simple as its form is known analytically. Quarks were introduced into this geometry using D7-brane probes, and following the work of [71], a more thorough investigation into the properties of this theory was carried out. The stable and unstable D7-brane flows were studied in some detail and the relationship between the quark mass and bilinear condensate was investigated. This relationship indicated that chiral symmetry is broken in the field theory dual to this geometry.

The spectrum of scalar fields living on the D7-brane surface were studied and compared with the results from the phenomenological pion Lagrangian introduced in chapter 3. The AdS/CFT results match to a high degree of accuracy with the Gell-Mann-Oakes-Renner relation. Next, the higher order interaction terms and the pion decay constant were studied and again compared with the chiral Lagrangian. These results matched remarkably well with experimental results, indicating that the $\frac{1}{N}$ corrections make only a small difference to these values.

Comparing the magnitude of the Gasser-Leutwyler coefficients with those calculated using naive-dimensional-analysis also gave a good match indicating that even in this non-supersymmetric deformation of the gauge-gravity correspondence, the duality holds well. Having studied the case of a single flavour of quark, the action for multiple D7-branes was investigated. The multi-flavour model gave exactly the same results for the pion decay constant and the Gasser-Leutwyler coefficients as the single flavour case. This result was understood having studied the interaction terms between the open strings on the D7-branes and those stretching between the D3- and D7-branes. The chiral symmetry group is not enhanced, because any non-Abelian extension is broken explicitly by the open string interaction terms.

As the metric and dilaton fields are known analytically in this geometry, the background was used as a testing-ground for new techniques, later applied to the more complicated geometries. It was discovered that one of the signatures of chiral symmetry breaking, is the presence of a gap between the D7-brane in the massless quark limit, and the singular structure causing the deformation. This gap is due to a potential felt by the D7-brane, and a simple procedure to calculate the potential felt by the brane was developed. This used a non-physical brane configuration to probe the region around the singularity using a circular wrapping technique. This allowed the equations of motion for the brane to be simplified to such an extent that they could be solved analytically. The analytical solution showed the repulsive potential expected in this case.

This background has a single free parameter, and it was found that changing

its value (corresponding to the size of the singularity) produces qualitatively different gauge theories. It was discovered that there is a lower bound on this parameter, which gives chiral symmetry breaking. There is another, slightly lower bound, which gives a theory with confinement. It is somewhat perplexing to find a gauge theory which does induce chiral symmetry breaking with a $\bar{q}q$ condensate but is not confining. It may be that stringy corrections to the geometry would bring these two bounds together, meaning that chiral symmetry breaking vanishes at the same point in parameter space where confinement stops.

Chapter 6 dealt with a supersymmetric geometry constructed from a lift of a five-dimensional supergravity solution to ten dimensions. The solutions to the field equations are known only numerically meaning that the equations of motion for the D7-brane cannot be solved analytically. When the $\bar{q}q$ condensate is calculated as a function of the quark mass, numerical results appear to show a finite condensate for non-zero quark mass. This condensate vanishes in the massless limit, however, the supersymmetry should not allow any condensate at all. The reason for this discrepancy came from using inappropriate coordinates. For this specific geometry, a change of variables for the coordinate system is known which produces a canonically normalised gauge theory on a D3-brane. In this system, the equations of motion for the D7-brane are equivalent to a D7-brane in the $AdS_5 \times S^5$ geometry, and the absence of a condensate can be calculated analytically.

The wrapping technique was applied to this geometry in the unphysical coordinate system and it was found that the repulsive potential necessary for chiral

symmetry breaking was absent. Though the absence of chiral symmetry breaking had already been proved analytically, it was useful to understand the unphysical coordinate system in order to study the non-supersymmetric background of chapter 7.

The geometry of chapter 7 was a generalisation of the previous one, this time with no supersymmetry. In the near singular limit, the equations of motion for the supergravity fields simplify greatly, and analytical solutions were found. Unlike the previous geometry, the physical coordinates for this one are not known. Quarks were introduced using D7-branes, however, it was not possible to extract a link between the quark mass and condensate due to the use of inappropriate coordinates.

The D7-brane wrapping technique was applied for this geometry and because the IR asymptotics was understood analytically, an analytical expression for the action was formulated for the circular brane configuration. It was found that the minimum action solution corresponded to the brane falling onto the singular surface. This indicated that, just as in the supersymmetric case, chiral symmetry is not broken in this background. It would be interesting to find the physical coordinates in which to describe the gauge theory, so that the brane flows indicate explicitly the absence of a chiral condensate.

The absence of a condensate in this background is more surprising than its absence in the previous geometry. However, the background of chapter 7 differs from the Constable-Myers geometry, in having a constant dilaton. In the regime of parameter space where the dilaton running vanishes in the Constable-Myers

geometry, chiral symmetry is restored. It may be that the running of the dilaton is a necessary ingredient for chiral symmetry breaking.

In chapter 8, the $\mathcal{N} = 2^*$ geometry was studied. This has a more complicated structure than the previous backgrounds because of the presence of extra closed string modes and the warped form of the five-sphere. Due to the symmetries of the background, it has not been possible to formulate a UV/IR flow for a D7-brane so no numerical results for the quarks and mesons were obtained.

Using the IR asymptotics, the equations of motion for the background fields were solved analytically. These solutions, when used in the action for a spherical D7-brane, showed the absence of a repulsive potential. No chiral symmetry breaking is allowed in this background due to its supersymmetry, and this is confirmed by the non-repulsive potential.

In chapter 9, the non-supersymmetric Yang-Mills* background was investigated. This geometry is dual to a field theory which is the closest to QCD of all those studied up to now. With the addition of quarks via a D7-brane probe, it would be interesting to compare the brane action to the chiral Lagrangian in order to investigate the relationships between the parameters of the two theories. However, the Yang-Mills* background describes a very complex geometry, specifically, the five-sphere is squashed to a pair of two-spheres and a deficit angle. The DBI action for a D7-brane probe in this background includes the NS-NS two-form which is switched on in this geometry. Due to the extra closed string modes and the non-trivial deformation, the equations of motion are very difficult to solve, analytically or numerically. A relaxation method was developed to attempt to

solve the flow equations for the brane running between the UV and the IR of the theory. However, the background was too complicated even for this and the brane wrapping technique was again invoked.

As in the previous sections, the IR behaviour of the fields were calculated analytically and it was found that, for most of the supergravity field solutions, there was a repulsive potential. However, this was not the case for some solutions which appear to retain the chiral symmetry. It would be interesting to study the difference between those IR solutions which do retain chiral symmetry and those which do not. This question remains open, pending further research.

Whereas in chapters 4 to 9, quark fields were introduced in order to formulate a more QCD-like field theory, the final chapter concentrated on a different aspect of the same problem. In all deformations of the AdS/CFT correspondence studied in the previous chapters, the UV of the field theory has been strongly coupled, in contrast to QCD.

The type IIA AdS-Schwarzschild geometry, corresponding to five-dimensional high temperature QCD, which reduces to four-dimensional QCD in the low energy limit, was studied. By defining the supergravity field boundary conditions at a finite radius, the strongly-coupled UV of the field theory was removed. At the same time, a higher-dimensional operator was introduced to account for the high-energy degrees of freedom which had been integrated out. This introduced two new free parameters to the theory: the cutoff and the coupling constant for the higher-dimensional operator. By linking the cutoff to the peak position of the potential felt by a scalar field, one of these degrees of freedom was removed

in order to constrain the theory. The masses of 0^{++} and 0^{-+} glueballs were calculated in this background as a function of the new coupling constant. These masses were compared to the small number of lattice data values available and it was found that, for the 0^{++} masses, the two values calculated on the lattice matched exactly those in the deformed geometry. Though there appears to be an anomalous data point for the 0^{-+} masses, whether or not this is included, the results with a cutoff are closer to the lattice data than those without.

The overall conclusion to be drawn from this thesis is that we have been able to use the AdS/CFT correspondence to investigate many of the properties of strongly-coupled, non-supersymmetric gauge theories. The results appear to match, to a high degree of accuracy, both calculations on the lattice and experiments. Whereas lattice calculations are extremely time and computer intensive, many of the calculations performed in this thesis were performed very quickly on a simple desktop computer. More research must be completed in order to understand the gauge-gravity duality, especially in the non-supersymmetric regime, and the correspondence in the presence of fundamental matter.

Many toy models are currently being developed [134, 90, 135] to study supergravity duals to QCD. One of the key conclusions being drawn seems to be that, even for the most naive models, the results match with lattice data and experimental results far more closely than might have been previously imagined. Even with arguments about universality, the similarity of the results appears astonishing. It may not be long before we have a model that mimics QCD to an accuracy which can be used in the building of hadron colliders in the future.

Appendix A

$AdS_5 \times S^5$ Parametrisations

The metric for the product of a five-dimensional anti-de-Sitter space and a five-sphere can be parametrised in a variety of ways. Different forms of the metric are used for simplifying calculations or to make a D-brane embedding easier to visualise. Below are some of the possible parametrisations all of which have been scaled such that no dimensionful quantities are explicit.

$$
\begin{aligned}
ds^2 &= r^2 dx_{//}^2 + \frac{1}{r^2}\left(dr^2 + r^2 d\Omega_5^2\right) \ , \\
ds^2 &= \left(\rho^2 + \omega_5^2 + \omega_6^2\right) dx_{//}^2 + \frac{1}{\left(\rho^2 + \omega_5^2 + \omega_6^2\right)}\left(d\rho^2 + d\omega_5^2 + d\omega_6^2 + \rho^2 d\Omega_3^2\right) \ , \\
ds^2 &= \left(y_1^2 + y_2^2 + y_3^2 + y_4^2 + y_5^2 + y_6^2\right) dx_{//}^2 + \frac{1}{\left(y_1^2 + y_2^2 + y_3^2 + y_4^2 + y_5^2 + y_6^2\right)} \sum_{i=1}^{6} dy_i^2 \ , \\
ds^2 &= r^2 dx_{//}^2 + \frac{1}{r^2}\left(dr^2 + d\theta^2 + \sin^2\theta d\phi^2 + \cos^2\theta d\Omega_3^2\right) \ , \\
ds^2 &= e^{2r} dx_{//}^2 + \left(dr^2 + d\Omega_5^2\right) \ , \\
ds^2 &= r^2 dx_{//}^2 + \frac{1}{r^2}\left(dr^2 + d\alpha^2 + \sin^2\alpha d\Omega_-^2 + \cos^2\alpha d\Omega_+^2\right) \ . \qquad \text{(A.1)}
\end{aligned}
$$

Bibliography

[1] D. Ivanenko and G. Sardanashvily, "The Gauge Treatment Of Gravity," Phys. Rept. **94**, 1 (1983).

[2] R. P. Feynman, "QED. The Strange Theory Of Light And Matter," http://www.slac.stanford.edu/spires/find/hep/www?irn=1631209SPIRES entry

[3] C. N. Yang and R. L. Mills, "Conservation Of Isotopic Spin And Isotopic Gauge Invariance," Phys. Rev. **96**, 191 (1954).

[4] E. S. Abers and B. W. Lee, "Gauge Theories," Phys. Rept. **9**, 1 (1973).

[5] P. W. Higgs, "Broken Symmetries And The Masses Of Gauge Bosons," Phys. Rev. Lett. **13**, 508 (1964).

[6] Y. A. Golfand and E. P. Likhtman, "Extension Of The Algebra Of Poincare Group Generators And Violation Of P Invariance," JETP Lett. **13**, 323 (1971) [Pisma Zh. Eksp. Teor. Fiz. **13**, 452 (1971)].

[7] J. Wess and B. Zumino, "A Lagrangian Model Invariant Under Supergauge Transformations," Phys. Lett. B **49**, 52 (1974).

[8] S. P. Martin, "A supersymmetry primer," arXiv:hep-ph/9709356.

[9] D. J. Gross and F. Wilczek, "Asymptotically Free Gauge Theories. 1," Phys. Rev. D **8**, 3633 (1973).

[10] E. Reya, "Perturbative Quantum Chromodynamics," Phys. Rept. **69**, 195 (1981).

[11] J. B. Kogut, "A Review Of The Lattice Gauge Theory Approach To Quantum Chromodynamics," Rev. Mod. Phys. **55**, 775 (1983).

[12] S. Weinberg, "Phenomenological Lagrangians," PhysicaA **96**, 327 (1979).

[13] A. Pich, "Chiral perturbation theory," Rept. Prog. Phys. **58**, 563 (1995) [arXiv:hep-ph/9502366].

[14] G. 't Hooft, "A Planar Diagram Theory For Strong Interactions," Nucl. Phys. B **72**, 461 (1974).

[15] G. 't Hooft, "A Two-Dimensional Model For Mesons," Nucl. Phys. B **75**, 461 (1974).

[16] A. V. Manohar, "Large N QCD," arXiv:hep-ph/9802419.

[17] W. J. Marciano and H. Pagels, "Quantum Chromodynamics: A Review," Phys. Rept. **36**, 137 (1978).

[18] O. Aharony, S. S. Gubser, J. M. Maldacena, H. Ooguri and Y. Oz, "Large N field theories, string theory and gravity," Phys. Rept. **323**, 183 (2000) [arXiv:hep-th/9905111].

[19] J. Polchinski, "String Theory Volume 1 – An introduction to the bosonic string," Cambridge, UK:Univ. Pr. (1998) 402 p. "String Theory Volume 2 – Superstring theory and beyond", Cambridge, UK:Univ. Pr. (1998) 531 p.

[20] M. Ademollo, H. R. Rubinstein, G. Veneziano and M. A. Virasoro, "Bootstrap Of Meson Trajectories From Superconvergence," Phys. Rev. **176**, 1904 (1968).

[21] M. Ademollo, G. Veneziano and S. Weinberg, "Quantization Conditions For Regge Intercepts And Hadron Masses," Phys. Rev. Lett. **22**, 83 (1969).

[22] G. F. Chew, S. C. Frautschi and S. Mandelstam, "Regge Poles In Pi Pi Scattering," Phys. Rev. **126**, 1202 (1961).

[23] M. E. Peskin and D. V. Schroeder, "An Introduction to Quantum Field Theory," http://www.slac.stanford.edu/spires/find/hep/www?irn=3485960.

[24] J. M. Maldacena, "The large N limit of superconformal field theories and supergravity," Adv. Theor. Math. Phys. **2**, 231 (1998) [Int. J. Theor. Phys. **38**, 1113 (1999)] [arXiv:hep-th/9711200].

[25] S. S. Gubser, I. R. Klebanov and A. M. Polyakov, "Gauge theory correlators from non-critical string theory," Phys. Lett. B **428**, 105 (1998) [arXiv:hep-th/9802109].

[26] E. Witten, "Anti-de Sitter space and holography," Adv. Theor. Math. Phys. **2**, 253 (1998) [arXiv:hep-th/9802150].

[27] F. Gliozzi, J. Scherk and D. I. Olive, "Supersymmetry, Supergravity Theories And The Dual Spinor Model," Nucl. Phys. B **122**, 253 (1977).

[28] P. Van Nieuwenhuizen, "Supergravity," Phys. Rept. **68**, 189 (1981).

[29] C. V. Johnson, "D-brane primer," arXiv:hep-th/0007170.

[30] E. Cremmer and S. Ferrara, "Formulation Of Eleven-Dimensional Supergravity In Superspace," Phys. Lett. B **91**, 61 (1980).

[31] S. Weinberg and E. Witten, "Limits On Massless Particles," Phys. Lett. B **96**, 59 (1980).

[32] E. D'Hoker and D. Z. Freedman, "Supersymmetric gauge theories and the AdS/CFT correspondence," arXiv:hep-th/0201253.

[33] L. Susskind, "The anthropic landscape of string theory," arXiv:hep-th/0302219.

[34] E. Witten, "String theory dynamics in various dimensions," Nucl. Phys. B **443**, 85 (1995) [arXiv:hep-th/9503124].

[35] J. Polchinski, "Dirichlet-Branes and Ramond-Ramond Charges," Phys. Rev. Lett. **75**, 4724 (1995) [arXiv:hep-th/9510017].

[36] G. T. Horowitz and A. Strominger, "Black strings and P-branes," Nucl. Phys. B **360**, 197 (1991).

[37] S. Weinberg, "Gravitation and Cosmology: Principles and Applications of the General Theory of Relativity," New York (US): Wiley (1972).

[38] E. Witten, "Bound states of strings and p-branes," Nucl. Phys. B **460**, 335 (1996) [arXiv:hep-th/9510135].

[39] I. L. Buchbinder and S. M. Kuzenko, "Ideas and Methods of Supersymmetry and Supergravity: Or a Walk Through Superspace," Bristol, UK: IOP (1998).

[40] N. Seiberg and E. Witten, "Monopoles, duality and chiral symmetry breaking in N=2 supersymmetric QCD," Nucl. Phys. B **431**, 484 (1994) [arXiv:hep-th/9408099].

[41] M. R. Gaberdiel, "An introduction to conformal field theory," Rept. Prog. Phys. **63**, 607 (2000) [arXiv:hep-th/9910156].

[42] G. 't Hooft, "Dimensional reduction in quantum gravity," arXiv:gr-qc/9310026.

[43] L. Susskind, "The World as a hologram," J. Math. Phys. **36**, 6377 (1995) [arXiv:hep-th/9409089].

[44] J. D. Bekenstein, "Entropy bounds and black hole remnants," Phys. Rev. D **49**, 1912 (1994) [arXiv:gr-qc/9307035].

[45] H. J. Kim, L. J. Romans and P. van Nieuwenhuizen, "The Mass Spectrum Of Chiral N=2 D = 10 Supergravity On S^5," Phys. Rev. D **32**, 389 (1985).

[46] D. Z. Freedman, S. S. Gubser, K. Pilch and N. P. Warner, "Renormalization group flows from holography supersymmetry and a c-theorem," Adv. Theor. Math. Phys. **3**, 363 (1999) [arXiv:hep-th/9904017].

[47] J. Distler and F. Zamora, "Non-supersymmetric conformal field theories from stable anti-de Sitter spaces," Adv. Theor. Math. Phys. **2**, 1405 (1999) [arXiv:hep-th/9810206].

[48] L. Girardello, M. Petrini, M. Porrati and A. Zaffaroni, "Novel local CFT and exact results on perturbations of N = 4 super Yang-Mills from AdS dynamics," JHEP **9812**, 022 (1998) [arXiv:hep-th/9810126].

[49] I. R. Klebanov and A. A. Tseytlin, "D-branes and dual gauge theories in type 0 strings," Nucl. Phys. B **546**, 155 (1999) [arXiv:hep-th/9811035].

[50] A. Karch, D. Lust and A. Miemiec, "New N = 1 superconformal field theories and their supergravity description," Phys. Lett. B **454**, 265 (1999) [arXiv:hep-th/9901041].

[51] K. Gawedzki, "Conformal field theory: A case study," arXiv:hep-th/9904145.

[52] P. H. Ginsparg, "Applied Conformal Field Theory," arXiv:hep-th/9108028.

[53] E. Witten, "Anti-de Sitter space, thermal phase transition, and confinement in gauge theories," Adv. Theor. Math. Phys. **2**, 505 (1998) [arXiv:hep-th/9803131].

[54] R. G. Leigh, "Dirac-Born-Infeld Action From Dirichlet Sigma Model," Mod. Phys. Lett. A **4**, 2767 (1989).

[55] M. R. Douglas and W. I. Taylor, "Branes in the bulk of anti-de Sitter space," arXiv:hep-th/9807225.

[56] A. I. Karanikas and C. N. Ktorides, "Extension of worldline computational algorithms for QCD to open fermionic contours," JHEP **9911**, 033 (1999) [arXiv:hep-th/9905027].

[57] S. R. Das, "Brane waves, Yang-Mills theories and causality," JHEP **9902**, 012 (1999) [arXiv:hep-th/9901004].

[58] M. K. Prasad and C. M. Sommerfield, "An Exact Classical Solution For The 'T Hooft Monopole And The Julia-Zee Dyon," Phys. Rev. Lett. **35**, 760 (1975).

[59] R. G. Leigh, "Dirac-Born-Infeld Action From Dirichlet Sigma Model," Mod. Phys. Lett. A **4**, 2767 (1989).

[60] M. Cederwall, A. von Gussich, A. Mikovic, B. E. W. Nilsson and A. Westerberg, "On the Dirac-Born-Infeld action for D-branes," Phys. Lett. B **390**, 148 (1997) [arXiv:hep-th/9606173].

[61] S. R. Coleman, J. Wess and B. Zumino, "Structure Of Phenomenological Lagrangians. 1," Phys. Rev. **177**, 2239 (1969).

[62] J. Gasser and H. Leutwyler, "Low-Energy Expansion Of Meson Form-Factors," Nucl. Phys. B **250**, 517 (1985).

[63] M. Gell-Mann, R. J. Oakes and B. Renner, "Behavior Of Current Divergences Under SU(3) X SU(3)," Phys. Rev. **175**, 2195 (1968).

[64] C. Vafa and E. Witten, "Restrictions On Symmetry Breaking In Vector - Like Gauge Theories," Nucl. Phys. B **234**, 173 (1984).

[65] H. Georgi, "Generalized dimensional analysis," Phys. Lett. B **298**, 187 (1993) [arXiv:hep-ph/9207278].

[66] A. V. Manohar, "Effective field theories," arXiv:hep-ph/9606222.

[67] A. Karch and E. Katz, "Adding flavor to AdS/CFT," JHEP **0206**, 043 (2002) [arXiv:hep-th/0205236].

[68] A. Karch, E. Katz and N. Weiner, "Hadron masses and screening from AdS Wilson loops," Phys. Rev. Lett. **90**, 091601 (2003) [arXiv:hep-th/0211107].

[69] M. Kruczenski, D. Mateos, R. C. Myers and D. J. Winters, "Meson spectroscopy in AdS/CFT with flavour," JHEP **0307**, 049 (2003) [arXiv:hep-th/0304032].

[70] T. Sakai and J. Sonnenschein, "Probing flavored mesons of confining gauge theories by supergravity," JHEP **0309**, 047 (2003) [arXiv:hep-th/0305049].

[71] J. Babington, J. Erdmenger, N. J. Evans, Z. Guralnik and I. Kirsch, "Chiral symmetry breaking and pions in non-supersymmetric gauge / gravity duals," Phys. Rev. D **69**, 066007 (2004) [arXiv:hep-th/0306018].

[72] C. Nunez, A. Paredes and A. V. Ramallo, "Flavoring the gravity dual of N = 1 Yang-Mills with probes," JHEP **0312**, 024 (2003) [arXiv:hep-th/0311201].

[73] P. Ouyang, "Holomorphic D7-branes and flavored N = 1 gauge theories," Nucl. Phys. B **699**, 207 (2004) [arXiv:hep-th/0311084].

[74] X. J. Wang and S. Hu, "Intersecting branes and adding flavors to the Maldacena-Nunez background," JHEP **0309**, 017 (2003) [arXiv:hep-th/0307218].

[75] S. Hong, S. Yoon and M. J. Strassler, "Quarkonium from the fifth dimension," JHEP **0404**, 046 (2004) [arXiv:hep-th/0312071].

[76] N. J. Evans and J. P. Shock, "Chiral dynamics from AdS space," Phys. Rev. D **70**, 046002 (2004) [arXiv:hep-th/0403279].

[77] B. A. Burrington, J. T. Liu, L. A. Pando Zayas and D. Vaman, "Holographic duals of flavored N = 1 super Yang-Mills: Beyond the probe approximation," JHEP **0502**, 022 (2005) [arXiv:hep-th/0406207].

[78] J. Erdmenger and I. Kirsch, "Mesons in gauge / gravity dual with large number of fundamental fields," JHEP **0412**, 025 (2004) [arXiv:hep-th/0408113].

[79] M. Kruczenski, L. A. P. Zayas, J. Sonnenschein and D. Vaman, "Regge trajectories for mesons in the holographic dual of large-N(c) QCD," JHEP **0506**, 046 (2005) [arXiv:hep-th/0410035].

[80] S. Kuperstein, "Meson spectroscopy from holomorphic probes on the warped deformed conifold," JHEP **0503**, 014 (2005) [arXiv:hep-th/0411097].

[81] A. Paredes and P. Talavera, "Multiflavour excited mesons from the fifth dimension," Nucl. Phys. B **713**, 438 (2005) [arXiv:hep-th/0412260].

[82] T. Sakai and S. Sugimoto, "Low energy hadron physics in holographic QCD," Prog. Theor. Phys. **113**, 843 (2005) [arXiv:hep-th/0412141].

[83] N. Evans, J. Shock and T. Waterson, "D7 brane embeddings and chiral symmetry breaking," JHEP **0503**, 005 (2005) [arXiv:hep-th/0502091].

[84] H. Nastase, "On Dp-Dp+4 systems, QCD dual and phenomenology," arXiv:hep-th/0305069.

[85] N. R. Constable and R. C. Myers, "Exotic scalar states in the AdS/CFT correspondence," JHEP **9911**, 020 (1999) [arXiv:hep-th/9905081].

[86] S. S. Gubser, "Dilaton-driven confinement," arXiv:hep-th/9902155.

[87] K. Ghoroku and M. Yahiro, "Chiral symmetry breaking driven by dilaton," Phys. Lett. B **604**, 235 (2004) [arXiv:hep-th/0408040].

[88] A. Kehagias and K. Sfetsos, "On running couplings in gauge theories from type-IIB supergravity," Phys. Lett. B **454**, 270 (1999) [arXiv:hep-th/9902125].

[89] J. M. Maldacena, "Wilson loops in large N field theories," Phys. Rev. Lett. **80**, 4859 (1998) [arXiv:hep-th/9803002].

[90] L. Da Rold and A. Pomarol, "Chiral symmetry breaking from five dimensional spaces," Nucl. Phys. B **721**, 79 (2005) [arXiv:hep-ph/0501218].

[91] N. Mahajan, "Revisiting 5D chiral symmetry breaking and holographic QCD models," Phys. Lett. B **623**, 119 (2005) [arXiv:hep-ph/0506098].

[92] R. C. Myers, "Dielectric-branes," JHEP **9912**, 022 (1999) [arXiv:hep-th/9910053].

[93] M. Kruczenski, D. Mateos, R. C. Myers and D. J. Winters, "Towards a holographic dual of large-N(c) QCD," JHEP **0405**, 041 (2004) [arXiv:hep-th/0311270].

[94] B. de Wit and H. Nicolai, "The Consistency Of The S^7 Truncation In D = 11 Supergravity," Nucl. Phys. B **281**, 211 (1987).

[95] M. Gunaydin, L. J. Romans and N. P. Warner, "Gauged N=8 Supergravity In Five-Dimensions," Phys. Lett. B **154**, 268 (1985).

[96] M. Pernici, K. Pilch and P. van Nieuwenhuizen, "Gauged N=8 D = 5 Supergravity," Nucl. Phys. B **259**, 460 (1985).

[97] M. Gunaydin, L. J. Romans and N. P. Warner, "Compact And Noncompact Gauged Supergravity Theories In Five-Dimensions," Nucl. Phys. B **272**, 598 (1986).

[98] D. Z. Freedman, S. S. Gubser, K. Pilch and N. P. Warner, "Continuous distributions of D3-branes and gauged supergravity," JHEP **0007**, 038 (2000) [arXiv:hep-th/9906194].

[99] K. Pilch and N. P. Warner, "N = 2 supersymmetric RG flows and the IIB dilaton," Nucl. Phys. B **594**, 209 (2001) [arXiv:hep-th/0004063].

[100] J. Babington, N. J. Evans and J. Hockings, "Secrets of the metric in N = 4 and N = 2* geometries," JHEP **0107**, 034 (2001) [arXiv:hep-th/0105235].

[101] J. Babington, D. E. Crooks and N. J. Evans, "A non-supersymmetric deformation of the AdS/CFT correspondence," JHEP **0302**, 024 (2003) [arXiv:hep-th/0207076].

[102] L. Girardello, M. Petrini, M. Porrati and A. Zaffaroni, "Confinement and condensates without fine tuning in supergravity duals of gauge theories," JHEP **9905**, 026 (1999) [arXiv:hep-th/9903026].

[103] A. Brandhuber and K. Sfetsos, "An N = 2 gauge theory and its supergravity dual," Phys. Lett. B **488**, 373 (2000) [arXiv:hep-th/0004148].

[104] N. J. Evans, C. V. Johnson and M. Petrini, "The enhancon and N = 2 gauge theory/gravity RG flows," JHEP **0010**, 022 (2000) [arXiv:hep-th/0008081].

[105] S. Randjbar-Daemi and M. E. Shaposhnikov, "On some new warped brane world solutions in higher dimensions," Phys. Lett. B **491**, 329 (2000) [arXiv:hep-th/0008087].

[106] J. Babington, D. E. Crooks and N. J. Evans, "A stable supergravity dual of non-supersymmetric glue," Phys. Rev. D **67**, 066007 (2003) [arXiv:hep-th/0210068].

[107] R. Apreda, D. E. Crooks, N. J. Evans and M. Petrini, "Confinement, glueballs and strings from deformed AdS," JHEP **0405**, 065 (2004) [arXiv:hep-th/0308006].

[108] L. Girardello, M. Petrini, M. Porrati and A. Zaffaroni, "The supergravity dual of N = 1 super Yang-Mills theory," Nucl. Phys. B **569**, 451 (2000) [arXiv:hep-th/9909047].

[109] J. Polchinski and M. J. Strassler, "The string dual of a confining four-dimensional gauge theory," arXiv:hep-th/0003136.

[110] N. J. Evans and M. Petrini, "Superfluidity in the AdS/CFT correspondence," JHEP **0111**, 043 (2001) [arXiv:hep-th/0108052].

[111] A. Khavaev, K. Pilch and N. P. Warner, "New vacua of gauged N = 8 supergravity in five dimensions," Phys. Lett. B **487**, 14 (2000) [arXiv:hep-th/9812035].

[112] K. Pilch and N. P. Warner, "N = 1 supersymmetric renormalization group flows from IIB supergravity," Adv. Theor. Math. Phys. **4**, 627 (2002) [arXiv:hep-th/0006066].

[113] M. Petrini and A. Zaffaroni, "The holographic RG flow to conformal and non-conformal theory," arXiv:hep-th/0002172.

[114] W. H. Press "Numerical Recipes in C. The Art of Scientific Computing," http://www.cs.brown.edu/research/vis/results/bibtex/Press-1992-MOD.bib

[115] P. Hasenfratz and F. Niedermayer, "Perfect lattice action for asymptotically free theories," Nucl. Phys. B **414**, 785 (1994) [arXiv:hep-lat/9308004].

[116] M. Luscher and P. Weisz, "Computation Of The Action For On-Shell Improved Lattice Gauge Theories At Weak Coupling," Phys. Lett. B **158**, 250 (1985).

[117] T. R. Morris, "A gauge invariant exact renormalization group. II," JHEP **0012**, 012 (2000) [arXiv:hep-th/0006064].

[118] S. Arnone, Y. A. Kubyshin, T. R. Morris and J. F. Tighe, "Gauge invariant regularisation via SU(N|N)," Int. J. Mod. Phys. A **17**, 2283 (2002) [arXiv:hep-th/0106258].

[119] C. Csaki, H. Ooguri, Y. Oz and J. Terning, "Glueball mass spectrum from supergravity," JHEP **9901**, 017 (1999) [arXiv:hep-th/9806021].

[120] C. Csaki, Y. Oz, J. Russo and J. Terning, "Large N QCD from rotating branes," Phys. Rev. D **59**, 065012 (1999) [arXiv:hep-th/9810186].

[121] J. A. Minahan, "Glueball mass spectra and other issues for supergravity duals of QCD models," JHEP **9901**, 020 (1999) [arXiv:hep-th/9811156].

[122] R. de Mello Koch, A. Jevicki, M. Mihailescu and J. P. Nunes, "Evaluation of glueball masses from supergravity," Phys. Rev. D **58**, 105009 (1998) [arXiv:hep-th/9806125].

[123] R. C. Brower, S. D. Mathur and C. I. Tan, "Glueball spectrum for QCD from AdS supergravity duality," Nucl. Phys. B **587**, 249 (2000) [arXiv:hep-th/0003115].

[124] H. Boschi-Filho and N. R. F. Braga, "QCD / string holographic mapping and glueball mass spectrum," Eur. Phys. J. C **32**, 529 (2004) [arXiv:hep-th/0209080].

[125] H. Boschi-Filho and N. R. F. Braga, "Gauge / string duality and scalar glueball mass ratios," JHEP **0305**, 009 (2003) [arXiv:hep-th/0212207].

[126] N. J. Evans, C. V. Johnson and M. Petrini, "Clearing the throat: Irrelevant operators and finite temperature in large N gauge theory," JHEP **0205**, 002 (2002) [arXiv:hep-th/0112058].

[127] K. A. Intriligator, "Maximally supersymmetric RG flows and AdS duality," Nucl. Phys. B **580**, 99 (2000) [arXiv:hep-th/9909082].

[128] A. Hashimoto, "Holographic description of D3-branes in flat space," Phys. Rev. D **60**, 127902 (1999) [arXiv:hep-th/9903227].

[129] N. Itzhaki, J. M. Maldacena, J. Sonnenschein and S. Yankielowicz, "Supergravity and the large N limit of theories with sixteen supercharges," Phys. Rev. D **58**, 046004 (1998) [arXiv:hep-th/9802042].

[130] P. Kraus, F. Larsen and S. P. Trivedi, "The Coulomb branch of gauge theory from rotating branes," JHEP **9903**, 003 (1999) [arXiv:hep-th/9811120].

[131] C. J. Morningstar and M. J. Peardon, "The glueball spectrum from an anisotropic lattice study," Phys. Rev. D **60**, 034509 (1999) [arXiv:hep-lat/9901004].

[132] B. Lucini and M. Teper, "SU(N) gauge theories in four dimensions: Exploring the approach to N = infinity," JHEP **0106**, 050 (2001) [arXiv:hep-lat/0103027].

[133] H. D. Politzer, "Reliable Perturbative Results For Strong Interactions?," Phys. Rev. Lett. **30**, 1346 (1973).

[134] J. Erlich, E. Katz, D. T. Son and M. A. Stephanov, "QCD and a holographic model of hadrons," arXiv:hep-ph/0501128.

[135] G. F. de Teramond and S. J. Brodsky, "The hadronic spectrum of a holographic dual of QCD," Phys. Rev. Lett. **94**, 201601 (2005) [arXiv:hep-th/0501022].